A WIRELESS SENSOR SYSTEM AND APPLICATION OF TRADITIONAL CHINESE PULSE DIAGNOSIS FOR INDIVIDUAL HEALTHCARE MONITORING

A WIRELESS SENSOR SYSTEM AND APPLICATION OF TRADITIONAL CHINESE PULSE DIAGNOSIS FOR INDIVIDUAL HEALTHCARE MONITORING

By

Wei Zhou

Bachelor of Engineering

McMaster University

Hamilton, Ontario, Canada

August 2009

A THESIS

SUBMITTED TO THE SCHOOL OF GRADUATE STUDIES IN PARTIAL FULFILLMENT OF THEREQUIREMENTS FOR THE DEGREE OFMASTER'S OF APPLIED SCIENCE

McMaster University

Hamilton, Ontario, Canada

MASTER OF APPLIED SCIENCE (2009) McMaster University

(Electrical and Computer Engineering) Hamilton, Ontario

TITLE: A WIRELESS SENSOR SYSTEM AND APPLICATIONS OF TRADITIONAL CHINESE PULSE DIAGNOSIS FOR INDIVIDUAL HEALTHCARE MONITORING

AUTHOR: Wei Zhou, B.Eng. (McMaster University)

SUPERVISOR: Professor M. J. Deen

NUMBER OF PAGES: 132

ABSTRACT

Home health care continues to be an important and challenging issue in most countries, especially for the elderly. To improve home health care, it would be useful to have wireless biomedical systems that can monitor various vital signs of the elderly and to provide such information to a health care professional. In the orient, one powerful tool in diagnosing and predicting health issues is the Traditional Chinese Pulse Diagnosis (TCPD) technique. The TCPD technique is through the examination of the artery pulse pattern on three points along the radial artery and it usually requires a doctor to conduct pulse palpation with their fingers. Therefore, the diagnosis relies significantly on the experience of the doctor. However, for the more widespread use of TCPD, one concept is to bring the doctor's "fingers" and "encode" the doctor's experience to an individual in a home care setting. Using existing technologies in biomedical sensor, data acquisition, communication and microelectronics, it is possible to construct a "smart" TCPD system.

In this thesis, a microcontroller based pulse monitoring system for TCPD's application in home care is proposed. The system consists of three main units for data acquisition, data processing and wireless transmission. The pulse data acquisition is with a liquid-filled digital pressure sensor module with the employment of applanation tonometry, a technique used in recording the peripheral artery waveform. Each sensor module is read by a corresponding microcontroller via its serial peripheral interface, and the measurement is then sent wirelessly to a personal computer (PC) via a 2.4GHz transceiver. The system was used to successfully record and transmit radial pulse pressure and body surface temperature measurements to a host PC. Pulse waveforms are then reproduced from the pulse pressure measurements to conduct offline analysis. The analysis is targeted to integrating TCPD diagnosis with quantitative pulse representation and measurement history, to use expert knowledge in classification and recognition, and therefore to provide supporting information for disease diagnosis and forecasting.

The work performed in this thesis presents the proof-of-concept research and system implementation in the design of an individual health monitoring system using the TCPD method. Basic pattern matching and parameter extraction/comparison are performed and verified. Finally, the research work presented here provides a solid foundation for future work in this field of TCPD and its application.

ACKNOWLEDGEMENTS

I would like to first express my sincere thanks and appreciation to my supervisor Prof. M. Jamal Deen for his continuous guidance all the way throughout this thesis and providing me the chance to achieve my academic goal. Prof. M. Jamal Deen's enormous knowledge in his field of research and ambitious towards new technology have set a great model for all his students, including me. His continuous support and technical advice were most helpful and enabled me to overcome lots of difficulties.

I would like to thank Dr. O. Marinov too for providing me countless helpful technical advice and teaching me several things.

I am also very grateful to be part of the McMaster University's Microelectronics Research Group. Everyone in this group are working together and helping each other. I would thank to all my colleges especially Munir El-Desouki, Waleed Shinwari, Mohammed Naser, Gefei Zhou and everyone else for their support.

In the end, I would like to express my sincere thanks and gratitude to my parents. Without their continuous support, I would never have the opportunity to achieve my academic goals.

Table of Contents

List of Figures

Chapter 1 Introduction

Health care is a fundamental issue for every country. The Canadian government spending for health care has been rising over the last decade. Among all the health care expenditures, the aged population, those whose age is 65 and above, occupies a significant percentage of health care costs. Further, individual health care for the aging population has become a challenging problem to most governments. Some of the challenges are due to the social and financial burden of chronic conditions, the increase of emergency occurrences, and the lack of efficient health models to provide a satisfactory solution [1]. Meanwhile, the growing population of aged people has made the individual health care even more difficult. In Canada, the number of elderly people, 65 years old and above, has increased rapidly in the past few decades and is expected to continue increasing [2],

Figure 1-1 shows the population percentage of individuals whose age are 65 and above. It also shows the composition of such age group by categorizing it into three sub age groups which are 65 years to 74 years, 75 years to 84 years and 85years and above, respectively. As shown, the trend of the aged population percentage has been increasing steadily at a pace of 1-2% per decade in the past few decades. At this rate, it will surpass 20% by the year of 2031.

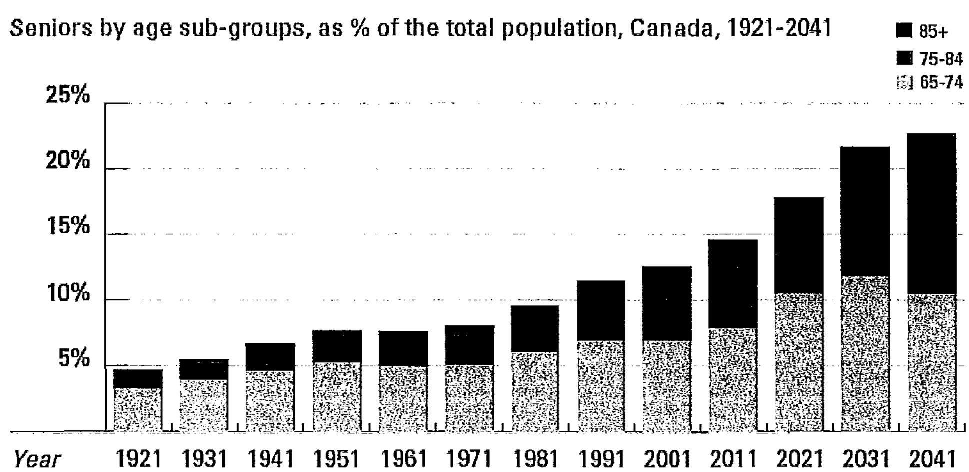

Figure 1-1 Seniors (age above 65) by age sub-groups, as percentage of the total population, Canada, 1921-2041 [2] .

Figure 1-2 shows the general population distribution in the year of 2001 and the prediction for the year of 2041. It categorizes population into male and female, and for each sex group, shows the weights of each age group. One important observation is the percentage of higher age that is predicted to significantly increase.

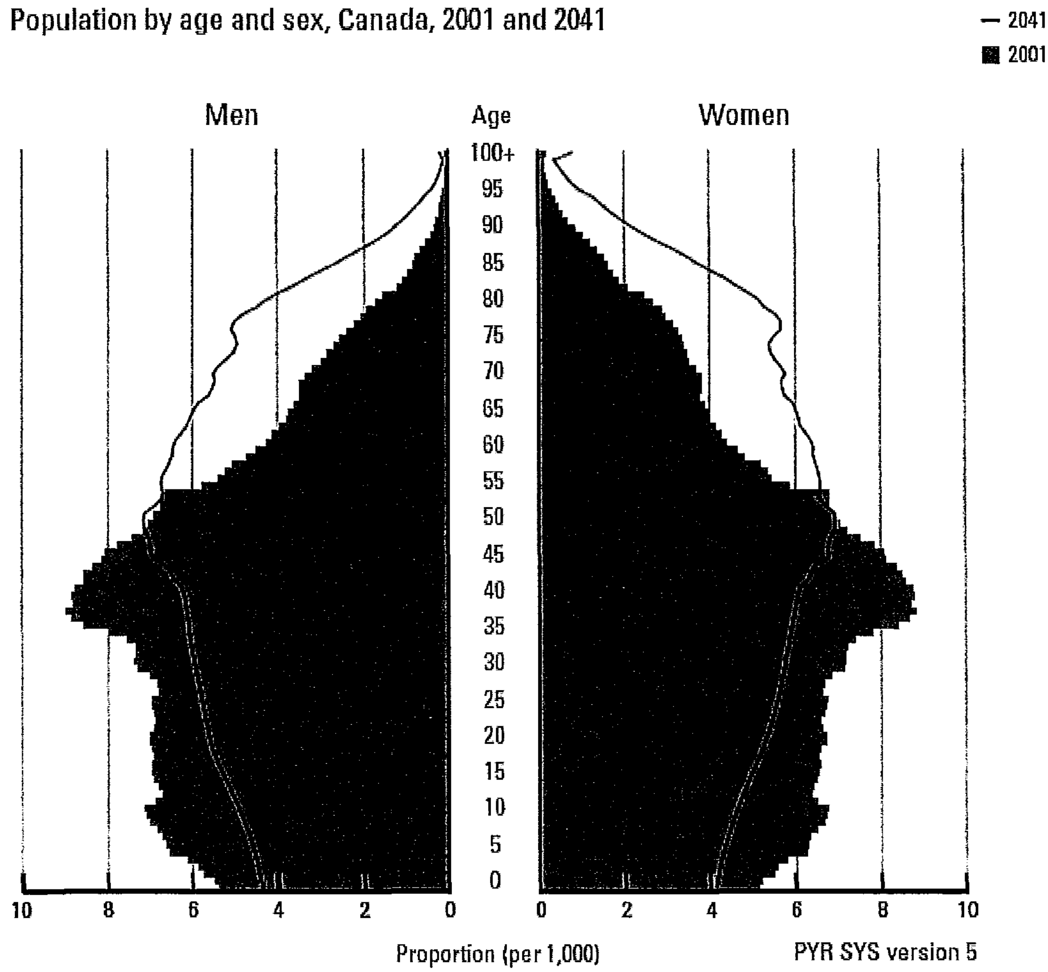

Figure 1-2 Population by age and sex, Canada, 2001 and 2041[3].

1.1 The Canadian Health Expenditure

In 2007, public- and private-sector spending on health care in Canada was estimated at $160 billion. This was about 4.1% more than in 2006 when inflation is taken into account, and about 3.2% more when both inflation and population growth are taken into account [4]. The health care spending outpaced the inflation and population growth for eleven consecutive years. As a share of Canada's gross domestic product (GDP), it continued the slow, steady increase of the previous five years, rising slightly from an estimated 10.4% in 2006 to an estimated 10.6% in 2007 [5].

Figure 1-3 shows the trends of the health care spending in the past few decades. In 2007, total health care spending per capita continued to grow, but the rate of growth has moderated since 2000. Growth in per capita spending peaked at 8.0% in 2000. The forecast spending increase of 5.7% in 2007 is in line with recent yearly growth rates: 5.4% in 2004, 6.1% in 2005 and an estimated 5.3% in 2006 [4]. Among all the health care spending, a major proportion goes to the people whose age is 65 and above. In the year of 2005 Canadians age 65 and older consumed an estimated 44% of provincial and territorial government health care spending; about the same proportion they had been consuming yearly since 1998 [4].

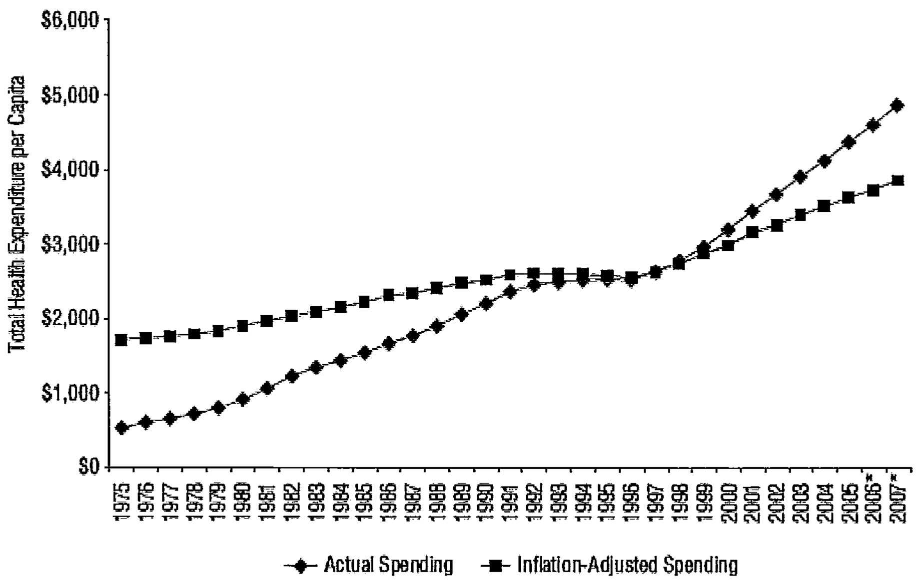

Figure 1-3 Total health care spending per capita in Canada [4]

In 2005, CIHI (Canadian Institute for Health Information) analyzed the extent to which projected increases in provincial and territorial government health care spending to 2026 may be due to population aging. The analysis kept everything constant except changes in population size and the proportion of Canadians that are seniors. For example, the health care system's operations and per capita health care use by different age groups were kept at 2002 levels. The analysis found that population aging would cause the add up of 1% per year to provincial and territorial government health care spending between 2002 and 2026 [6]. Taking inflation into account, the "pure aging effect" can be expected to increase provincial and territorial governments' real per capita spending from $2,321 in 2002 to $2,940 by 2026 [6]. In figure 1-4, the 2005 Canadian health care expenditure by age and gender is given.

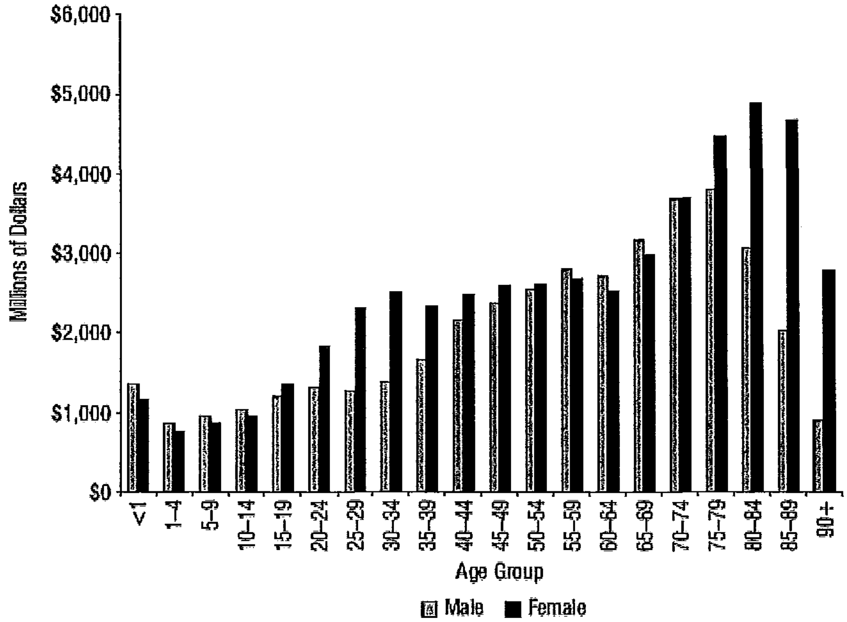

Figure 1-4 Total Provincial and Territorial Government Health Expenditure, by Age and Sex, Canada, 2005 [4].

1.2 Individual Home Monitoring

With the growing aged population and the continuously increased cost in health care, individual health care has been growing in importance. For the elderly, through prompt reporting of health or emergency conditions, some severe illness can be detected early. In Canada one common phenomenon is older people who live by themselves. For these elderly persons, it is often difficult to achieve prompt reporting of their health conditions. Further, because it is not feasible to have the health caregiver provide continuous individual health care to each person due to the cost and availability of trained care providers.

One complementary approach is to have devices that monitor certain biological signals of people and detect occurrences of emergency situations at home. In fact, the rapid development of microelectronic technology in the past few decades has made many kinds of home monitoring techniques accessible by the general public. There are several approaches. One is to have stationary monitoring device that tracks the movements of the individual and reports an emergency if abnormal activities are detected. Another approach is to use an implantable device. A third approach is to use a wearable device that monitors specific biological signals and report the health condition accordingly.

The stationary systems have limited access to the actual human health conditions compared to the wearable or implantable devices. The implantable device has less flexibility and people are reluctant to have a device implanted in their body, unless it is absolutely necessary. Therefore, wearable devices seem to be the most promising way for health condition monitoring. In the following sections, implementation and techniques for each type of monitoring device are discussed to provide an overview to home monitoring systems.

1.2.1 Stationary home monitoring system

Stationary home monitoring devices are normally designed to detect accidents such as falls that occur to elder people living independently. Falls are recognized as one of the major health hazard for older people. The estimated incidence falls for both institutionalized and independent persons aged 75 or higher is thirty percent per year [7]. To detect falls effectively, the monitoring device should be able to track the unusual movement or to detect the abnormal conditions of the subject.

1.2.1.1 Camera based fall detector

One type of existing system is camera based fall detector called SIMBAD (Smart Inactivity Monitor using Array-Based Detectors) [8]. The idea of such monitoring system is to use a camera integrated with an intelligent detection system capable of tracking the subject and detecting risks. However, normal camera may appear intrusive and using machine interpretation of camera images could be complex and difficult. In this case, the IRISYS (Infrared Integrated Systems) thermal imaging sensors have been used as a camera [8]. The IRISYS sensor can locate and track a thermal target in the sensor's field of view and provides size, location and velocity information. One detection system is connected to the sensor system. The detection system consists of five subcomponents: Tracker, Subtle-motion detector, Fall detector, Inactivity monitor and High-level reasoner [8]. Figure 1-5 shows the whole architecture of SIMBAD.

Tracker is subsystem of the main detection system which is based on an elliptical-contour gradient-tracking system that identifies and tracks elliptical target in data provided by the IRISYS sensor. The tracker will track a moving subject which either has higher temperature or lower temperature compared to the background. It will also provide real-time estimates of subject's position, velocity, shape and size. Another subcomponent is Fall detector. The Fall detector employs a neural network that classifies falls using vertical-velocity estimates derived either directly from IRISYS sensor data or from the tracker. The Subtle-motion detector indentifies small movements in the sensor's field of view. Since such movements generate limited responses that may not activate the tracker and therefore would be ignored otherwise. The Inactivity monitor examines the subject's inactive period based on the output from the tracker and subtle-motion detector. The data output from all the aforementioned components will be integrated in the High-level reasoner. The High-level reasoner performs the reasoning required based on the data provided by other components and issue alarms for excessive periods of inactivity (according to the risk map) and detected fall [8].

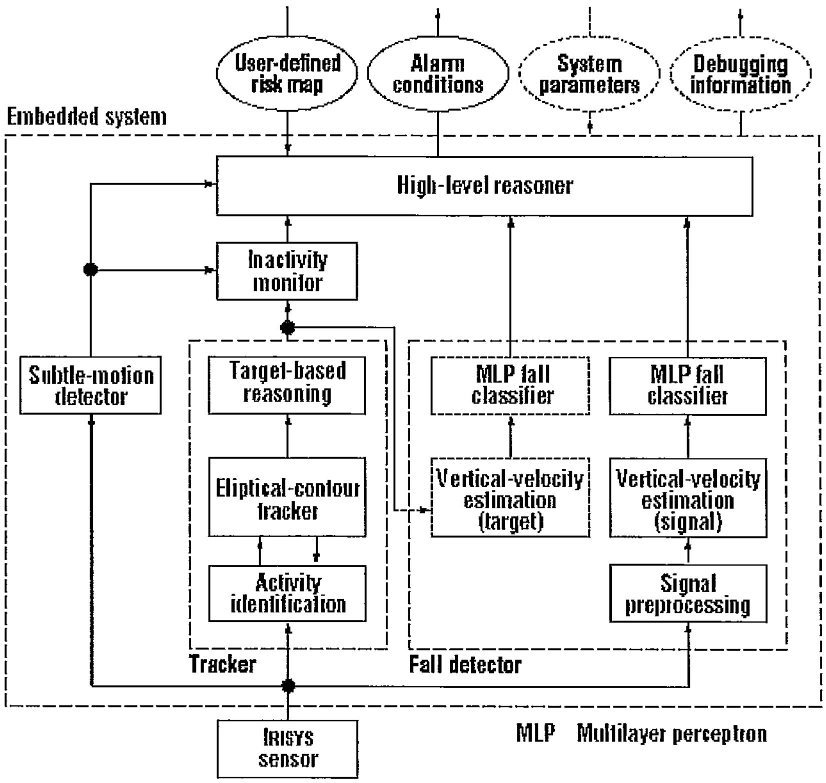

Figure 1-5 The prototype architecture for the SIMBAD (Smart Inactivity Monitor using Array-Based Detectors) system. Dashed boxes indicate subsystems; dotted boxes, ovals, and arrows indicate optional or debugging components and data flow [8].

An example of the SIMBAD usage and set up is shown in the figure below (Figure 1-6).

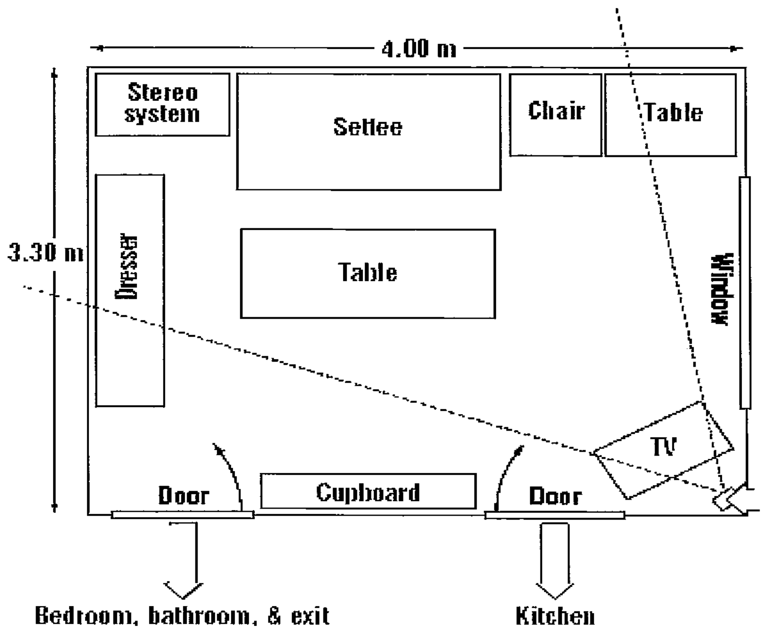

Figure 1-6 Setup for the SIMAD prototype. Dotted line illustrates the sensor's approximated field of view [8].

1.2.1.2 Floor-Vibration based fall detector

This kind of monitoring system is designed to monitor the vibrations introduced when a person falls. It is based on the observation that human activities such as walking or running can cause measurable vibrations on the floor [9]. And when a human falls, the impact would cause a specific vibration pattern that is transmitted throughout the floor. In this section, a Smart and Passive Floor-Vibration based Fall Detector for Elderly [10] is studied. The system is based on the hypothesis that it is possible to detect human falls by monitoring the vibration patterns in the floor. It implies two essential requirements: the first one is the vibration signature of the floor generated by falls is significantly different from those generated by normal activities like walking; and the second is that the vibration signature of the floor generated by a human falling is significantly different from those generated by objects falling on the floor [10]. The implementation of this system (see Figure 1-7) includes a piezoelectric sensor, it is then coupled to the floor surface by means of mass and spring arrangement and combined with battery-powered pre-processing electronics to evaluate the floors vibration patterns and then generate binary fall signal. The signal can be transferred wirelessly to communication gateway [10].

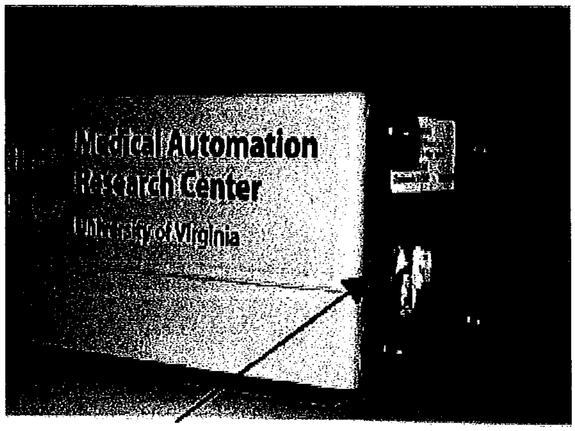

Piezo Transducer

Figure 1-7 Floor vibration based fall detector [10]

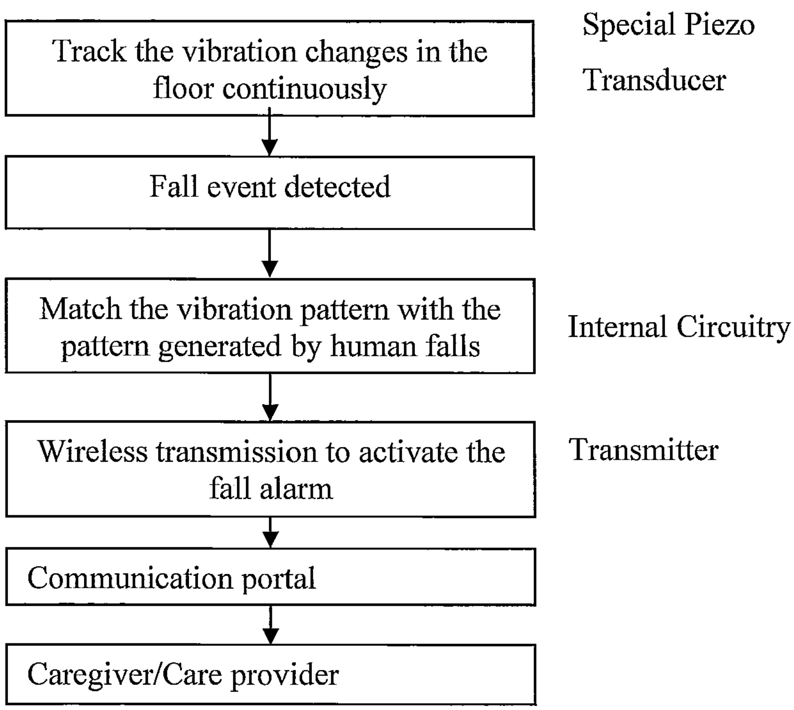

Figure 1-8 Working principle of the floor vibration based fall detector, reproduced from [10].

The result is this system can detect the impact of a human fall and distinguish it from object falling, the following figures (Figure 1-9 (a) and (b)) show the different signal pattern from a Rescue Randy falls and a 15 lbs object falls [10].

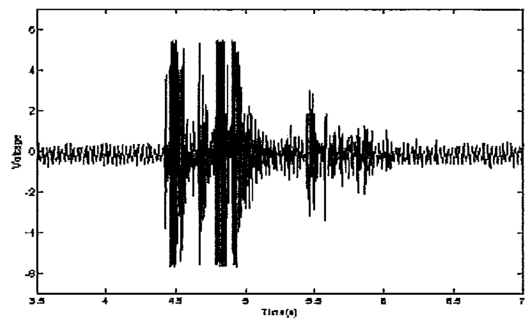

Figure 1-9 (a) Pre-amplified signal from the piezo sensor showing the vibration pattern of the floor following the event of a Rescue Randy fall at a distance of 20 feet from the sensor, on Mezzanine concrete floor covered with linoleum [10].

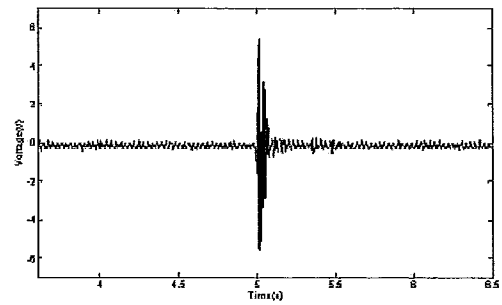

Figure 1-9 (b) Pre-amplified signal from the piezo sensor showing the vibration pattern of the floor following a 15 lb object fall, at a distance of 2 feet from the sensor, on Mezzanine concrete floor covered with linoleum [10].

1.2.2 Body implantable monitoring system

The body implantable electronic device is an important subfield in biomedical engineering. The world's first transistorized, battery-powered, wearable pacemaker was invented in1957 [11]. The pacemaker monitors the impulses in the heart and generates electrical pulses to stimulate the heart operation when required. The fast development in microelectronics technologies has enabled many novel design and manufacturing approaches for biomedical implantable systems. In this section, a prototype the Novel Long-Term Implantable Blood Pressure Monitoring System is discussed.

This system measures pressure by means of measuring the diameter change of the blood vessel while the heart is beating. It employs an instrumented elastic cuff, wound around a blood vessel, and operating in a linear "diameter vs. pressure" region of the vessel for real time blood pressure monitoring [12]. The concept is shown in Figure 1-10.

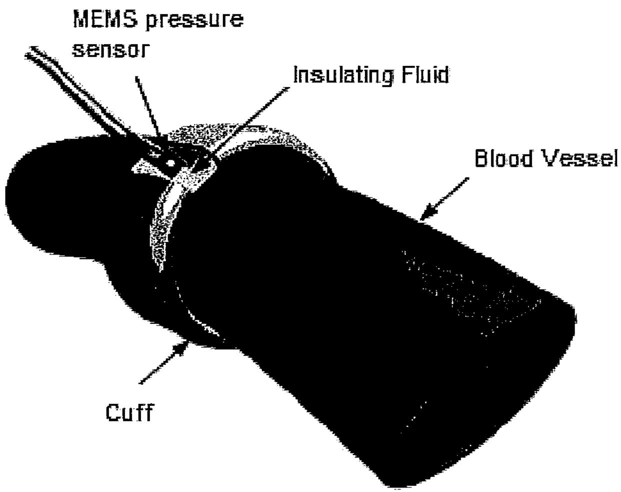

Figure 1-10 Implantable blood pressure monitoring system, reproduced from [12].

The fluid in the cuff is incompressible, the volume of the fluid is constant and it is reasonable to assume that the cuff cross-sectional area is constant [12]. Figure 1-11 shows the cross section of the cuff monitoring system.

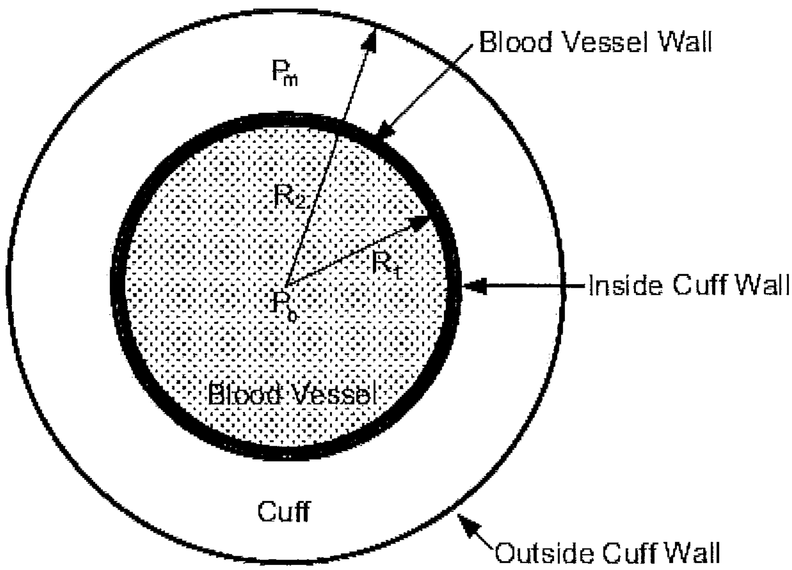

Figure 1-11 Cross section of cuff wound around blood vessel, the inner circle represents the cross section of the blood vessel while the outer circle is the cross section of the cuff [12].

The following equations [12] can be derived from the analysis.

$$\Delta P_m = \Delta P_b - \Delta P_w \tag{1-1}$$

$$\Delta P_w = [(K_{BW} + K_{insideCW}) / K_{Total}] \times \Delta P_b \tag{1-2}$$

$$\Delta P_m = (1 - \frac{K_{BW} + K_{insideCW}}{K_{Total}}) \times \Delta P_b = \eta \times \Delta P_b \tag{1-3}$$

$$\frac{\Delta R_2}{\Delta R_1} = \frac{R_1}{R_2} \tag{1-4}$$

$$\eta = \frac{\frac{R_1}{R_2} K_{OutsideCW}}{K_{BW} + K_{InsideCW} + \frac{R_1}{R_2} K_{OutsidCW}} \tag{1-5}$$

where ΔP_m, ΔP_b, and ΔP_w represent the pressure change measured by the sensor in the cuff, the blood pressure change in the blood vessel, and the pressure change exerted on the blood vessel wall and inside cuff wall, respectively. K_{BW}, $K_{insideCW}$, and K_{Total} are the elastic modulus of the blood vessel wall, the cuff inside wall, and the total equivalent elastic modulus associated with the blood vessel wall and the cuff, respectively, and η is the scaling factor [12].

The study shows that in a certain blood pressure range, the blood vessel walls exhibit nearly constant elastic modulus as shown in the Figure 1-12.

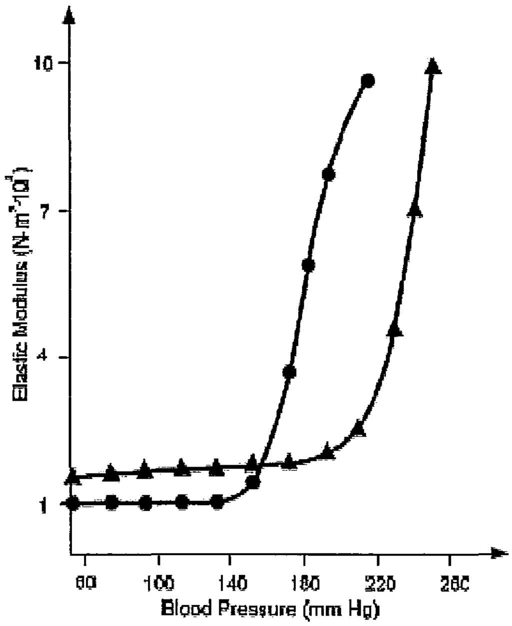

Figure 1-12 Elastic modulus K vs. blood pressure in 8 week old rats [13][14]

●normotensive, ▲hypertensive

Therefore a constant scaling factor can be achieved for in vivo blood pressure monitoring within the linear region. Then the blood pressure waveform can be expressed by the following equation

$$P_b(t) = \frac{1}{\eta}[P_m(t) - P_{Bias}] \qquad [12]$$

where $P_m(t)$ and $P_b(t)$ are the pressure measured in the cuff and blood vessel as a function of time, respectively. P_{Bias} is the cuff bias pressure which can be obtained before implant. The measurement result is shown below, as the cuff is measuring the pressure waveform of the elastic tube. The experiment set up is given in the Figure 1-13, and the measurement result is given in Figure 1-14.

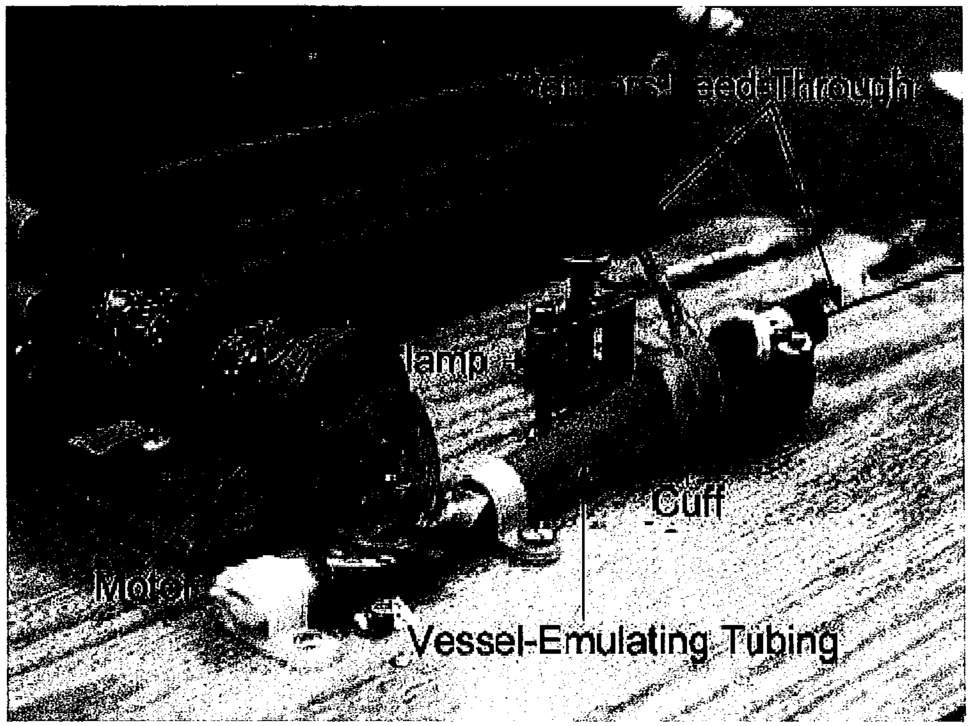

Figure 1-13 Experiment setup. The tube acts as the blood vessel, while motor push one end of the tube to simulate the blood flow pattern [12]

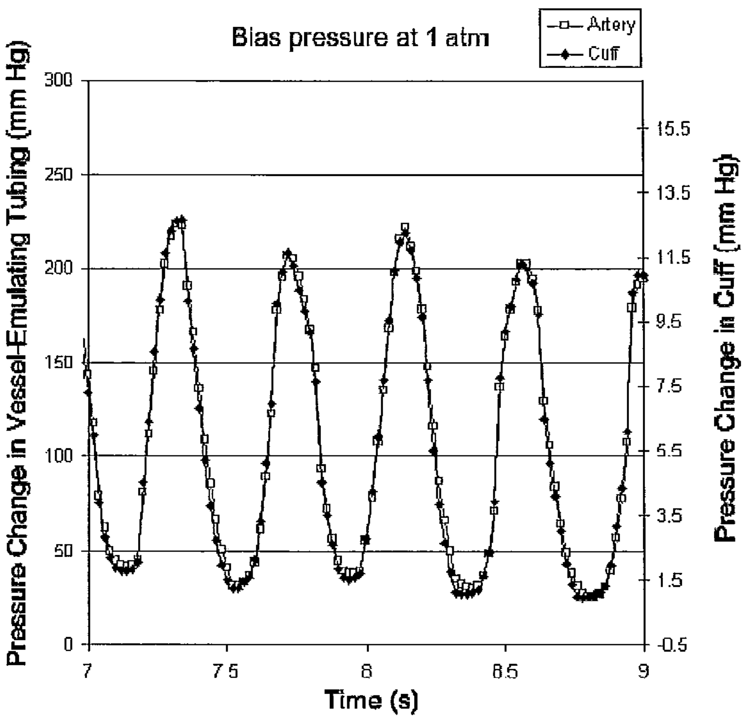

Figure 1-14 Pressure waveforms in vessel-emulating tubing and cuff [12]

1.2.3 Wearable non-invasive monitoring system

"Speedy" Wrist watch integrated fall detector

Wearable non-invasive monitoring system can monitor more specific biological signal from human body than stationary systems. Most of the wearable systems are designed in a wrist watch like template to make them more easily acceptable. More importantly, the radial artery is located at the wrist which contains rich information of the cardio system. A wrist watch integrated fall detector called "*Speedy*" [15] is discussed in this section to give an overview of the concept and implementation of such systems.

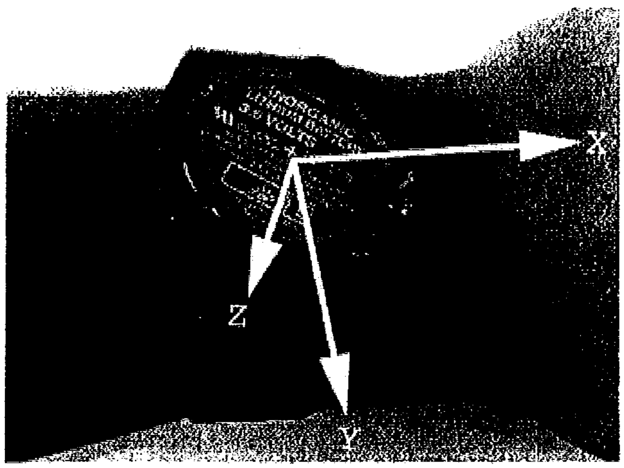

Figure 1-15 Illustration of the wrist watch integrated fall detector"*Speedy*" and its axes [15]

The detection of falls is based on the norm of the acceleration (described below). Two accelerometers are used to measure the acceleration in all three axes simultaneously. During a fall, the net acceleration can only be less than the static acceleration, which is the acceleration result by gravity.

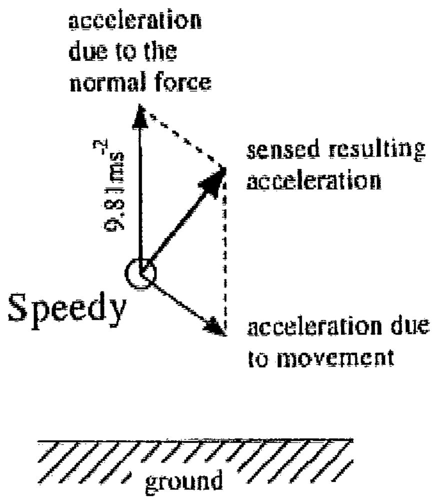

Figure 1-16 Resulting acceleration vector during a fall [15]

Through the measurements from the accelerometers, *Speedy* calculates the norm of the three axes acceleration vector $|n|=\sqrt{a_x^2+a_y^2+a_z^2}$. Integration is done to obtain the velocity of *Speedy:* $v_1 = \int(\sqrt{a_x^2+a_y^2+a_z^2}-9.81)dt$ [15]. The advantage of this approximation is it is not dependent on the orientation or even the rotation of *Speedy*. However, this approximation is correct for vertical movements only. Also, fast accelerated movements towards the ground will result in an incorrect estimated velocity [15]. A second integral is used to solve this problem. $v_2=\sqrt{(\int a_x dt)^2+(\int a_y dt)^2+(\int a_z dt)^2}-\int 9.81 dt$ [15]. The second estimation is good as long as the device is not rotating during fall. However, through experiment and in real world applications, the two velocity estimations will not be wrong at the same time [15].

The system then uses $|n|, v_1, v_2$ as the input to the detection algorithm. The detection algorithm can be concluded as follow (Figure 1-17).

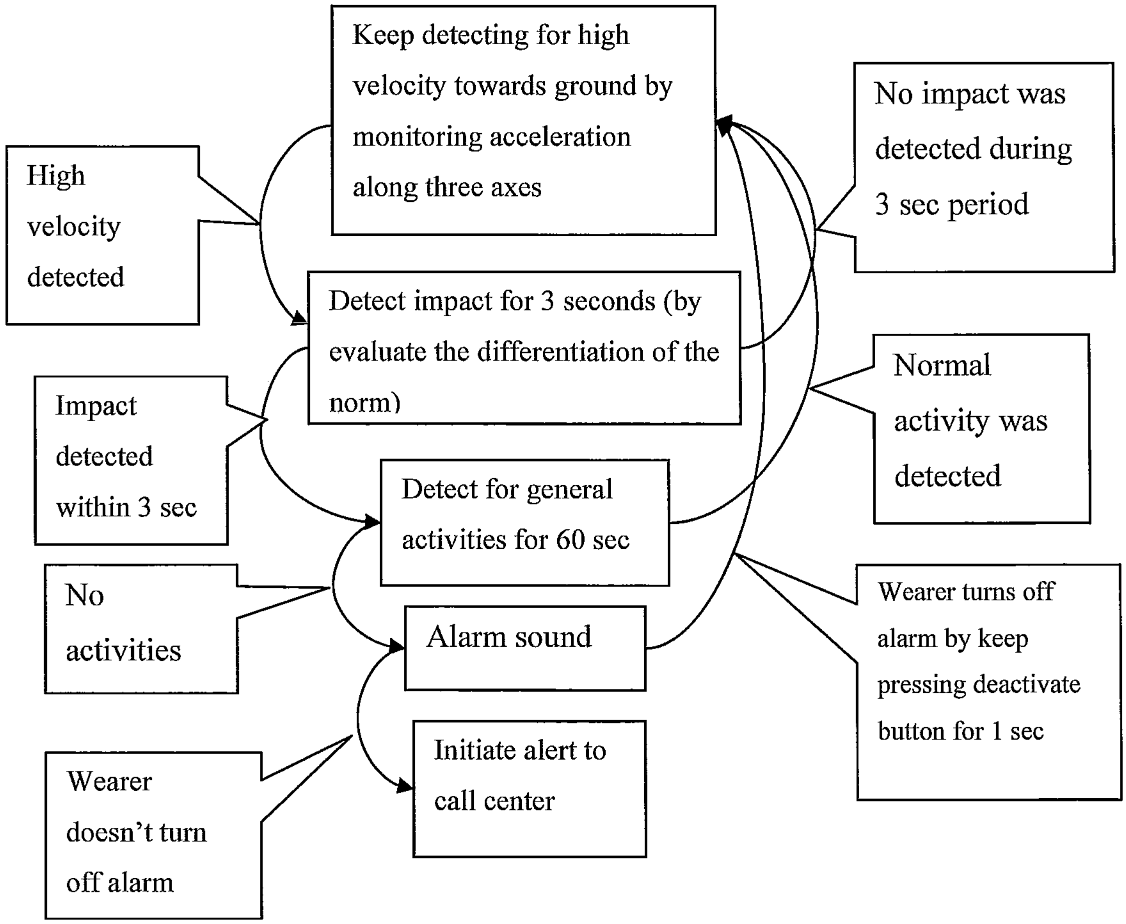

Figure 1-17 Detection algorithm of *Speedy*

Sometimes a gyroscope is integrated in the fall detection system to determine the direction of the arm which further assists the detecting of fall.

1.3 Thesis motivation

Wireless microelectronic system and its application in Traditional Chinese Medicine

This section contains the discussion of fundamentals of Traditional Chinese Medicine (TCM) and especially Traditional Chinese Pulse Diagnosis (TCPD). The methods of diagnosis of TCPD and pulse pattern classification are introduced, along with the current research on quantitative pulse classification standards. The challenges and problems in TCPD diagnosis will be discussed. Moreover, the possible application of TCPD in individual monitoring based on the existing quantitative scheme is discussed. In later part of this section, the proposal for a microelectronic system that records the pulse pattern generated from radial artery for TCPD analysis presented. It is designed to be wrist-worn with wireless transmitting function. The monitoring system and TCPD application in such field can provide useful information for further clinical studies and researches.

1.3.1 Traditional Chinese Pulse Diagnosis overview

Traditional Chinese Medicine (TCM) has been an important complementary and alternative medicine. It emphasizes treatment based on pattern discrimination. This means that although TCM practitioners first make a disease diagnosis, that the treatment is based more on the pattern discrimination than on the disease diagnosis [16]. One fascinating nature about pattern discrimination in TCM is the patterns, in most of the cases, are contributing to the signs of the early stage of certain diseases. In other words, if certain patterns are observed, then it is likely that their corresponding disease is occurring.

Traditional Chinese Pulse Diagnosis (TCPD) is one of the main methods of four diagnosis method in TCM along with inspection, auscultation/olfaction and inquiry [17]. It employs the same concept as TCM, which is pattern recognition and discrimination. The only difference is that it limits the pattern being examined to the behaviour and change of the radial pulse pattern. The doctors diagnose the patients by mean of using finger tips to palpate the pulse beating at the three points, namely *Cun*, *Guan*, and *Chi* as shown in Figure 1-18, along the radial artery. By analyzing the pressure fluctuation signal of the pulse, the doctors can detect and predict some symptoms that ECG cannot. Further, TCPD can deduce the positions and degree of pathological changes. It is a convenient, inexpensive, painless, bloodless, non-invasive, no-side effect method [18]. An experienced doctor can distinguish the different pulse patterns and use them to make a diagnosis. In practice, TCPD requires high level of skills from the doctor and greatly rely on the subjective judgement from the doctor. This affects the reliability and repeatability of the diagnosis, which limits the practical applications in clinical medicine. There are many researches [19], [20], [21], [22], [24], [28] devoted on the classification of the pulse pattern and attempting to establish a quantitative model for pulse classification in TCPD.

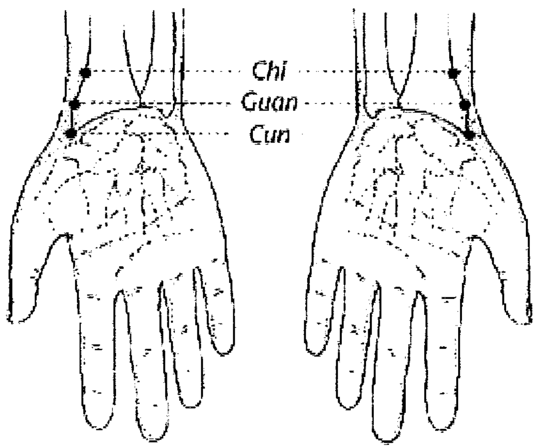

Figure 1-18 Position of the *Cun*, *Guan*, and *Chi* [25]

The figure above shows the locations of *Cun*, *Guan*, and *Chi*. Each location corresponds to or reflects organs in a certain region of the human body. It is said the *Cuan* position corresponds to the region of the body from the bottom of the chest to the top of the head; the *Guan* position corresponds to the area of the body located between the diaphragm and the navel; and the *Chi* position corresponds to the region of body that is below the navel [16].

1.3.2 Disease forecasting and pulse patterns in Traditional Chinese Pulse Diagnosis

In TCPD, the early detection of disease is based on the abnormal symptoms felt in the pulse. The rational is that the pathologic changes of a person's body condition are reflected in the wrist-pulse waveforms. Clinical studies demonstrate [26] that patients with hypertension, hypercholesterolemia, cardiovascular disease, and diabetes, exhibit premature loss of arterial elasticity and endothelial function, which eventually resulted in decreased flexibility of vasculature, and heightened stress to the circulatory system. The wrist-pulse shape, amplitude, and rhythm are also altered in correspondence with the hemodynamic characteristics of blood flow [16]. In TCPD, the pulses are assessed by five major criteria: Depth, Frequency, Rhythm, Quality and Strength [17]. The pulses are then classified into 12 detailed patterns - Hurried pulse, Rapid pulse, Soggy pulse, Wiry pulse, Surging pulse, Intermittent pulse, Fine pulse, Normal pulse, Choppy pulse, Knotted pulse, Slippery pulse, and Slow pulse [27]. Example pulse waveforms are shown below (Figure 1-19) to provide a visual impression of each kind of pulses.

1. **Hurried** Pulse: A rapid pulse with irregular intermittence, often due to excessive heat with stagnation of blood, or retention of phlegm or undigested food.

2. **Rapid** Pulse: A pulse with increased frequency (more than 90 beats per minute), usually indicating the presence of heat.

3. **Soggy** Pulse: A superficial, thin, and soft pulse which can be felt on light touch like a thread floating on water, but grows faint on hard pressuring, indicating deficiency conditions or damp retention.

4. **Wiry** Pulse: A pulse that feels straight and long, like a musical instrument string, usually occurring in liver and gallbladder disorders or severe pain.

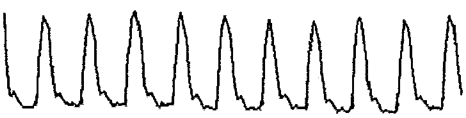

5. **Surging** Pulse: A pulse beating like dashing waves with forceful rising and gradual decline, indicating excessive heat.

6. **Intermittent** Pulse: A slow pulse pausing at regular intervals, often occurring in exhaustion of internal organs, severe trauma, or being seized by terror.

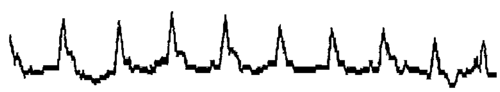

7. **Fine** Pulse: A pulse felt like a fine thread, but always distinctly perceptible, indicating deficiency of blood or other deficiency states.

8. **Normal** Pulse: A normal pulse with smooth, even, forceful and frequency that is between 60 to 90 beats per minute.

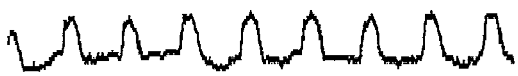

9. **Choppy** Pulse: A pulse coming and going choppily with small, finem slow, joggling tempo like scraping bamboo with knife, indicating sluggish blood circulation due to deficiency of blood or stagnation of blood.

10. **Knotted** Pulse: A slow pulse pausing at irregular intervals, often occurring in stagnation of blood.

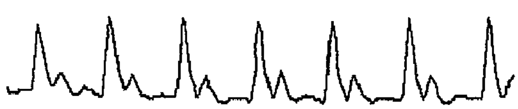

11. **Slippery** Pulse: A pulse like beads rolling on a plate, found in patients with phlegm-damp or food stagnation. A slippery and rapid pulse may indicate pregnancy.

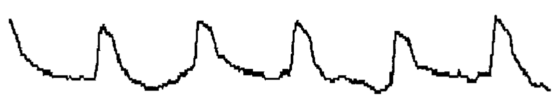

12. **Slow** Pulse: A pulse with reduced frequency, which is less than 60 beats per minute. Usually indicating endogenous cold.

Figure 1-19 Waveforms of 12 basic patterns in TCPD and brief explanations, reproduced from [26]

Although till now, in most clinical practises, the practitioners are still using their subjective judgement on classification and diagnosis of the pulse pattern and diseases, quantification of pulse recognition standard is one of the biggest trends in modern TCM researches [20][28].

1.3.3 Traditional Chinese Pulse Diagnosis and individual health care

Most of the individual monitoring systems available are targeting the collection of biological information from the human body. Aside from promptly reporting of real time biological signals, it is important for us to further examine the general health condition of the person. TCPD has its disadvantages due to the lack of experienced practitioners. Also, the patient is required to visit the doctor for diagnosis on a regular basis. It limits the number of patients that a doctor can take care of and further restricts the application of TCPD to general health care. The proposed idea, shown in figure 1-20, is to have a portable system that can collect the basic information from individuals for general TCPD assessment. In this way, the doctor can review a patient's general health condition remotely.

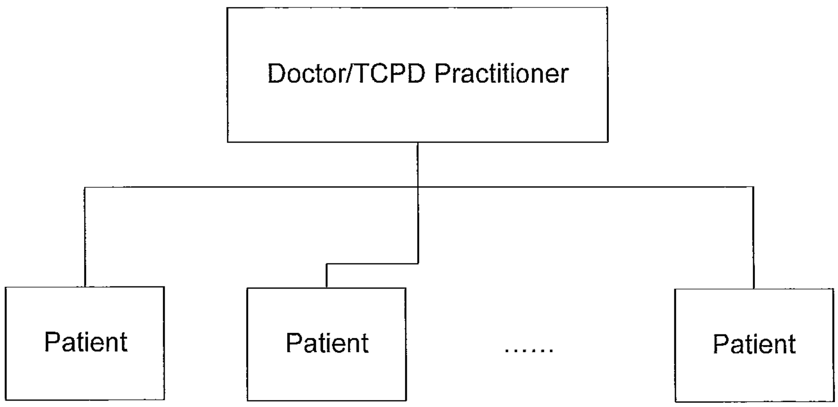

(a) Conventional TCPD diagnosing scheme

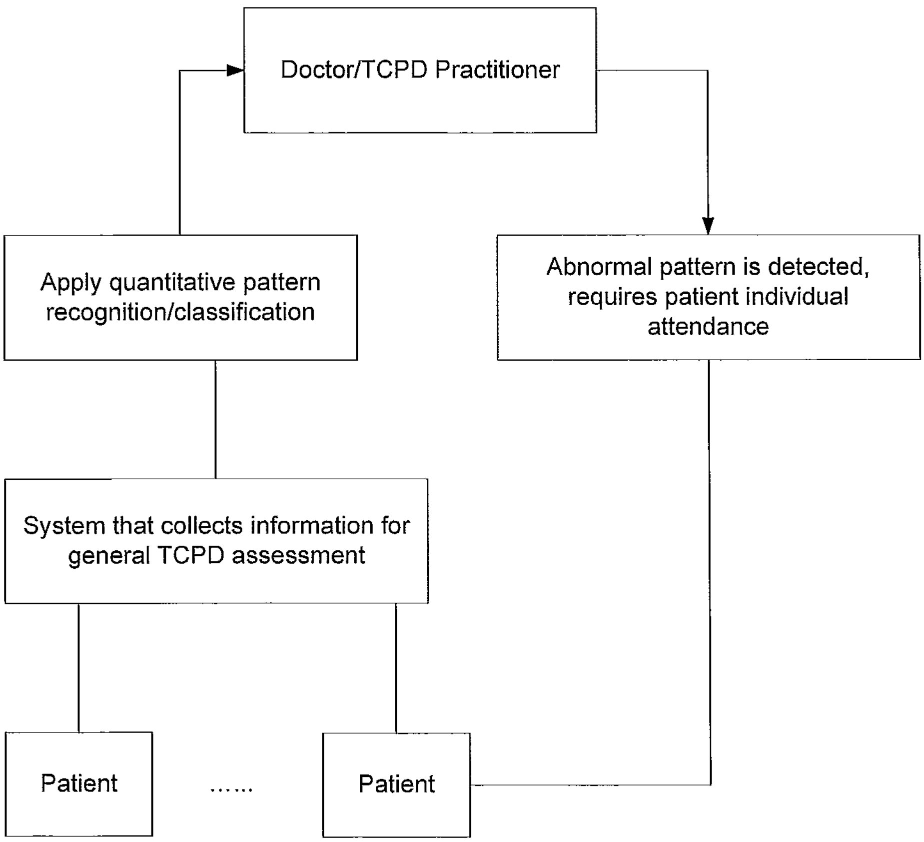

(b) Proposed system and scheme to assist TCPD diagnosing

Figure 1-20 Comparison between a. conventional TCPD diagnosing scheme and b. Proposed scheme in assisting TCPD diagnosing

The idea of the proposed scheme shown in figure 1-20 is to provide the doctor with the option of remote access to an individual's pulse waveforms, which would then allow each doctor to assess the general health condition of a larger population.

1.3.4 Proposed system in assisting TCPD diagnosis and individual home care

The objective of this work is to design a prototype system that non-invasively measures the biological signals from a human body and then wirelessly transmit the signals to a PC for analysis, for instance using TCPD. Through this work, we can further obtain insights on the usage of sensors, microcontroller and wireless transceiver in biomedical applications.

The system should have the following functions

- Measure the pressure non-invasively from radial artery
- Measure body temperature
- Digital processing, data saving and filtering
- Wireless data transmission to PC for data analysis
- Reconstruct and analyze the pulse waveform

1.4 Contribution

In this thesis, the design procedure, detailed implementation and real time measurement results from human radial artery are discussed. The data processing and analyses techniques are presented. Most of the system is built with off-the-shelf components to provide a cost effective solution.

1.5 Thesis Organization

This thesis is organized as follows. In Chapter 2, an introduction of body biological signals measurement techniques is given; and then a comprehensive study of several wrist-worn monitoring systems is presented. For each system, the detail functions and advantages/disadvantages are discussed. In Chapter 3, the design and implementation of the wireless sensor system with three pressure/temperature sensors used to record radial pulse wave for TCPD applications is presented. In Chapter 4, discussion of measurement results and waveform analysis are provided. In Chapter 5, a summary of this work and recommendations for further improvements in the wireless TCPD monitoring system are presented.

Chapter 2 Literature review

In this Chapter, the biological signals that can be measured from a human wrist are defined. Various techniques in acquiring these signals are discussed. Then, a detailed discussion of the existing wrist-worn monitoring system is presented in order to provide a solid background to understand the implementation of microelectronic systems in medicine. The overall performance of these systems is evaluated at the end of each section.

The objective of this review is first to provide a clear understanding of how and why certain biological signals are measured. The second objective is to provide a sound understanding of the concept, design, and implementation of wrist-worn monitoring systems. The third objective is to collect ideas on how to approach this kind of monitoring device and to provide cost effective solutions.

2.1 Biological signals from human wrist

The radial artery is one of the major arteries with oxygenated blood in a human forearm. It commences at the bifurcation of the brachia, just below the bend of the elbow, and passes along the radial side of the forearm to the wrist. It then winds backward, around the lateral side of the carpus, beneath the tendons of the Abductor pollicis longus and Extensores pollicis longus and brevis to the upper end of the space between the metacarpal bones of the thumb and index finger. Finally it passes forward between the two heads of the first Interosseous dorsalis, into the palm of the hand, where it crosses the metacarpal bones and at the ulnar side of the hand [29].

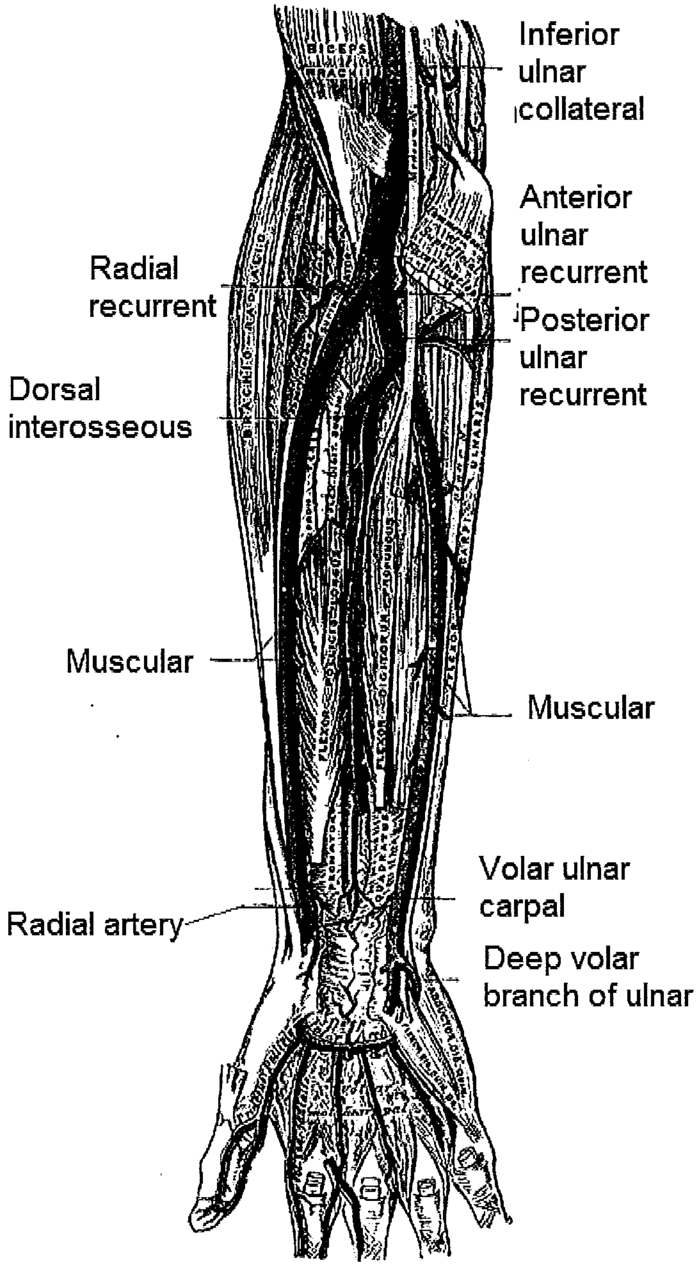

Figure 2-1 Arm anatomy, reproduced from [29]

From the anatomy of the radial artery, it can be observed that the radial artery meets the wrist on top of the radial bone which can act like a rigid support beneath the radial artery. This gives a big advantage in measuring the blood flow and pressure inside the artery. On the other hand, in Traditional Chinese Medicine, the wrist radial artery is recognized as a great important meeting-point of the blood vessels, and therefore can reflect conditions of certain organs [16].

One straightforward measurement from the wrist radial artery is the artery pressure. In addition to the artery pressure, the body surface temperature (BST) and blood oxygenation can also be obtained by non-invasive measurement techniques.

2.1.1 Blood Pressure and its measuring techniques

2.1.1.1 Blood Pressure

Blood pressure (BP) refers to the force exerted by circulating blood on the walls of a blood vessel (Figure 2-2). It constitutes one of the principle vital signs [30] and is a very important measurement result, especially in older people. If the blood pressure goes either too high or too low, then the human body could be in a dangerous condition.

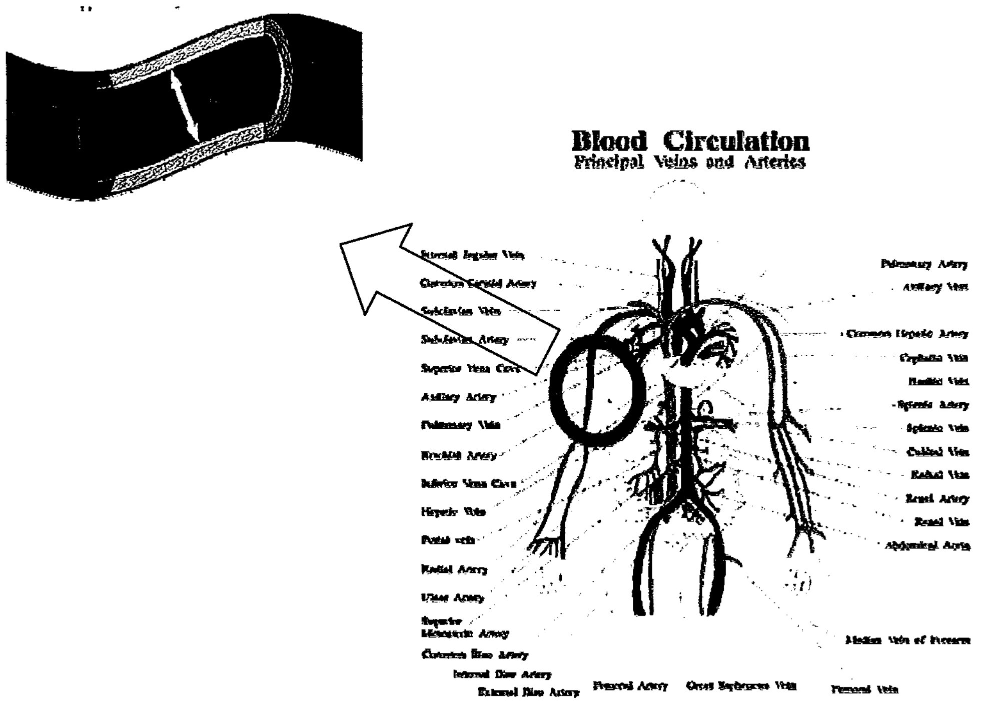

Figure 2-2 Blood pressure illustration [30]

When describing the blood pressure, there are two pressure values. One is systolic pressure and the other one is diastolic pressure. The systolic pressure refers to the peak pressure which occurring at the beginning of the cardiac cycle. The diastolic pressure refers to the pressure during the resting phase of the cardiac cycle. The optimal systolic pressure is less than 120 mmHg and the optimal diastolic pressure is less than 80 mmHg [31]. However the blood pressure is different for each person and even varies for the same person during the day. Excessively high pressure is considered as hypertension. The classification of the human blood pressure is given in Figure 2-3.

Category	*Systolic blood pressure (mmHg)*	*Diastolic blood pressure (mmHg)*
Optimal blood pressure	<120	<80
Normal blood pressure	<130	<85
High-normal blood pressure	130–139	85–89
Grade 1 hypertension (mild)	140–159	90–99
Grade 2 hypertension (moderate)	160–179	100–109
Grade 3 hypertension (severe)	≥180	≥110
Isolated systolic hypertension (Grade 1)	140–159	<90
Isolated systolic hypertension (Grade 2)	≥160	<90

This classification equates with that of the ESH[50] and that of WHO/ ISH,[52] and is based on clinic blood pressure values. If systolic blood pressure and diastolic blood pressure fall into different categories, the higher value should be taken for classification.

Figure 2-3 British Hypertension Society classification of blood pressure levels [31]

2.1.1.2 Blood pressure measurement techniques

The current techniques in obtaining blood pressure (BP) measurements can be classified into two categories: invasive and non-invasive. Invasive BP measurement is the most accurate method to determine BP [30]. It is commonly done, in a hospital, by an anaesthesiologist or a surgeon placing a catheter into the artery. Figure 2-4 demonstrates the procedure.

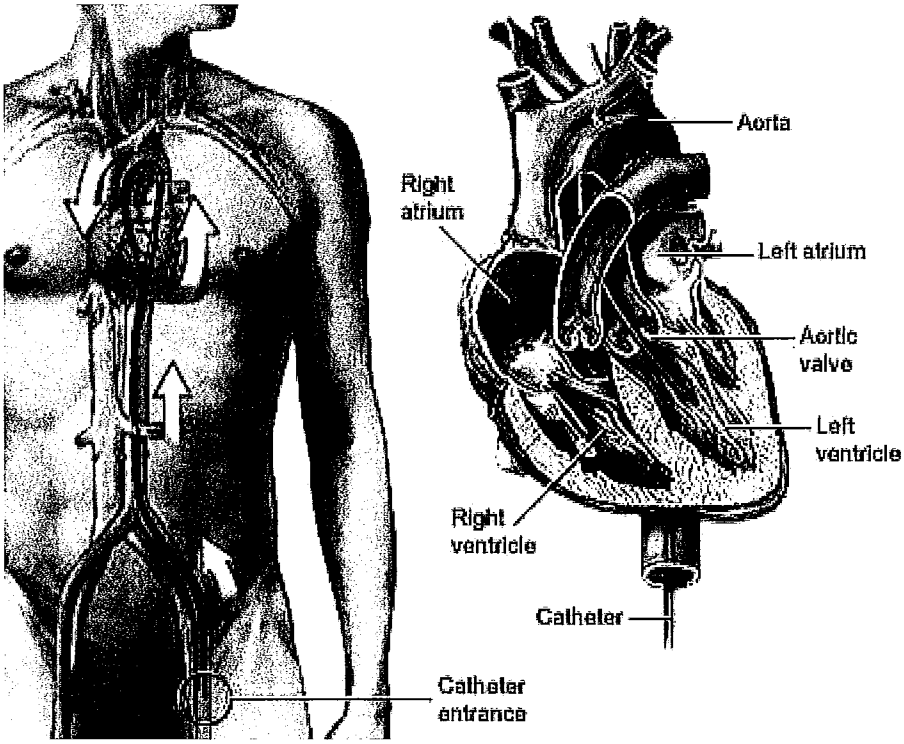

Figure 2-4 Cardiac catheterization [32]

Although invasive arterial blood pressure measurement with intravascular catheter is considered as the most accurate method, it is difficult and uncomfortable to apply in a real time monitoring system. However, in ambulatory monitoring, when the high accuracy is not required, the patient would rather choose system that is easy to implement and comfortable to wear. Therefore, in this section we will focus on the non-invasive measurement techniques that could possibly be employed in ambulatory blood pressure monitoring.

2.1.1.3 Oscillometric method

This is probably the most common method in measuring blood pressure. It requires an inflated cuff around the wrist, an air pump and sensors. The working principle is similar to the traditional auscultatory method [30], except that the doctor's ear is replaced with electronic sensors.

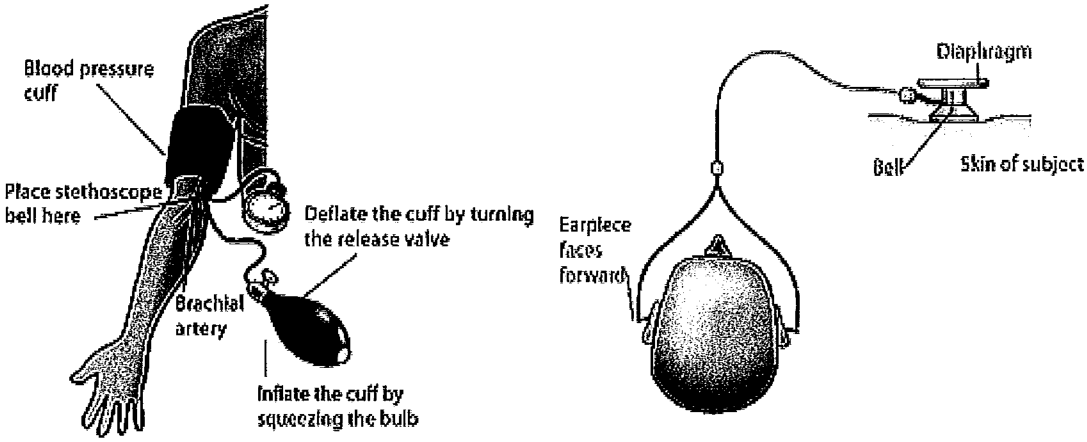

Figure 2-5 Auscultatory method measures blood pressure [33]

The theory of measurement can be explained as the following. A inflatable cuff is wrapped around your upper arm and kept in place. A tube leads out of the cuff to a rubber bulb. Another tube leads from the cuff to the reservoir of a pressure measurement unit. Then, the pressure in the cuff is shown on the pressure measurement unit. Air is then blown into the cuff and increasing pressure and tightening is felt on the upper arm. The doctor puts a stethoscope to your arm and listens to the sound while the air is slowly let out again. The sound is called Korotkoff sound which is named after the Russian doctor and scientist Nikolai S. Korotkoff [34], it first occurs at the point where the cuff pressure equals to the systolic pressure. This sound will slowly become more distant and finally disappear and this is when the diastolic pressure is measured [35].

2.1.1.4 Applanation tonometry

Applanation tonometry is the method used by Goldmann and Perkins tonometers. It infers the intraocular pressure from the force required to flatten (applanate) a constant area of the cornea [36]. In the application of blood pressure measurement, it refers to the use of an externally applied micromanometer-tipped probe to continuously record peripheral pulse waveforms [37], [38]. Accurate recording with this method requires that the vessel wall be flattened by the probe so that the transmural forces are perpendicular to the arterial surface [39]. There are studies that have shown that reasonable estimates of central aortic pressure waveforms can be obtained by tonometry from the carotid artery [40], [41]. This technique is suboptimal. However, because the artery is surrounded by loose tissue, it is difficult to ascertain and consistently achieve optimal applanation [41].

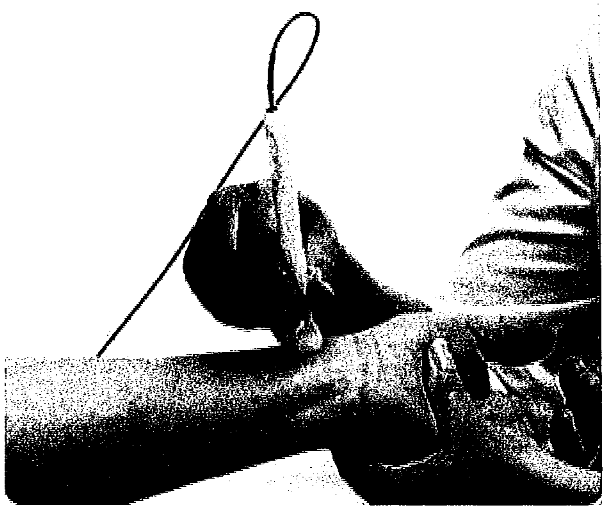

Figure 2-6 Radial artery tonometer [23]

In contrast to the carotid artery, the radial artery is very accessible and well supported by bony tissue, making optimal applanation easier to achieve. The main disadvantage of using the radial pulse is that the pressure contour changes appreciably as it travels from the aorta to more peripheral sites, so that radial pressures cannot be used directly as a surrogate for central aortic pressure [42]. However, it may be possible to estimate the central aortic pressure wave from radial tonometry data with the use of mathematical transformation as proposed by Karamanoglu et al [43] by using a single group-averaged transfer function (TF) to reconstruct aortic pressures.

The ARX (AutoRegressive-eXogenous) linear parametric model [44] has been proposed by Chen CH [40] to estimate the blood pressure. The expressions for radial tonometer discrete measurement T and aortic pressure P are

$$T(t) = -a_1T(t-1) - a_2T(t-2) - ... - a_{na}T(t-nb) + -b_1P(t-1) + b_{nb}P(t-nb) \quad (2\text{-}1)$$

$$P(t-1) = -\frac{b_2}{b_1}P(t-2) - ... - \frac{b_{nb}}{b_1}P(t-nb) + \frac{1}{b_1}T(t) + \frac{a_1}{b_1}T(t-1) + ... + \frac{a_{na}}{b_1}T(t-na) \quad (2\text{-}2)$$

where $T(t)$ and $T(t-I)$ $[I = 1,2..]$ are outputs representing the present and previous radial tonometer discrete measurements; and $P(t-I)$ is the previous input (aortic pressure) discrete measurement. The "*a, b*'s" are the parameters to be estimated using the model. Equation (2-1) is the transfer function and to obtain aortic pressure from the tonometer measurement; the inverse transfer function is given by equation (2-2). The study [40] suggested that the minimal order of this transfer function, in order to achieve a similar spectral estimate as given by nonparametric methodology (Fourier transformation) during the steady state, is 5; which means five pairs of (*a, b*) coefficients.

2.1.2 Heart Rate

Heart rate (HR) is very basic, but at the same time, an important biological signal. The common method used is Electrocardiogram (ECG). The measurement requires each hand to touch one of the two electrodes in order to obtain the HR reading. One novel method uses the change of infra-red (IR) reflection caused by wrist artery change due to pulse added volume, to estimate the HR.

The concept is that the emitter emits an optical IR signal at the surface of the body tissue, this signal is then to be reflected, refracted and absorbed by body tissues. And then sensor or multiple sensors are located at a distance about 10 mm to detect the signal.Under ideal steady-state condition, the received signal contains both a constant and a time varying component. The constant component is generally due to baseline absorption of blood, soft tissue, bone and reflection/refraction/scattering losses. The varying component relies on the expansion of the tissue due to varying blood pressure [45].

2.1.3 Body surface temperature

To measure body temperature, the most straight forward way is to use a thermometer. One alternate technique can be applied to measure body surface temperature is a temperature integrated circuit (IC). Temperature IC has the advantages of small size, low power consumption and easy integration with other microelectronic devices.

2.1.4 Blood oxygenation

Oxygenation refers to the amount of oxygen in a medium. In blood, it may be taken to be synonymous with saturation, which describes the degree to which the oxygen-carrying capacity of hemoglobin is utilized, normally 98-100% [46].

The blood oxygenation level can be measured directly by examining the patient's blood. An alternate non-invasive method to measure the blood oxygen level is with Pulse oximetry. A sensor is placed on a thin part of the patient's anatomy, usually a fingertip or earlobe, or in the case of a neonate, across a foot; then red and infrared light is passed from one side to the other. The difference in absorbance of each of the two wavelengths is measured, allowing determination due to the pulsing arterial blood alone, excluding venous blood, skin, bone, muscle, fat, and (in most cases) fingernail polish. Based upon the ratio of changing absorbance of the red and infrared light caused by the difference in color between oxygen-bound (bright red) and oxygen unbound (dark red or blue, in severe cases) blood hemoglobin, a measure of oxygenation (the per cent of hemoglobin molecules bound with oxygen molecules) can be made [47].

2.2 Quantitative scheme for Traditional Chinese Pulse Diagnosis

As mentioned in the introduction chapter, Traditional Chinese Pulse Diagnosis judges disease by means of palpation of the radial pulse from Cun, Guan, Chi, respectively. The diagnosis is done by an experienced doctor and it heavily relies on the subjective judgement of the doctor. Many researchers have been working to establish a global quantitative standard of pulse diagnosis. The quantification scheme proposed by Jian-Jun Shu [26] can be used as a reference in pulse classification.

The pulse waveform in human radial artery is the net effect of a forward incident wave and a backward reflected wave that is reflected by the end of the limb. In this research [26], the pulse is described numerically by the summation of two Gamma density functions.

$$F(t \mid \alpha, \beta, \Delta, A, B) = Af(t \mid \alpha, \beta, 0) + Bf(t \mid \alpha, \beta, \Delta) \tag{2-3}$$

where $f(t \mid \alpha, \beta, \Delta) = (t-\Delta)^{\alpha} e^{-\beta(t-\Delta)/10},\ t \geq \Delta$ (2-4)

Therefore, $F(t \mid \alpha, \beta, \Delta, A, B) = At^{\alpha} e^{-\beta t/10} + B(t-\Delta)^{\alpha} e^{-\beta(t-\Delta)/10}$ [26] (2-5)

$F(t \mid \alpha, \beta, \Delta, A, B)$ represents the net waveform. $Af(t \mid \alpha, \beta, 0)$ is the incident forward wave and $Bf(t \mid \alpha, \beta, \Delta)$ represents the backward reflected wave. The parameters A and B are amplitude of incident and reflected waves, respectively. Δ is the phase shift between two waves, or its time delay. Patterns can be classified into thirteen general patterns; and each of them is given nine indices [26]. With the use of the indices, the typical pulse waveforms can be generated by computer.

2.3 Existing home monitoring devices

2.3.1 Wrist-worn integrated health monitoring device with tele-reporting [48]

This system [48] integrates several functions in one device. Its functions includes the Fall Detection, Heart Rate estimation, Blood Pressure measurement, estimation of Blood Oxygenation level, estimation of Respiration Rate, measurement of Body Surface Temperature and Communication through cell phones. The system employs several microelectronic technologies that are used for portable wireless systems. The device overview is given in the following figures (Figure 2-7and Figure 2-8).

Figure 2-7 System overview [48].

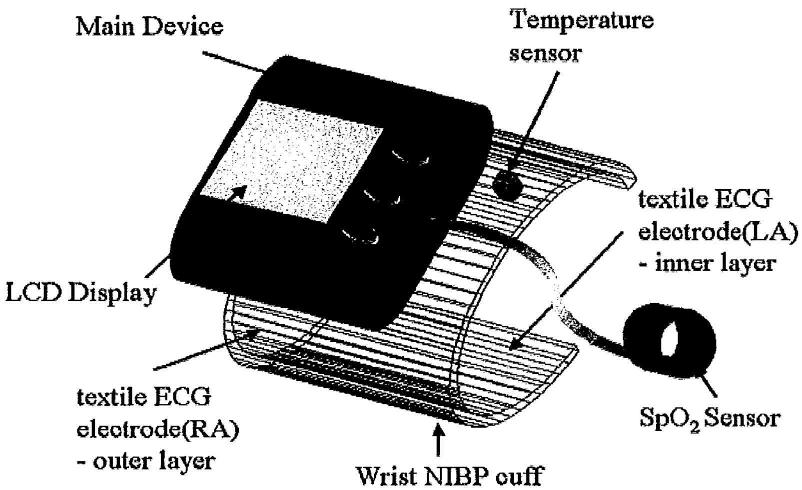

Figure 2-8 Schematic drawing of the wrist-worn integrated health monitoring device with tele-reporting [48]

The system consists of components as shown in Figure 2-9. A data acquisition board (DAQ board) that receives the multi channel inputs from the fall detector, pulse Sp02 sensor (blood oxygenation detector), ECG monitor, blood pressure sensor cuff, and temperature sensor are integrated in the system. The measurement data is transmitted to PC for analysis or wirelessly to a cell phone for emergency alert.

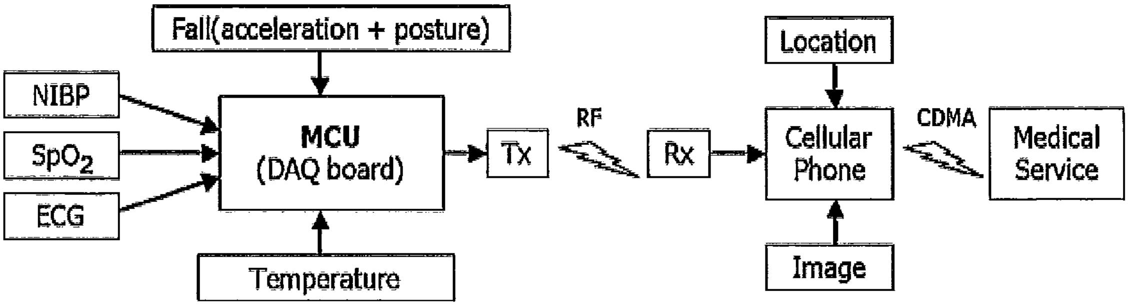

Figure 2-9 Block diagram for the Wrist-worn integrated health monitoring device with tele-reporting [48].

In this system, the non-invasive blood pressure measurement is done by employing the Oscillometric method. A wrist cuff is used to surround the wrist; it contains a motor, a pump and a solenoid valve. During the measurement, the cuff will inflate to tighten the radial artery. Then the procedure is the same as the measurement taken on the brachial artery. For each measurement, the cuff will be first inflated, and then deflated, and the whole process is powered from a battery. The blood oxygenation measurement is done with an oximeter. A model 8000H oximeter manufactured by NONIN, USA is integrated. Heart rate is measured through Single Channel Electrocardiogram. There is an inner electrode and an outer electrode, the inner electrode is attached to left cuff and, to obtain heart rate measurement, the right hand should touch the outer layer. The body surface temperature is measured using IC temperature sensor model TC1047 from Microchips, USA.

The fall detector in this system integrates an accelerometer to detect the acceleration and a gyroscope to detect the orientation of the device. The detection algorithm is illustrated below (Figure 2-10).

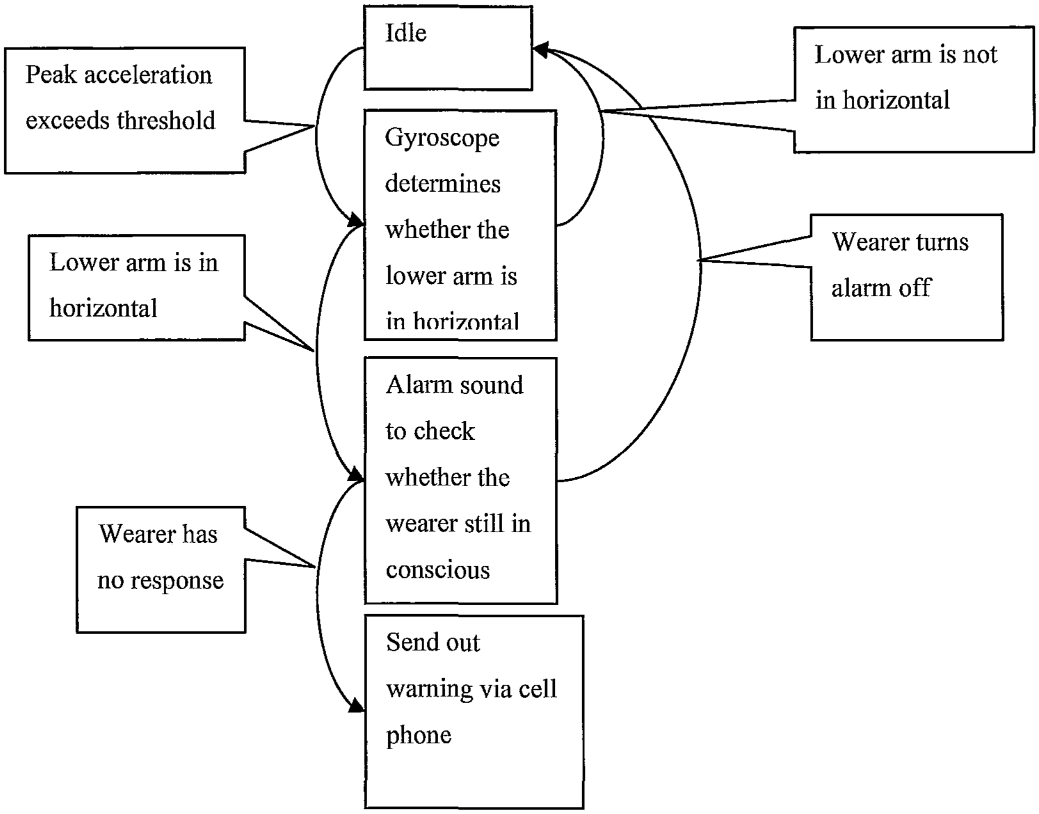

Figure 2-10 Fall detection algorithm for wrist-worn integrated health monitoring device with tele-reporting

Tele-reporting in this system uses RF-transceiver manufactured by LINX tech, USA. TXM-LC (transmitter module) and RXM-LC (receiver module) operating at 433 MHz, 10mW, FM.) and cellular phone for short and long range transmission. The RXM-LC is connected to a cellular phone (IM-3000 SK Teletech, Korea) via RS-232 connection with 38400-Baud rate [48].

2.3.1.1 Performance overview

The overall size of the device is 60 × 50 × 20 mm^3, excluding the wrist cuff. The system requires two 1.5V AAA-sized batteries; but the battery life was not studied. The user interface is shown in Figure 2-11 and Figure 2-12. It includes data displaying for the ECG waveform, SpO2 concentration display, blood pressure reading and data logging.

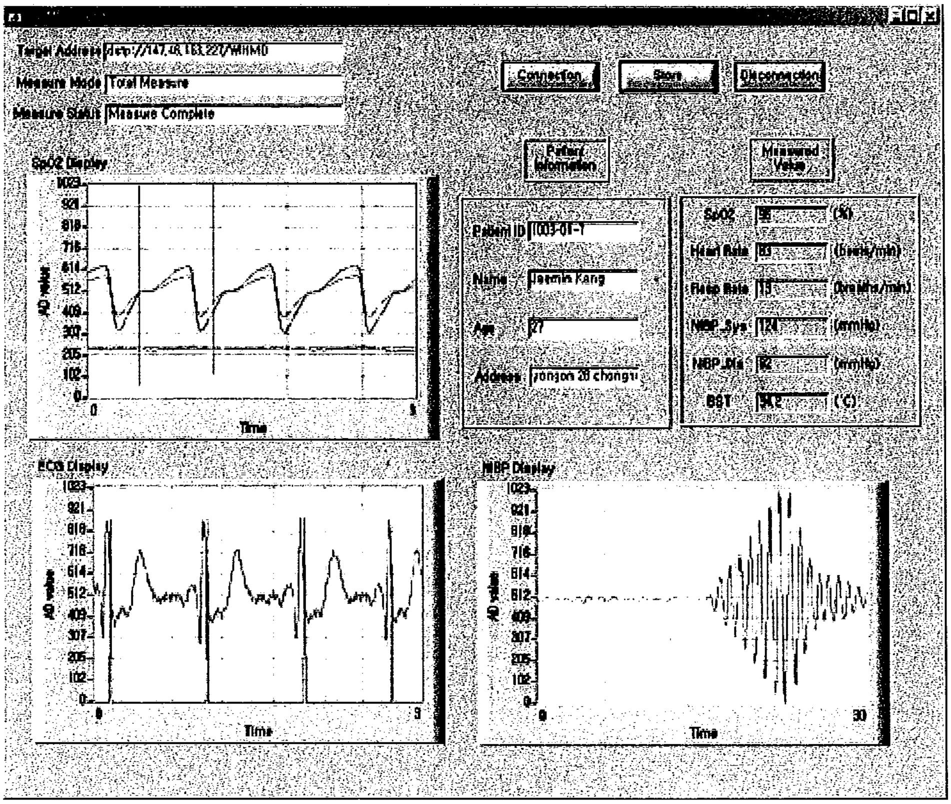

Figure 2-11 Data acquisition program for the performance evaluation test [48].

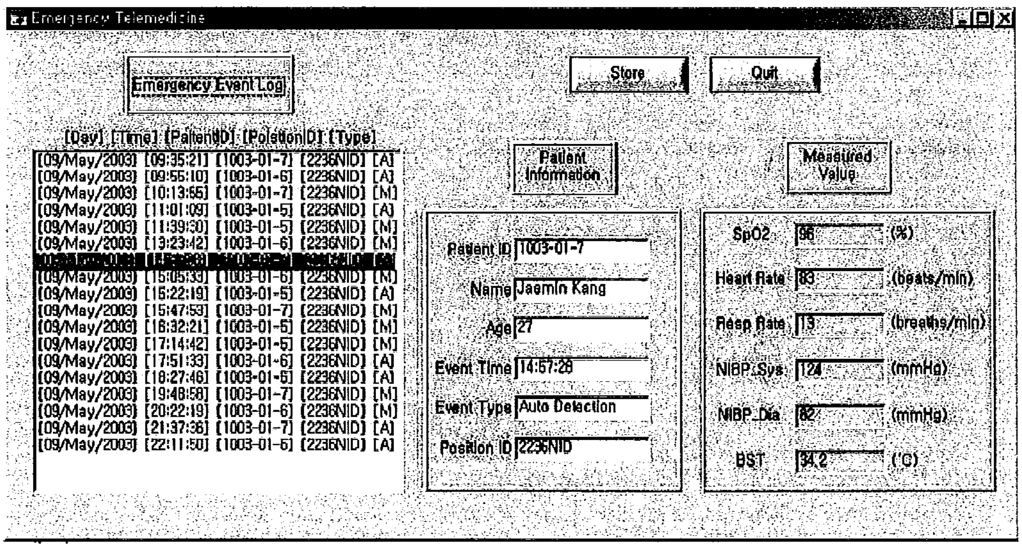

Figure 2-12 Example for tele-reporting interface [48].

The performance of the device is summarized in the table below (Figure 2-13). The results for ECG respiration rate and fall are from human trials. Blood pressure, SpO2, and ECG heart rate are from simulator. The body surface temperature measurement is from test set-up.

	NIBP	SpO2	ECG(Heart Rate)	ECG(Respiration Rate)	BST	Fall
Evaluation Method	simulator	simulator	simulator	Human trial	Test set-up	Human trial
	BPPump2M, Bio_tek,USA	Oxitest plus7, DNI Nevada Inc, USA	PS214B, DNI Nevada Inc, USA	WebDoc Spiro™, Elbio Inc, Korea	temperature-controlled chamber	150 simulated cases
Operation Range	40-270mmHg	80-99%	40-240 BPM	8-18 Breaths/min	25-40 °C	normal fall
Number of tests	100	100	100	50	20	150
Performance parameter	Error range	Error range	mean % error	mean % error	mean % error	Detection rate
	Within ±5mmHg	Within ±2 %	1%	1.8%	1.5%	91.3%

Figure 2-13 Performance summary [48].

2.3.2 Wrist-located pulse detection using IR reflection due to pulse added volume of arterial blood [49]

This prototype employs a novel radial pulse detecting method without physical contact of the radial artery.

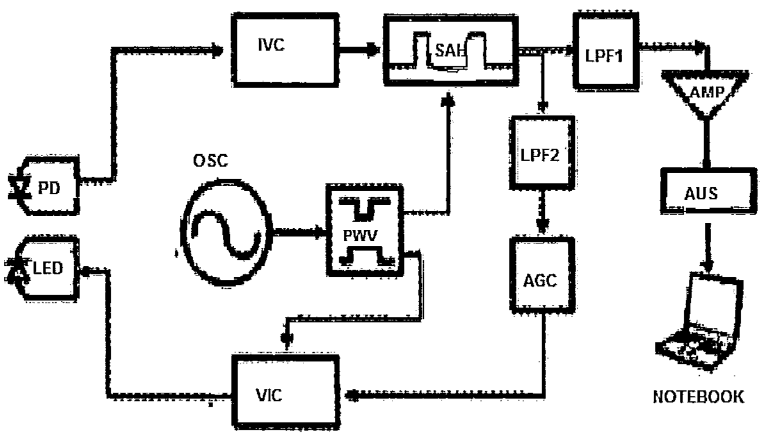

Figure 2-14 Block diagram of the aBVP detection system, reproduced from [49]. SAH: sample and hold, PWV: pulse width variation.

This system consists of an optical sensor and a detector. An infra red LED is placed near the radial artery and radiates at 900nm wavelength. At a distance 10mm away, a photodiode detects the reflected signal from tissues such as arterial blood vessel, venous blood, capillaries, muscle, and skin. Due to the blood volume change in the radial artery caused by heart beating, the pulse duration can be derived from the measurement of the reflected signal. The comparison in Figure 2-15 is the ECG measurement and the measurement from the prototype. It shows that the pulse measured by IR reflection on the radial artery can be used as an estimation of HR based on the ECG measurement.

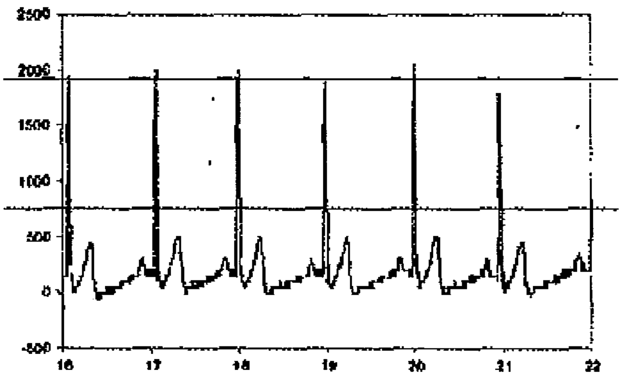

a. Waveform from ECG

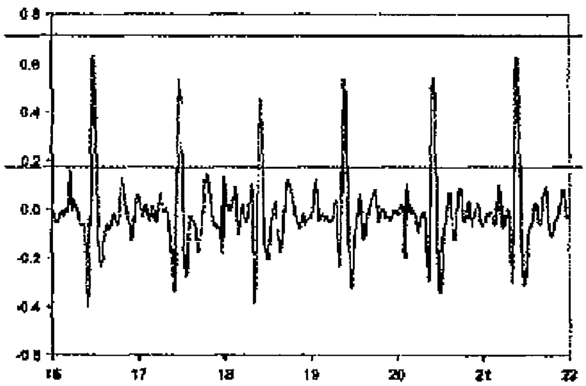

b. Waveform from the prototype

Figure 2-15 Comparison of the ECG waveform and the prototype waveform [49]

2.4 Chapter summary

This chapter showed that the various biological signals can be obtained from the wrist and their acquisition techniques are discussed, along with the potential application of Traditional Chinese Pulse Diagnosis in ambulatory monitoring. The techniques can be concluded in the following table.

Blood pressure	**Oscillometric** **Tonometry** **Implantation**
Blood oxygen level	**Pulse oximetry**
Heart rate	**ECG** **IR reflection** **Tonometry**
Body surface temperature	**IC type temperature sensor**
Fall detection	**User-activated fall alarms** **Automatic wearable fall detector** **Camera based detection** **Floor vibration detection**

Figure 2-16 Table of measurement techniques summary

The current application of TCPD mainly relies on the experience of doctors and practitioners in clinics and hospitals. The global trend for TCPD is to set up a quantitative acquisition and diagnosis scheme. The quantitative scheme proposed in the literature review can be used as a reference in assisting the doctor's diagnosis. The key requirements for home monitoring devices are

- Keep a history of the measurement.
- Provide basic analysis of pulse pattern.
- Make the whole system as a tool of the doctor. Provide the measurement which is readable to the doctor and let the doctor judge the health condition.

As mentioned in Chapter 1, the home monitoring devices can be categorized into three types which are stationary home monitoring devices, body implantable devices and non-invasive device that measures biological signals. Each of them has its own advantages and disadvantages. In this chapter, the implementation and performance of each type of technique are discussed. The purpose is to provide the reader with a brief overview of home monitoring devices that are available, and also to study the implementation of such devices

Chapter 3 Implementation of the sensor system

The goal of this research is to design a portable sensor system which can simultaneously capture pulse waveforms at Cun, Guan, Chi, the body surface temperature and then wirelessly transmit the measurements to a personal computer (PC). The measurements will be logged in the PC and data analyses will be carried out. The analysis is based on the methods described in Traditional Chinese Pulse Diagnosis (TCPD) towards the preliminary approach to the expert system. The TCPD data can be analyzed offline using pulse classification indices, or sent to experienced physicians for further analyses.

3.1 Components selection

To achieve the desired functions of the portable sensor system, the selection of suitable components is very important. In this section, we compare several approaches by choosing different components, and state reasons why the selected components are chosen. The components will be classified into three categories - measurement units (sensor), process/control units (microcontroller) and communication units (wireless transceiver).

3.1.1. Pressure sensor

The signals to be measured are both pulse strength and pulse waveform from Cun, Guan, and Chi. The human blood pressure is normally ranged from 80~120 mmHg (1.55~2.32Psi), with a resting heart rate between 60 and 100 beats per minute (bpm) [50]. Suitable choices for pressure sensors must consider their response over a low range of force or pressures sensor with adequate ranges of electrical output. Given the size and measuring range in this design, there are three types of sensors we can choose. They are load cell, piezoresistive force or piezoresistive pressure sensors.

3.1.1.1 Load cell

A load cell is an electrical transducer that is used to convert a force into an electrical signal. This conversion is indirect and happens in two stages. Through a mechanical arrangement, the force being sensed deforms a strain gauge (alternatively: strain gage). The resistance strain gauge most commonly consists of an insulating backing which supports metallic foil pattern [51]. The word "strain" is the deformation of the solid material due to applied force. The foil is deformed and therefore results the changes in its electrical resistance [52]. The resistance change is amplified and measured by using a Wheatstone bridge. An example of a sub-miniature load cell is shown in Figure 3-1. In Figure 3-2, the strain gauge and Wheatstone bridge are shown.

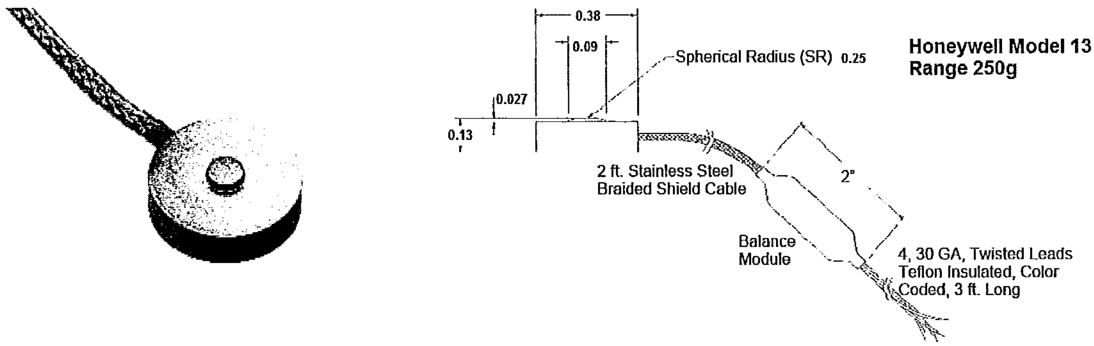

Figure 3-1 Sub-miniature load cell [51]

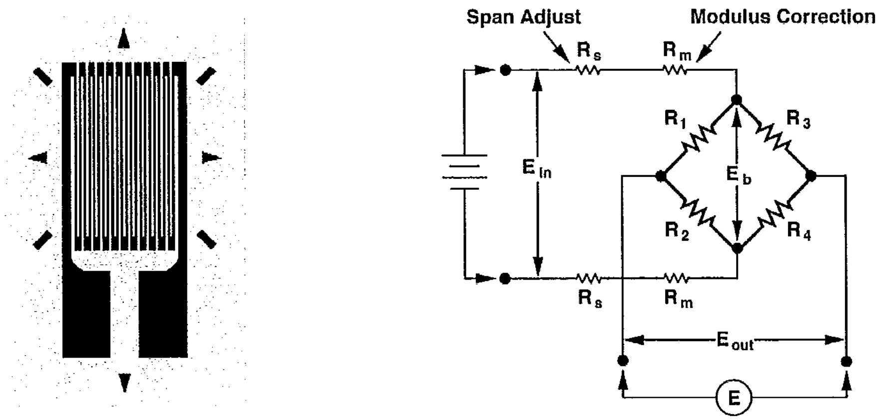

(a) (b)

Figure 3-2 Circuit used in load cells. a. Strain gauge [53] (varies its resistance as a linear function of the strain). b. Wheatstone bridge used in most load cells [54].

However, one important disadvantage of using a load cell for our portable sensor system is that the placement of the load cell will create an off-axis loading problem.

The force exert by the blood vessel will always be perpendicular to the vessel wall, but the mechanical deformation of the load cell is along its axis. Therefore, the placement angle which is between the axis of the load cell and the surface of the skin will affect the force being measured. This is schematically shown in Figure 3-2.

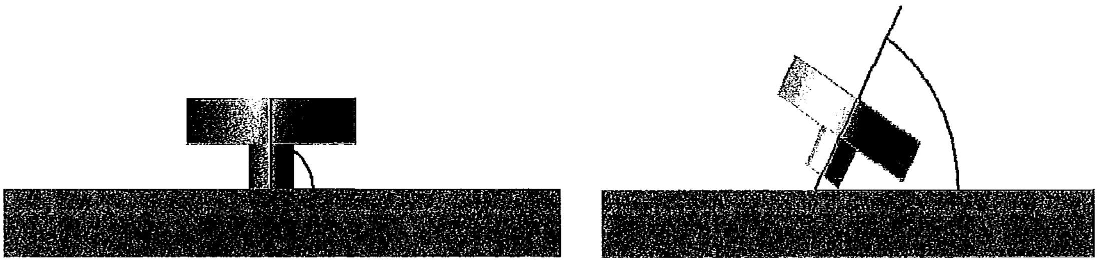

(a) (b)

Figure 3-3 Possible placement of the load cell between skin surface. (a) Perpendicular and (b) Non-perpendicular to the skin's surface. Note the different angles.

3.1.1.2 Piezoresistive force sensor

Another approach is to use a piezoresistive force sensor. Piezoresistive force sensors are devices that use the piezoresistive effect to measure pressure, acceleration, strain or force by converting the sensed signal into an electrical signal [55]. The piezoresistive sensor shown in Figure 3.4 is made by Tekscan [56]. The force sensor is an ultra-thin, flexible, printed circuit. The force sensor is constructed of two layers of the substrate (polyester/polyimide) film. On each layer, a conductive material (silver) is applied, followed by a layer of pressure-sensitive ink. An adhesive is then used to laminate the two layers of the substrate together, thus forming the force sensor. The active sensing area is defined by the silver circle on top of the pressure-sensitive ink. Silver extends from the sensing area to the connectors at the other end of the sensor, forming the conductive leads [56].

Compared to the load cell, the piezoresistive force sensor has more compact design and relatively high accuracy, but a low linearity. Although the sensor is made flat, which has no off-axis loading problem, given the anatomy of the wrist, we may find it is difficult to mount the sensor to create a firm contact between the sensor surface and the radial pulse.

(a) FlexiForce A201 piezoresistive force sensor

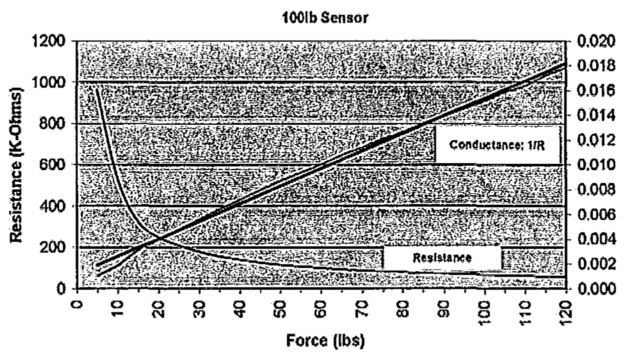

(b) Sensor response, resistance vs. force

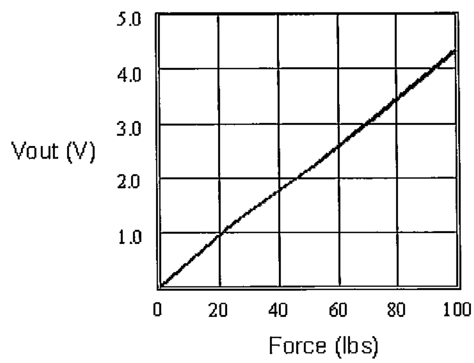

(c) Sensor response, voltage vs. force

Figure 3-4 Tekscan FlexiForce A201 piezoresistive force sensor [56].

A magnetic resonance image (MRI) of the left wrist's cross section is given in Figure 3-5. The view in the figure is looking from the elbow towards hand. As shown, the radial artery we are measuring is surrounded by the radial bone from below and the longus Palmaris tendon from the upper right. When we are performing the measurement, the radial artery has to be pushed against the radial bone in order to record the pulse. This is hard to do with flat surface sensor because to the radial artery is half hidden under the longus Palmaris tendon.

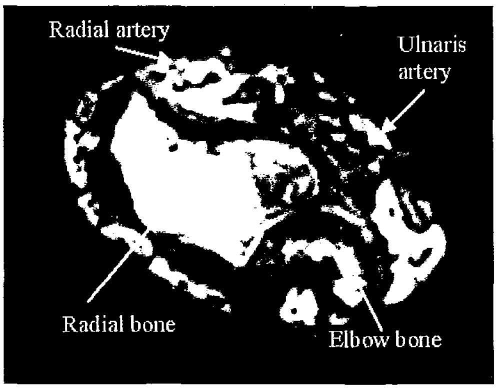

Figure 3-5 MRI of left wrist's cross-section [57]

To find a suitable sensor, we recall how a doctor uses their finger tips to palpate the pulse. Thus, we should find a sensor which has a round sensing surface just like the finger tip. With such a sensor, we should be able to create a rigid contact between radial artery pulse and the sensor. However, it was difficult to find an off-the-shelf sensor with the shape of a finger tip. Therefore, we customized our sensor based on existing off-the-shelf ones.

3.1.1.3 Piezoresistive pressure sensor

The sensor we use is the *MS5536C* (see Figure 3-6), a packaged piezoresistive digital pressure sensor manufactured by Itersema [58], a company specializing in measurement devices. This type of pressure sensor is a gage sensor, having a pressure range from -400mbar ~1000mbar (-5.8Psi ~ 14.5Psi or -300mmHg ~ 750mmHg) with 0.1mbar resolution [58]. There are two major reasons why this sensor was selected - small size and added capability of measuring temperature.

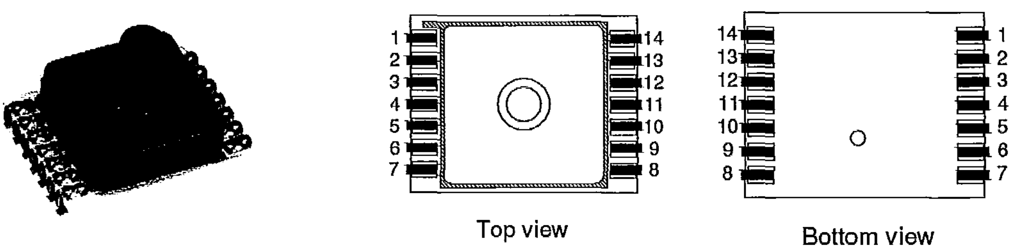

(a) (b)

Figure 3-6 Digital pressure sensor Intersema MS5536C (a) Pressure sensor and (b) Top and bottom views of the pin layout [58]

This device includes a piezoresistive sensor and an internal analog-to-digital converter (ADC). The communication is done by 3-wire serial interface (SPI). Digital pressure and temperature information is sent as 16-bit data word. In addition, 64-bits of individually calibrated compensation coefficients are stored, allowing for software compensation of process spread and temperature effects [58]. Also, the sensor operates with 3V, as compared to most other sensors which require 5V. The detailed customization is described in the Hardware design section.

The pin description of the pressure sensor is provided in the table below.

PIN DESCRIPTION

Pin Name	Pin	Type	Function
N/C	1		Not Connected
VDD	2	P	Positive Supply Voltage
MCLK	3	I	Master Clock (32.768kHz)
DIN	4	I	Data Input
DOUT	5	O	Data Output
SCLK	6	I	Serial Data Clock
GND	7	G	Ground
N/C	8		Not Connected
N/C	9		Not Connected
N/C	10		Not Connected
N/C	11		Not Connected
N/C	12		Not Connected
PV	13	N	Negative Programming Voltage
PEN	14	I	Programming Enable

Figure 3-7 MS5536C pin description [58]

3.1.2. Microcontroller

The data output from the sensors can be either analog or digital. If it is analog, then we need to convert it into digital form for further processing. There are three sensors that simultaneously capture the pulse pressure. All measurements are to be first saved in the system, and then transferred to a PC for offline storage and analysis. Therefore, the processing/control units should have A/D conversion, storage and communication module(s). Based on these criteria, microcontrollers would be a very suitable choice.

There is a wide selection of microcontrollers available, and many of them meet our requirements. We selected the *AVR Atmega8L* which is manufactured by Atmel. The *Atmega8L* is a high-performance, low-power, RISC (Reduced Instruction Set

Computer) architecture *AVR* 8-bit microcontroller. The block diagram below shows the architecture of the microcontroller. *Atmega8L* has two 8-bit timers/counters and a 16-bit timer/counter, a programmable USART interface, and a SPI (three-wire) interface. The memory is 8kBytes of in-system self-programmable Flash memory, 512 Bytes EEPROM and 1kByte internal SRAM. It is available in PDIP, TQFP or MLF packages.

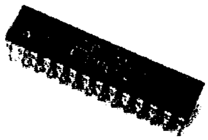

(a) 28PDIP

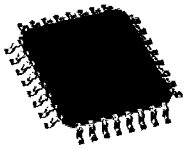

(b) 32TQFP

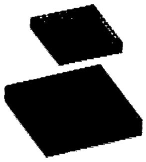

(c) 32MLF

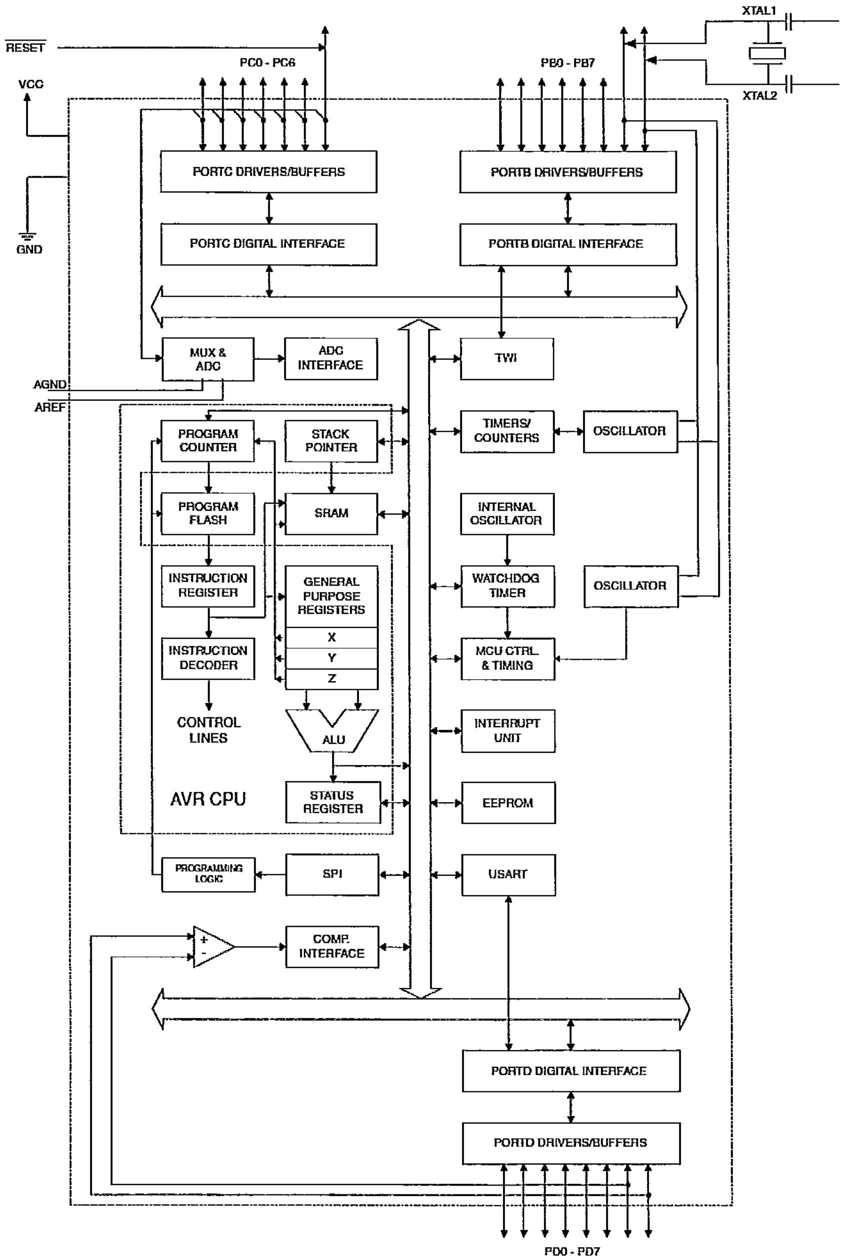

(d) Block diagram

Figure 3-8 AVR Atmega8L (a) in PDIP package; (b) in a TQFP package; (c) in a MLF package; and (d), its block diagram [59]

3.1.3. Wireless transceiver

3.1.3.1 Protocol

To pick suitable components, we first need to understand the wireless application of our design. The information to be sent wirelessly from the microcontroller to the PC is the pressure and temperature data from the sensor. The data is in the form of 8-bit packets, sent via USART to PC COM port. Under normal circumstances, the microcontroller will be operating at a frequency of 2MHz, giving us a maximum transmission baud rate of 250kBps [59]. However, to reduce transmission error, the signal rate will be limited to less than 28.8kBps [59]. Other than the data to be transmitted, we also need to take the transmission range into consideration. If we are to design a system that communicates with a wireless receiver attached to a PC or another device at home, 50m should be enough distance.

Now, let us examine what technologies are available to us. Common wireless options are Bluetooth (IEEE 802.15.1), Ultra Wideband (IEEE 802.15.3a), ZigBee (IEEE 802.15.4) and Wi-Fi (IEEE 802.11a/b/g). Each of them is targeting different applications. The figure below shows the wireless landscape [61].

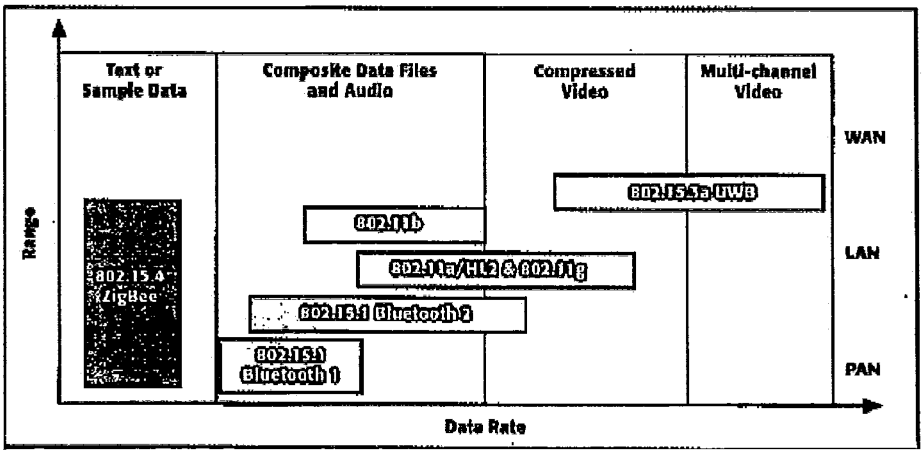

Figure 3-9 Wireless landscape [61]

The Bluetooth standard is based on a wireless radio system designed for short-range and cheap devices to replace cables for computer peripherals. This range of applications is known as wireless personal area network (WPAN). Bluetooth uses

2.4GHz frequency band and supports a maximum signal rate of 1MBps. The nominal range for a Bluetooth device is 10m [62].

UWB has recently attracted much attention as an indoor short-range, high-speed wireless communication system [63]. The huge bandwidth (3.1-10.6GHz) and high speed (up to 110MBps) can satisfy most of multimedia applications [61].

ZigBee is defined for low-rate WPAN (LR-WPAN) for supporting simple devices that consume minimal power and typically operate in the personal operating space (POS) of 10m. ZigBee provides self-organized, multi-hop, and reliable mesh networking with long battery life [64], [65]. Its operating frequencies are 868/915MHz, 2.4GHz and it supports a maximum signal rate of 250kBps with a nominal transmission range of under 100m [61].

Wireless fidelity (Wi-Fi) is especially for wireless local area networks (WLAN). It allows users to access the internet at broadband speeds. It operates at 2.4GHz or 5GHz frequency, with a maximum signal rate of 54MBps and its transmission range is up to 100m [61]. The two tables below compares the performance of the 4 systems.

Standard	Bluetooth	UWB	ZigBee	Wi-Fi
IEEE spec	802.15.1	802.15.3a	802.15.4	802.11a/b/g
Frequency band	2.4 GHz	3.1-10.6 GHz	868/915 MHz; 2.4 GHz	2.4 GHz; 5GHz
Max signal rate	1 Mb/s	110 Mb/s	250Kb/s	54 Mb/s
Nominal range	10 m	10 m	10-100 m	100 m
Nominal TX power	0 – 10 dBm	-41.3 dBm/MHz	(-25) – 0 dBm	15 – 20 dBm
Number of RF channels	79	(1 – 15)	1/10; 16	14 (2.4 GHz)
Channel bandwidth	1 MHz	500 MHz – 7.5 GHz	0.3/0.6 MHz; 2 MHz	22 MHz
Modulation type	GFSK	BPSK, QPSK	BPSK (+ASK), O-QPSK	BPSK, QPSK COFDM, CCK, M-QAM
Spreading	FHSS	DS-UWB, MB-OFDM	DSSS	DSSS, CCK, OFDM
Coexistence mechanism	Adaptive freq. hopping	Adaptive freq. hopping	Dynamic freq. selection	Dynamic freq. selection, transmit power control
Basic cell	Piconet	Piconet	Star	BSS
Extension of the basic cell	Scatternet	Peer-to-peer	Cluster tree, Mesh	ESS
Max number of cell nodes	8	8	>65000	2007
Encryption	E0 stream cipher	AES block cipher (CTR, counter mode)	AES block cipher (CTR, counter mode)	RC4 stream cipher (WEP), AES block cipher
Authentication	Shared secret	CBC-MAC (CCM)	CBC-MAC (ext. of CCM)	WPA2 (802.11i)
Data protection	16-bit CRC	32-bit CRC	16-bit CRC	32-bit CRC

(a)

Standard IEEE Spec.	Bluetooth 802.15.1	UWB 802.15.3	ZigBee 802.15.4	Wi-Fi 802.11a/b/g
Max data rate (Mbit/s)	0.72	110	0.25	54
Bit time (us)	1.39	0.009	4	0.0185
Max data payload (bytes)	339 (DH5)	2044	102	2312
Max overhead (bytes)	158/8	42	31	58
Coding efficiency (%)	94.41	97.94	76.52	97.18

(b)

Figure 3-10 A Comparison of (a) Bluetooth,UWB, ZigBee and Wi-Fi protocols. (b) Typical system parameters of the wireless protocols [61].

The information to be transmitted is just data samples, so all four protocols can meet this requirement. However, ZigBee and Bluetooth consume significantly less power compare to UWB and Wi-Fi (Figure 3-11). ZigBee requires even less power since it can “sleep” most of the time and is only activated during Tx and Rx. Considering all these factors, we chose ZigBee as our wireless communication protocol.

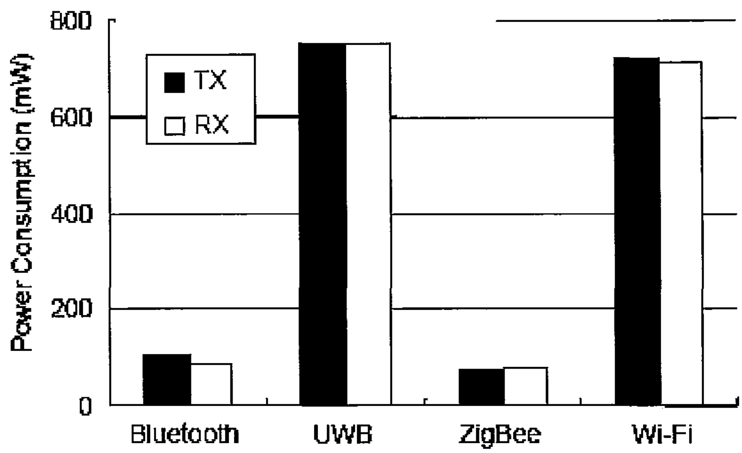

Figure 3-11 Comparison of power consumption [61]

3.1.3.2 Transceiver

The ZigBee transceiver we chose is the XBee Series 1 which is manufactured by Digi. XBee is an embedded RF module. It operates at 3V, which is the same voltage supply as our sensor and microcontroller.

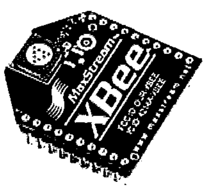

(a) XBee 802.15.4 Series 1

Platform	XBee® 802.15.4 (Series 1)
Performance	
RF Data Rate	250 kbps
Indor/Urban Range	100 ft (30 m)
Outdoor/RF Line-of-Sight Range	300 ft (100 m)
Transmit Power	1 mW (+0 dBm)
Receiver Sensitivity (1% PER)	-92 dBm
Features	
Serial Data Interface	3.3V CMOS UART
Configuration Method	API or AT Commands, local or over-the-air
Frequency Band	2.4 GHz
Interference Immunity	DSSS (Direct Sequence Spread Spectrum)
Serial Data Rate	1200 bps - 250 kbps
ADC Inputs	(6) 10-bit ADC inputs
Digital I/O	8
Antenna Options	Chip, Wire Whip, U.FL, & RPSMA
Networking & Security	
Encryption	128-bit AES
Reliable Packet Delivery	Retries/Acknowledgments
IDs and Channels	PAN ID, 64-bit IEEE MAC, 16 Channels
Power Requirements	
Supply Voltage	2.8 - 3.4VDC
Transmit Current	45 mA @ 3.3VDC
Receive Current	50 mA @ 3.3VDC
Power-Down Current	<10 uA @ 25° C
Regulatory Approvals	
FCC (USA)	OUR-XBEE
IC (Canada)	4214A-XBEE
ETSI (Europe)	Yes
C-TICK Australia	Yes
Telec (Japan)	Yes

(b) XBee 802.15.4 Series 1 specification

Figure 3-12 XBee 802.15.4 Series 1 (a) transceiver and (b) specifications. [66]

3.2 System architecture

3.2.1 Block diagram

With all the key components selected, the next target is to implement the sensor system. Since TCPD requires simultaneous monitoring of the three points - Cun, Guan and Chi, then there should be three sensors along the wrist. The digital output of each sensor will be available after conversion by the on-chip ADC, and it must be read immediately, otherwise the data will be replaced by the next reading. Each digital pressure sensor will be connected to a microcontroller. The simultaneous data from each sensor will be temporarily stored in its corresponding microcontroller, and then transferred to the master device, which is also a microcontroller. The *XBee* transceiver will be only connected to the master device, and another receiver is connected with PC via the RS232 – COM port. The block diagram below shows the system architecture.

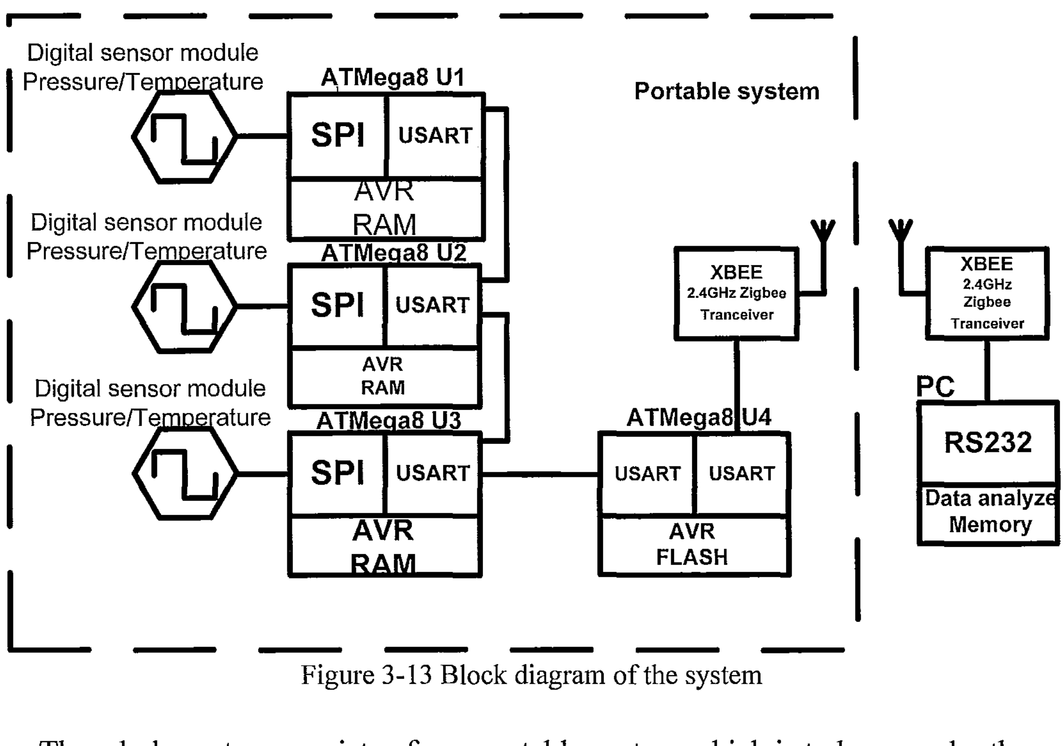

Figure 3-13 Block diagram of the system

The whole system consists of one portable system which is to be worn by the user, and one receiving/processing system which involves the PC. The portable portion can be divided into one master level and one slave level. The slave level consists of three digital pressure sensors and their corresponding microcontrollers, labelled as U1, U2 and U3; the master level consisting of one microcontroller, is labelled as U4, plus a ZigBee transceiver.

3.2.2 Algorithm

3.2.2.1 Reading the sensor

The *MS5536C* digital pressure sensor consists of one piezoresistive sensing film whose resistance changes as the pressure changes. The pressure is converted into an electrical voltage by an internal Wheatstone bridge circuit. The analog output from the circuit will enter the sensor's interface IC. The interface IC does the analog-to-digital (AD) conversion, digital filtering and provides the compensation coefficient for the temperature effects.

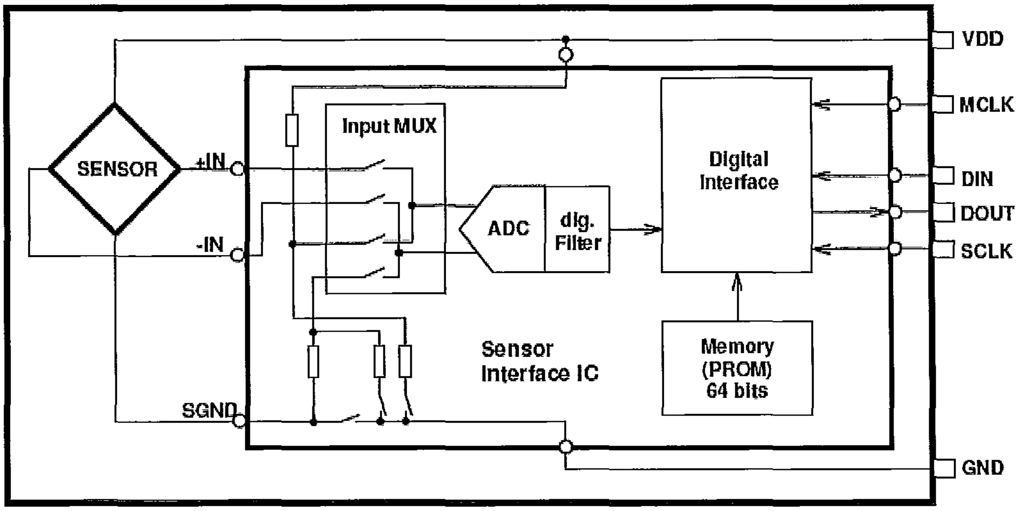

Figure 3-14 Block diagram MS5536C [58]

The *MS5536C* communicates with microcontroller through the SPI (Serial-Peripheral-Interface or Three-Wire interface). In order to get the pressure readings from the sensor, the microcontroller needs to first read the calibration parameters from the sensor, then read the pressure and temperature parameters. The real pressure and temperature is obtained through a calculation using these parameters. The flowchart below shows the reading process with an example.

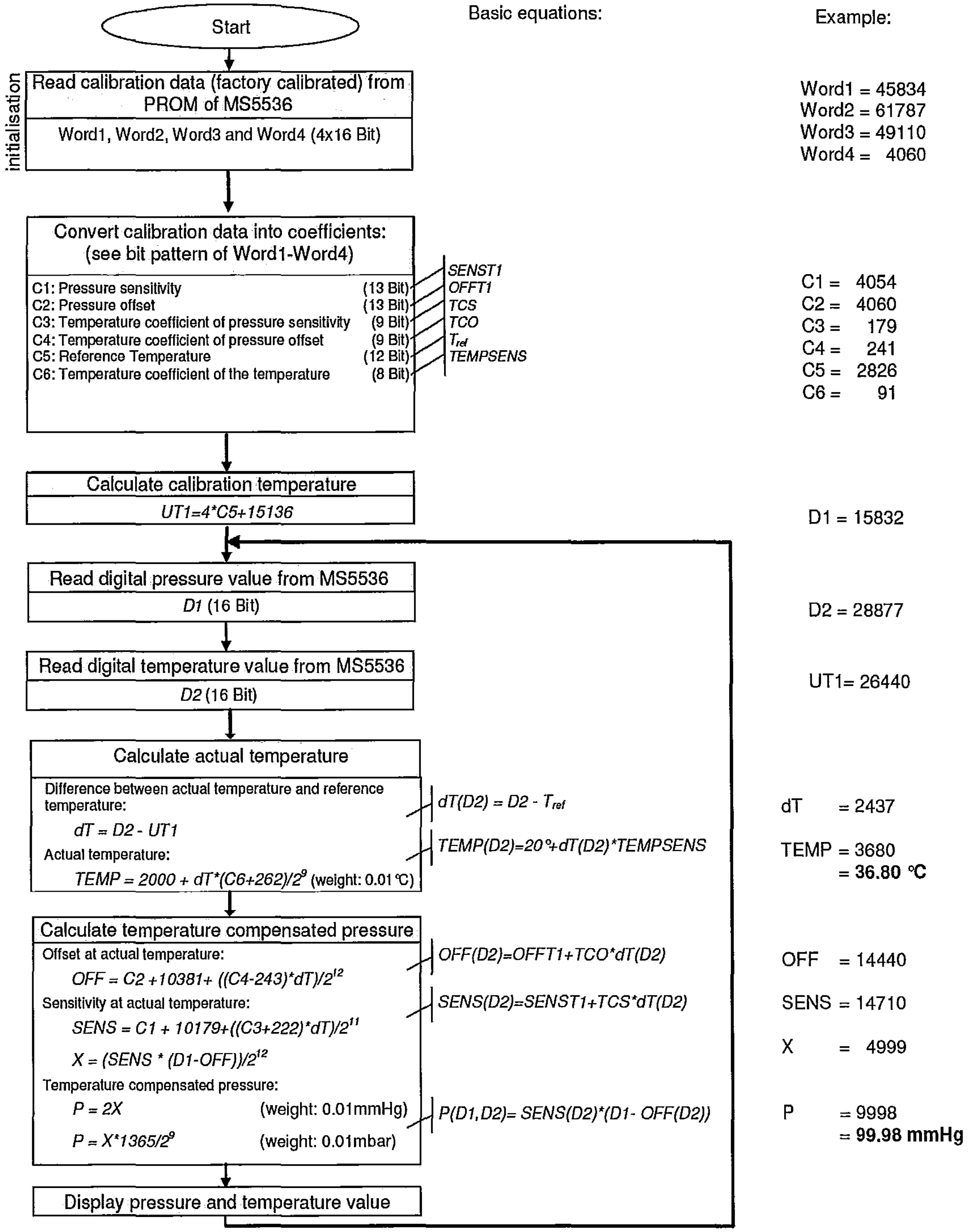

Figure 3-15 Flowchart for pressure/temperature reading and software compensation [58].

The calibration coefficients C1...C6 are extracted from the calibration data word W1...W4. Each word is two bytes wide. Figure 3-15 shows the arrangement of coefficients C1...C6 in W1...W4.

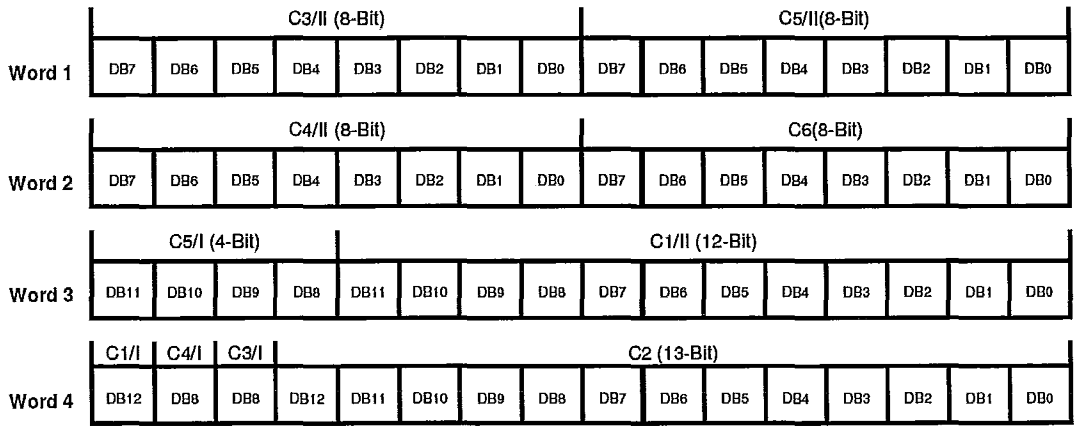

Figure 3-16 Bit pattern of calibration data (C1..6) in Word1 to Word4 [58]

3.2.2.2 Data structure and data flow

The data read from each of the sensor will be stored and transferred by its corresponding microcontroller. In order to avoid data collision, we arranged the microcontrollers in a serial path. The data from each microcontroller is labelled to avoid confusion. The following diagram shows the data structure.

Calibration data

- 6 arrays contain 6 bytes each, 2 arrays contain 3 bytes each. A total of 42 bytes
- Cx_H refers to the High byte of C1..6 in the U(x+1)
- Cx_L refers to the Low 8 byte if C1..6 in the U(x+1)
- D2H refers to the High byte of D2 in all unit
- D2L refers to the Low byte of D2 in all unit

C0_H	C0_H[0]	C0_H[1]	C0_H[2]	C0_H[3]	C0_H[4]	C0_H[5]	High 8 bits of C1..6 from U1
	C1H	C2H	C3H	C4H	C5H	C6H	
C0_L	C0_L[0]	C0_L[1]	C0_L[2]	C0_L[3]	C0_L[4]	C0_L[5]	Low 8 bits of C1..6 from U1
	C1L	C2L	C3L	C4L	C5L	C6L	
C1_H	C1_H[0]	C1_H[1]	C1_H[2]	C1_H[3]	C1_H[4]	C1_H[5]	High 8 bits of C1..6 from U2
	C1H	C2H	C3H	C4H	C5H	C6H	
C1_L	C1_L[0]	C1_L[1]	C1_L[2]	C1_L[3]	C1_L[4]	C1_L[5]	Low 8 bits of C1..6 from U2
	C1L	C2L	C3L	C4L	C5L	C6L	
C2_H	C2_H[0]	C2_H[1]	C2_H[2]	C2_H[3]	C2_H[4]	C2_H[5]	High 8 bits of C1..6 from U3
	C1H	C2H	C3H	C4H	C5H	C6H	
C2_L	C2_L[0]	C2_L[1]	C2_L[2]	C2_L[3]	C2_L[4]	C2_L[5]	Low 8 bits of C1..6 from U3
	C1L	C2L	C3L	C4L	C5L	C6L	
D2H	D2H[0]	D2H[1]	D2H[2]				High 8 bits of D2 from U1..3
	D2H	D2H	D2H				
D2L	D2L[0]	D2L[1]	D2L[1]				Low 8 bits of D2 from U1..3
	D2L	D2L	D2L				

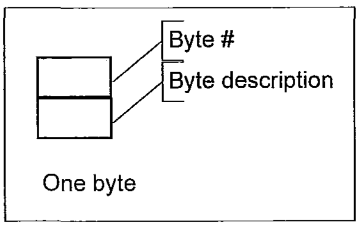

(a) Data structure for Calibration parameters

Shifting data
- 3 arrays contain 3 bytes each, a total of 9 bytes
- count refers to the measurement ID of D1 in all units, 0x00~0xff
- D1H refers to the High byte of D1(digital pressure measurement) in all units
- D1L refers to the Low byte of D1 (digital temperature measurement) in all units

count	count[0]	count[1]	count[2]
	Hex'xx'	Hex'xx'	Hex'xx'
D1H	D1H[0]	D1H[1]	D1H[2]
	D1H	D1H	D1H
D1L	D1L[0]	D1L[1]	D1L[2]
	D1L	D1L	D1L

High 8 bits of C1..6 from U1

Low 8 bits of C1..6 from U1

High 8 bits of C1..6 from U2

Master unit memory arrangement
- either located in data flash or on PC
- requires 2304 bytes, approx 13 sec measurement

(b) Data structure for Shifting data

	U1			U2			U3		
0	count[0]	D1H	D1L	count[1]	D1H	D1L	count[2]	D1H	D1L
1	.			.			.		
2	.			.			.		
.	.			.			.		
.	.			.			.		
.	.			.			.		
244	.			.			.		
255	count[0]	D1H	D1L	count[1]	D1H	D1L	count[2]	D1H	D1L

(c) Data structure for data storage in Master unit

Figure 3-17 Data structure (a) Calibration parameters. (b) Shifting data. (c) Storage in Master unit.

The data in the microcontroller system is categorized into three types - *Calibration parameters*, *Shifting data* and storage in Master unit (U4).

Calibration parameters are extracted from calibration words from the digital sensor and temperature parameters. Each parameter is labelled by putting it in the corresponding array. There are six calibration parameters from each sensor - C1 to C6.

There are also three temperature parameters from all sensors, one from each. Each calibration parameter will occupy 1 byte, whereas each temperature parameter will occupy two bytes (High byte and Low byte). The whole structure of *Calibration data* will occupy 42 bytes in total. *Calibration data* will only be read at the beginning of each acquisition cycle.

Shifting data stores the single real-time measurement from all sensors. The structure consists of three arrays - *Count*[], *D1H and D1L. Count*[] keeps track of the sample number and provides a label for each sample in all slave units. There are three elements in *Count*[], representing three corresponding slave units. For instance the value of *Count*[1] represents the current sample number in microcontroller U1. At the beginning of each acquisition cycle, the numbers in *Count*[] will be reset to zero, and they are increased by one every time a new sample is measured. *D1H* stores the high byte of the measured pressure parameter from all three units, whereas *D1L* stores the low byte of the pressure parameter. *Shifting data* occupies 9 bytes, and it is updated whenever a new sample arrives. Therefore, after each measurement, the data must be stored.

The length of each acquisition cycle is set to 256 data points, and the separation between every adjacent data points is 50ms. That gives us 12.8s of continuous monitoring for each acquisition cycle. The complete cycle is stored in the Master microcontroller. There are two reasons that we divide the monitoring process into separate cycles. One is to reduce the length of continuous data to reduce transmission error. Another one is to read temperature parameter once in a while to limit the pressure error introduced by temperature effect. The three flowcharts below shows the detailed data path and flow for cycle initialization and data sampling within each cycle.

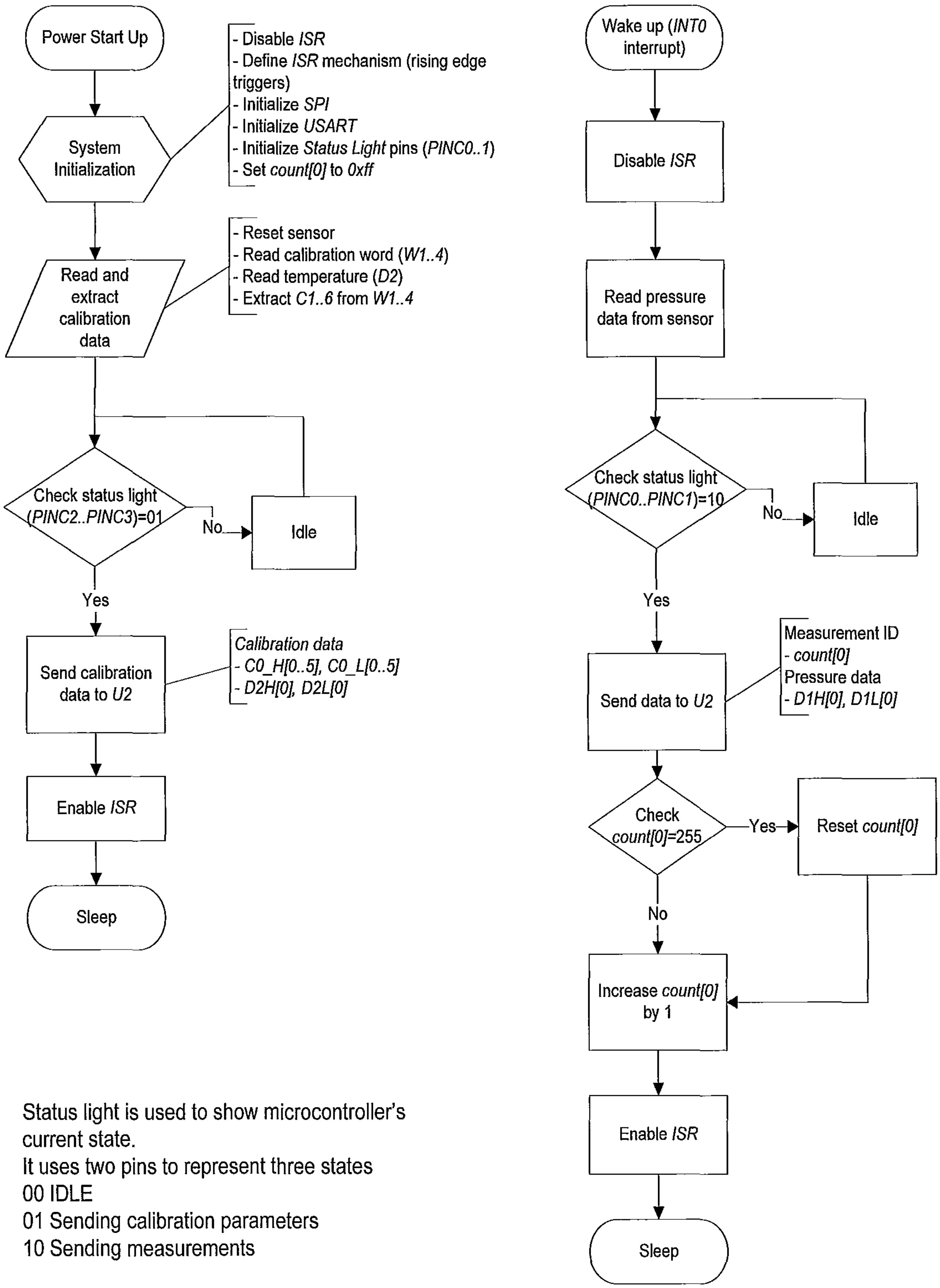

(a) Flowchart of microcontroller U1 from slave level

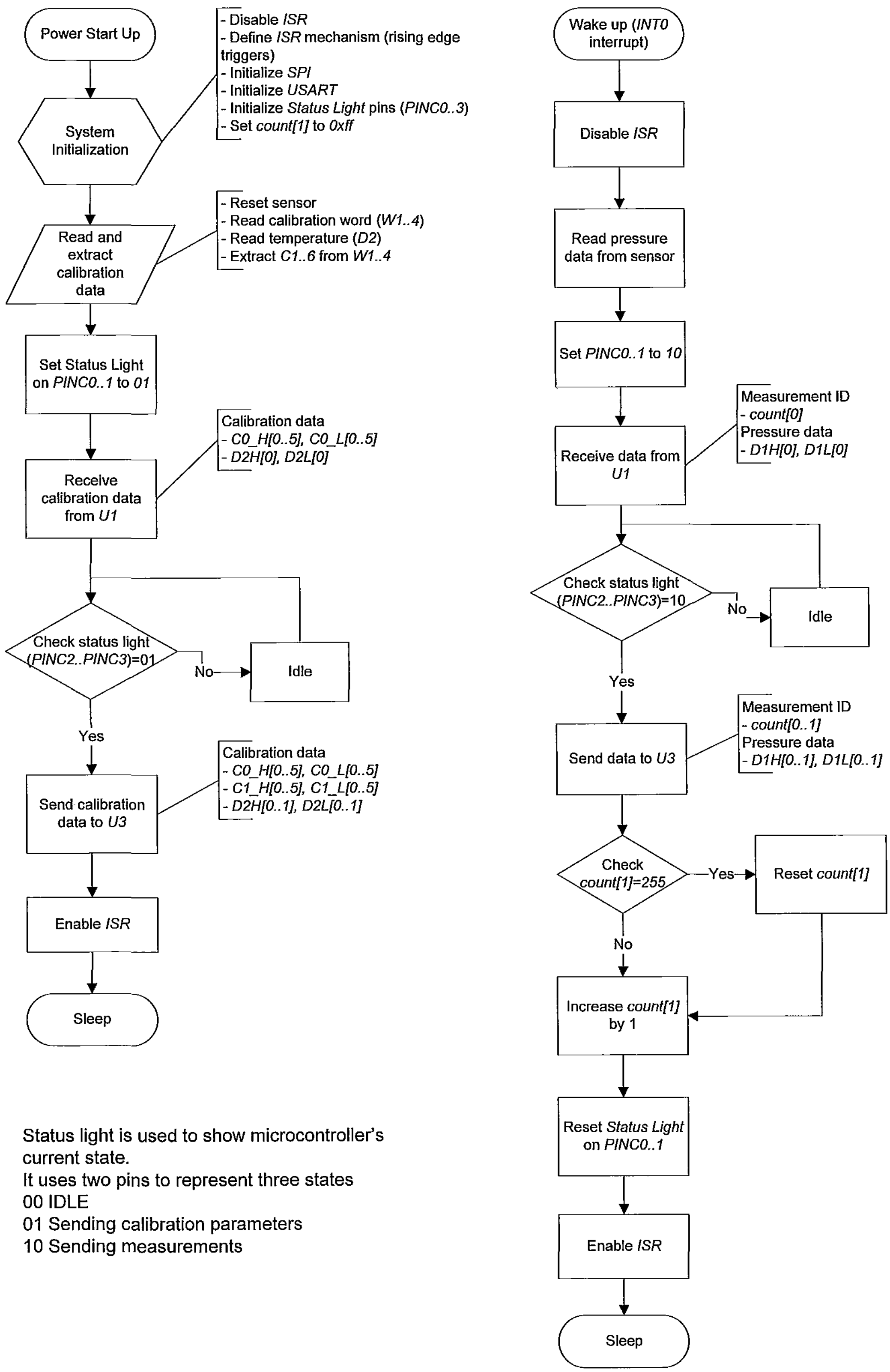

(b) Flowchart of microcontroller U2 from slave level

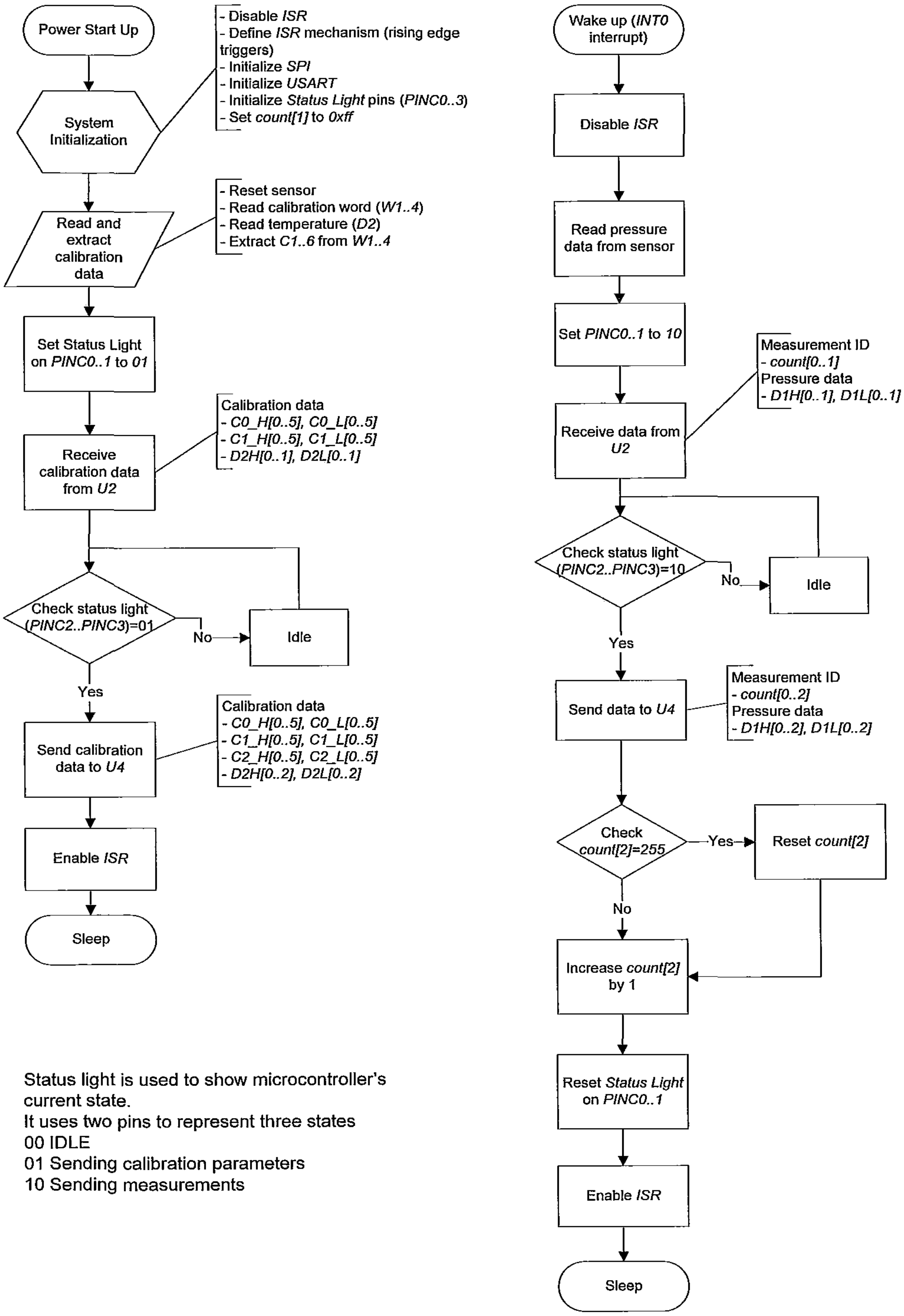

(c) Flowchart of microcontroller U3 from slave level

Figure 3-18 Flowchart from slave level microcontrollers.

Figure 3-18 illustrates the detailed working procedure of microcontroller U1, U2 and U3 There are two major processes - parameter acquisition and data acquisition.

Parameter acquisition is to acquire the calibration coefficients and temperature from the sensor. It is only perform at power start up. Data acquisition acquires the pressure measurement from the sensor. Then, U1, U2, and U3 will read the pressure from the sensor when they receive interrupt signals from U4.

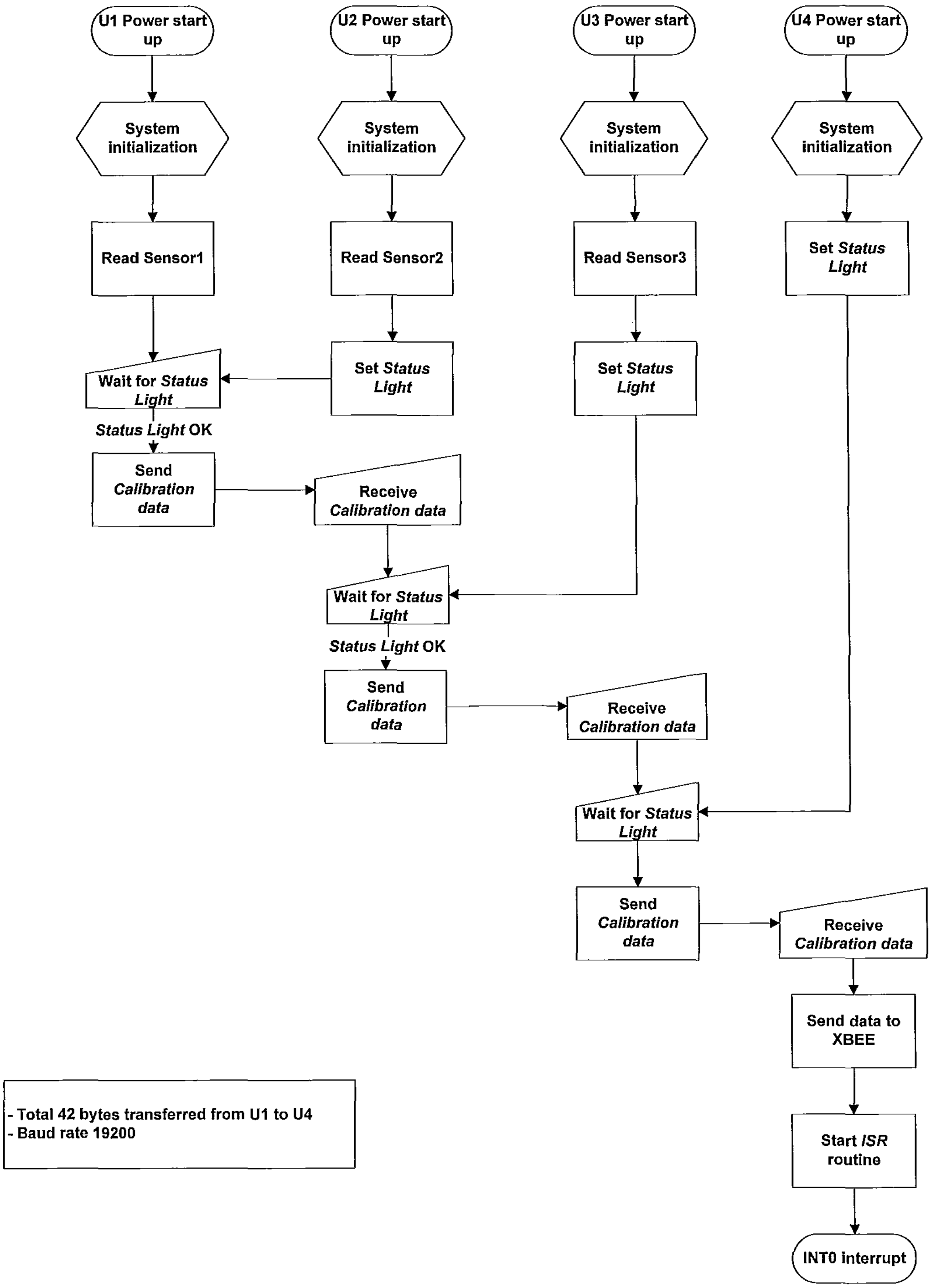

(a) Overall flowchart of initialization at the beginning of each acquisition cycle

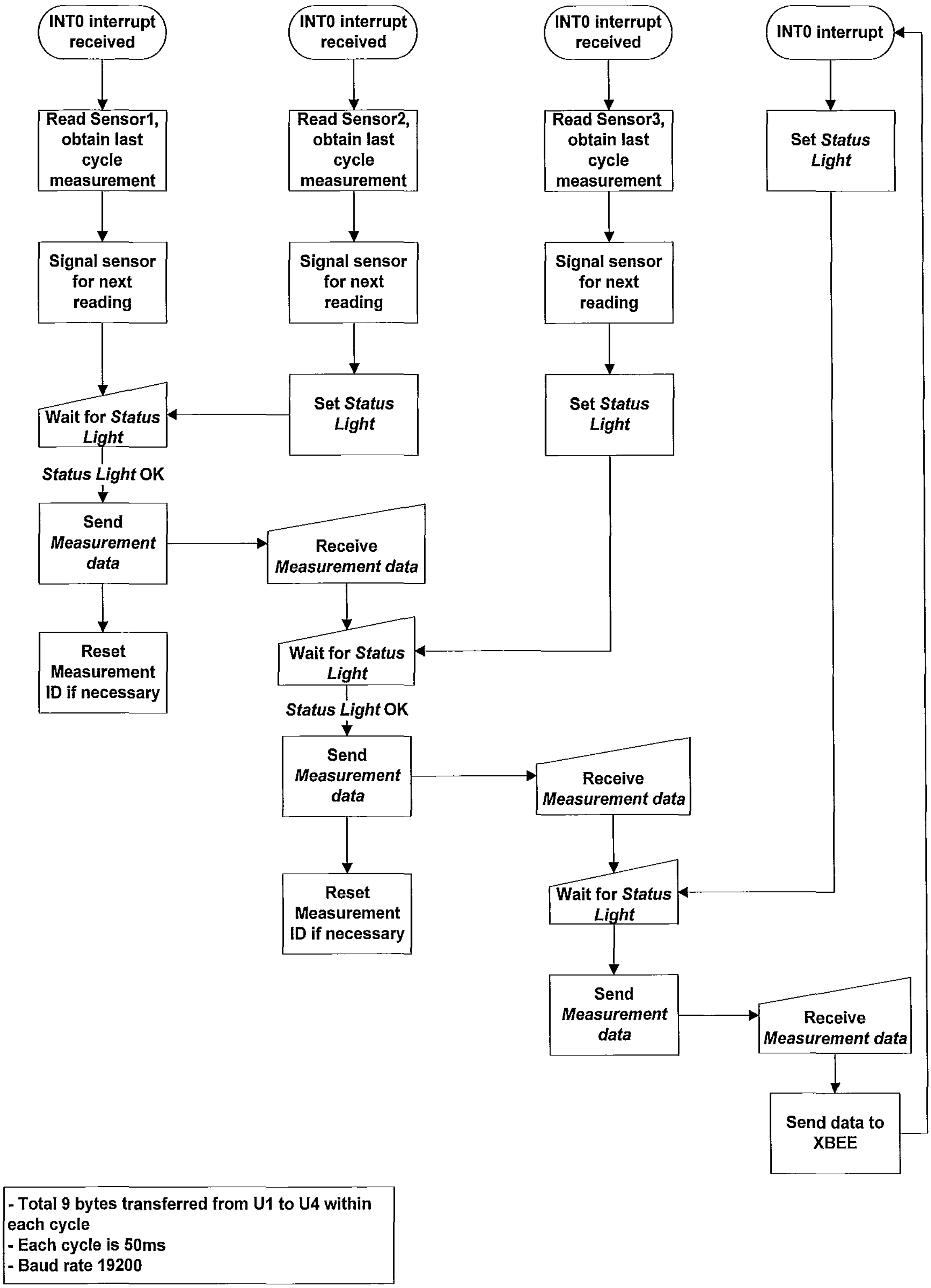

(b) Overall flowchart of data sampling in each acquisition cycle

Figure 3-19 System overall flowcharts

Figure 3-19 shows the overall system flowcharts. In Figure 3-19(a), the working procedure of parameter acquisition upon system start-up is given. After parameter acquisition, U4 will initialize data acquisition by declaring INT0 interrupt. The flowchart for each data acquisition cycle (acquire one pressure point) is given in Figure 3-19(b).

3.3 Hardware design

3.3.1 Liquid Filled Sensor module

As mentioned earlier in 3.1.1.2, it is difficult to find a off the shelf sensor that meets our requirement. Therefore we have to customize the sensor we have chosen. The basic idea of the sensor module is to have a soft spherical shape front end that is firm enough to stand pressure at the same time, which acts like human finger tip, to retrieve the pulse from the radial artery. Through some simple experiments, the idea of liquid filled sensor module arises. The following Figure 3-19 show the details of the pressure sensor module.

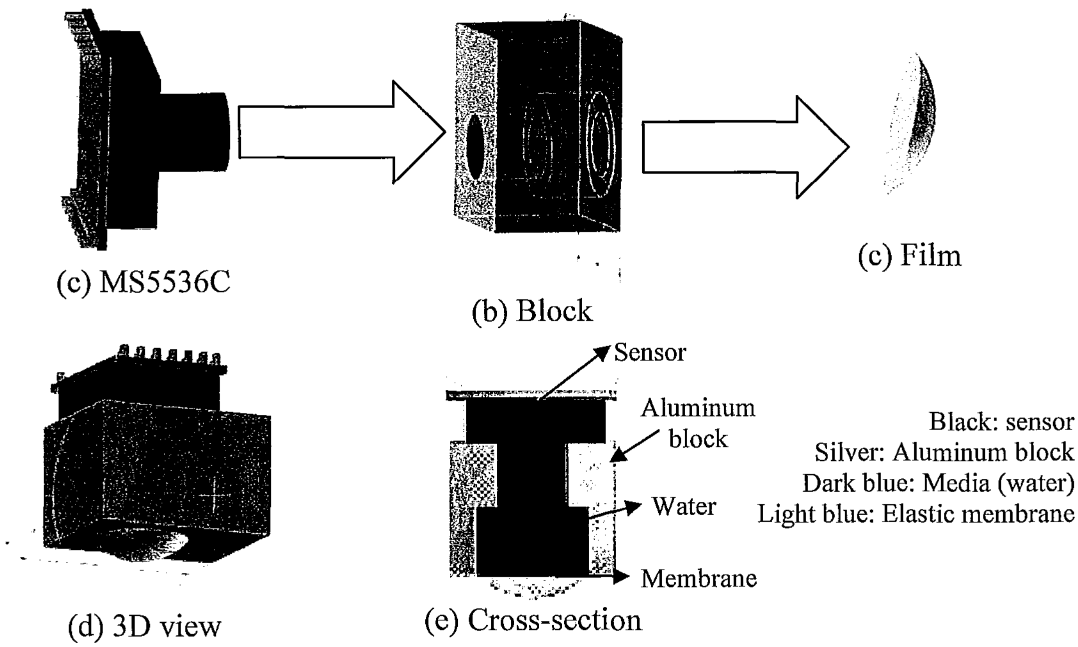

Figure 3-20 Sensor module, 3D and cross section view.

The single sensor module consists of a digital pressure sensor (black), an aluminum block (silver) and an elastic membrane (light blue). The digital sensor is glued at one end of the block; the elastic film (rubber latex) is glued at the opposite side. To establish electrical connection, a PCB is soldered at the bottom of the sensor. The complete prototype is shown in the figure below.

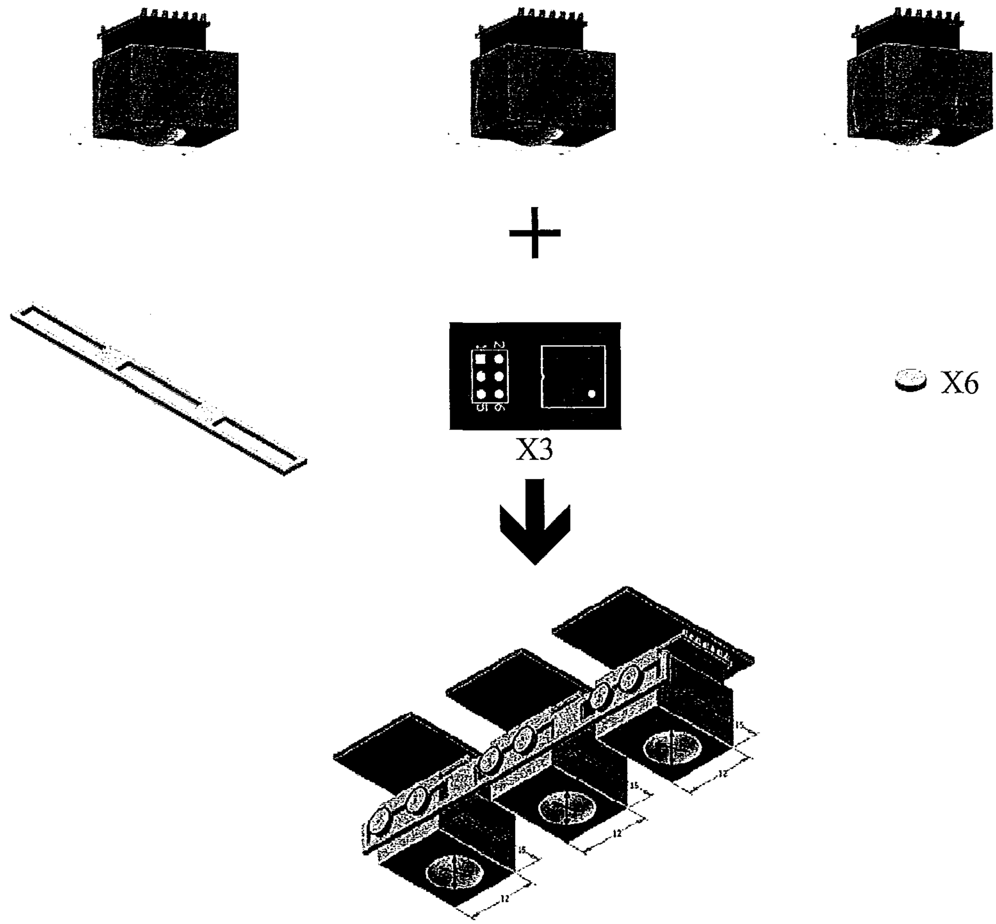

Figure 3-21 Sensor module assembly.

The sensor module assembly consists of three digital sensor modules, one positioning rack with a few screws, and three PCB connectors. The positioning rack will keep aligned and in place, the sensors. The PCB connector is soldered at the back of each digital sensor module to provide I/O connections.

3.3.2 Schematic drawing

The schematic drawing showing the electrical connections between slave level and master level microcontrollers is shown in Figure 3-22.

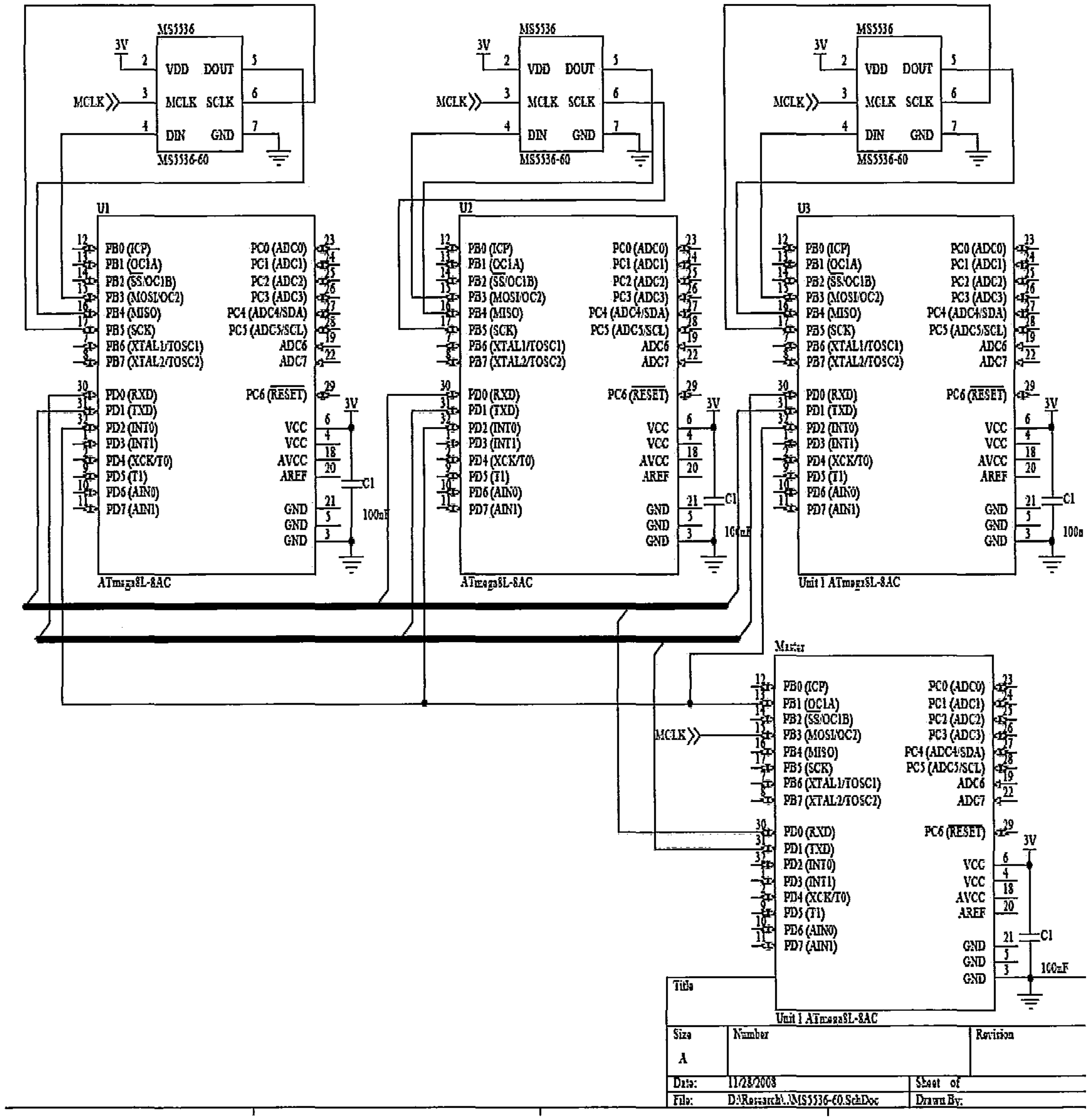

Figure 3-22 Circuit diagram for the sensor module and microcontroller using Protel

Chapter 4 Experimental results and analysis

4.1 Experiment target

From the discussion earlier in Section 1.3, the crucial information for TCPD assessment is the change of radial pulse pressure felt by the doctor's finger. In real diagnosis, the absolute amplitude of pressure felt by the doctor will not contribute significantly to the doctor's decision. Instead, the doctor would pay most of attention to the change of pulse strength, frequency, depth etc. [17]. Therefore, the measurement needed is the one that can accurately reflect the change of the amplitude. To obtain these changes, it is necessary to have continuous measurement of the radial pulse pressure.

The measurements are done by using the sensor module that is built as described in Hardware design, Section 3.3. The data is read and processed using a microcontroller system and then wirelessly transmitted with a Zigbee transceiver. With the sensor module, the tonometry measurement of the radial pulse amplitude at any given time can be taken. Also, the continuous measurement of the amplitude can be obtained, and this will form the pulse waveform. Note that both the radial tonometry measurement and central aortic pressure recording by cardiac catheterization can produce a waveform that reflects the changing pressure. But blood pressure measured by a conventional ocsilometric cuff can only give the systolic and diastolic pressure and no information of pulse waveform itself. The peak and baseline amplitude in the waveform corresponds to the diastolic pressure and systolic pressure, respectively. The radial pulse pressure measured by the tonometer is proportional to brachial pressure. In the conventional ocsilometric method, what are being measured are the peak brachial pressure which is during heart contraction and the resting state pressure. Central aortic pressure differs from cuff brachial pressure and radial tonometry measurement in amplitude. The amplitude is not proportional either.

Since the TCPD technique is mainly based on the change in pressure, then the experimental results analyses will be focussing on these aspects.

4.2 Experiment setup

Figures 4-1 and 4-2 show the experimental prototype set-up and its relative dimensions.

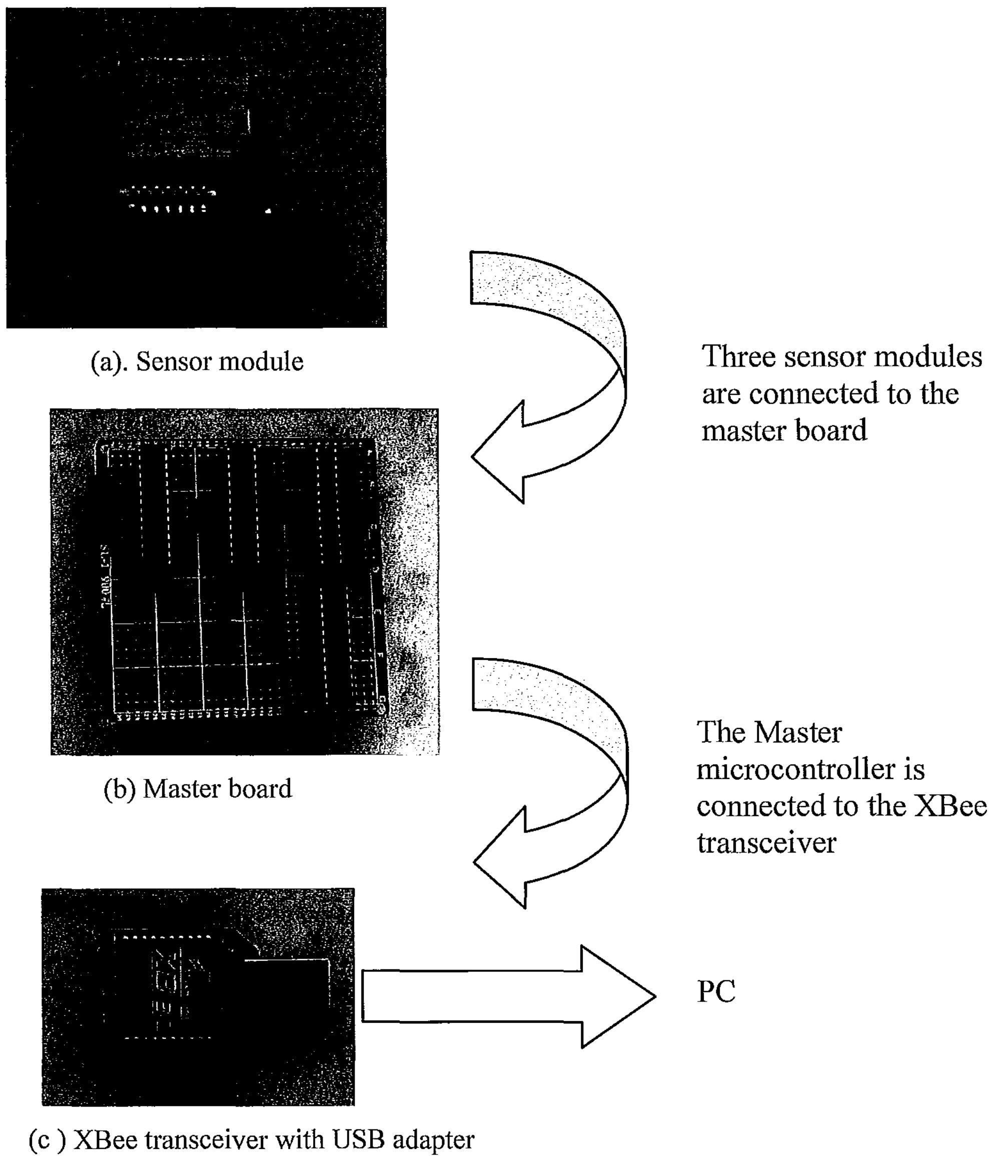

Figure 4-1 Experiment prototype setup

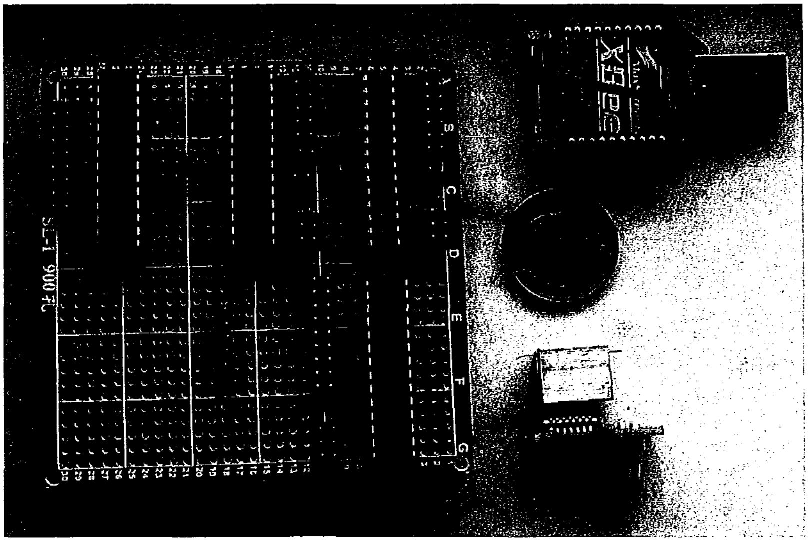

Figure 4-2 Experiment prototype setup overview

4.3 Experiment results

The experiments are conducted on healthy subjects aged 22 to 56 years. The results below are 5 seconds period measurement from Cun, Guan and Chi; and a longer period measurement from Cun only. The sample rate is 20 Hz, which means that time interval between adjacent data points is 50ms.

4.3.1 Wireless function

The wireless function is tested by comparing the measurement transmitted by cable and measurement transmitted by wireless transceiver. The procedure is first to split the USART output on the up-level microcontroller, then one branch is connected to the ATMEL development board which is linked with PC through RS232 port. Another branch of the USART output is wired with the Zigbee transmitter, and the receiver is connected with second RS232 port on PC. Separate data logging software are used on the PC to simultaneously monitor two the ports. Figure 4-3 below shows the measurement transmitted by cable versus transmitted by wireless transceiver. One problem which occurred in wireless transmission is the first 8 to 10 data bytes are always missing, which resulted in missing the first 4 to 5 pressure measurements. The reason is because on power start-up, the ZigBee transceiver will first initialize its network which requires a few hundred milliseconds, and the transmission can only take place after this initialization.

4 pressure measurements are missing in the wireless transmission (shown in figure 4-3b)

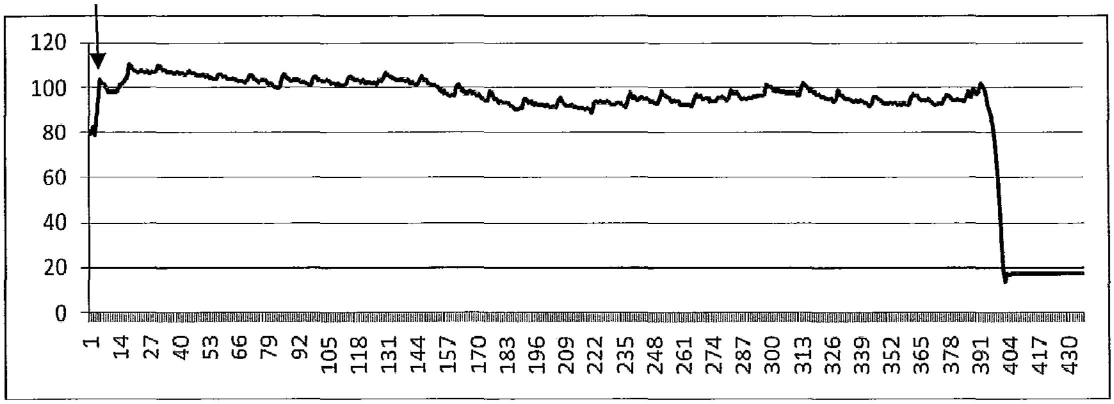

(a) Measurements transmitted by cable

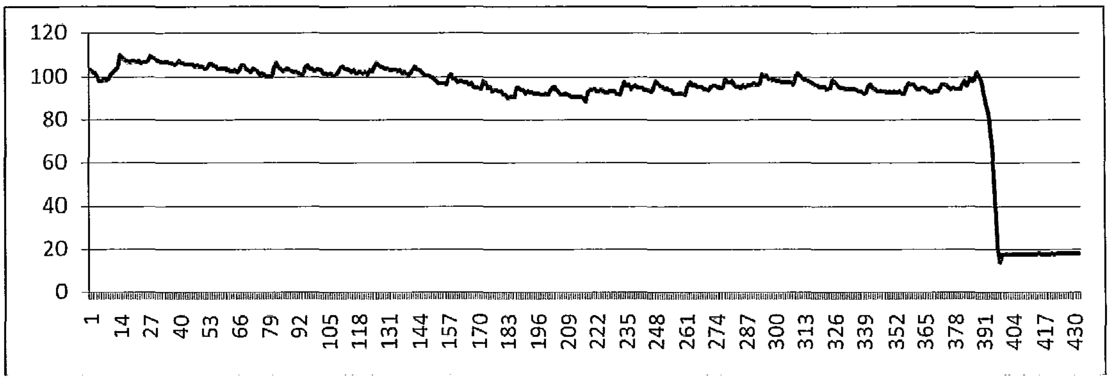

(b) Measurements transmitted by by wireless transceiver

Figure 4-3 Comparison of measurement (a). transmitted by cable and (b)wirelessly

4.3.2 Measurements

The pressure measurement system developed measured the radial tonometry pulse pressure. The data samples measured by the pressure sensor modules are read by their corresponding microcontrollers. Then, the microcontroller transmits the data to the wireless transmitter via USART and the receiver is connected to one of the USB port on PC. The COM port reading software is used to read the data from the receiver, which is in Hex format. These discrete data points are imported into Excel for further processing. The figures below show some of the results from the wireless sensor system.

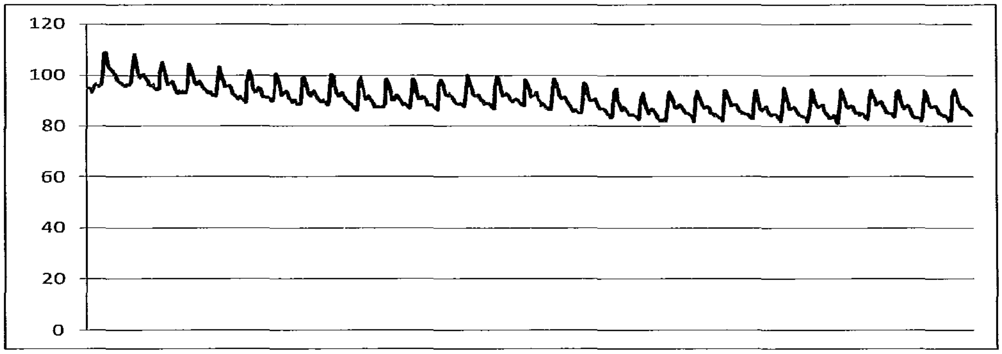

Figure 4-4. Fifteen seconds waveform measurement from Cun in a male 56 years.

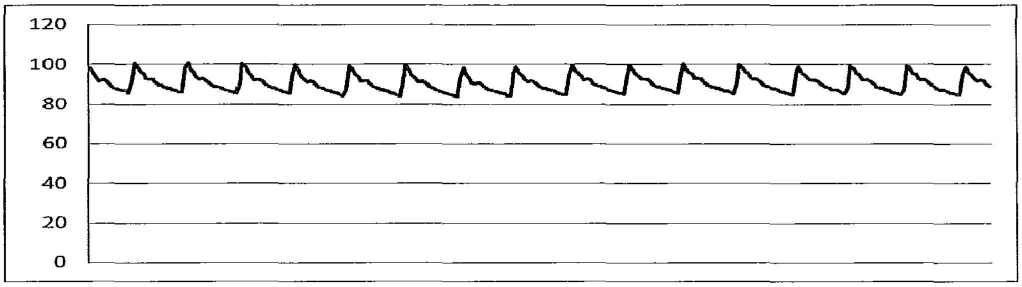

Figure 4-5. Fifteen seconds waveform measurement from Cun in a male 23 years.

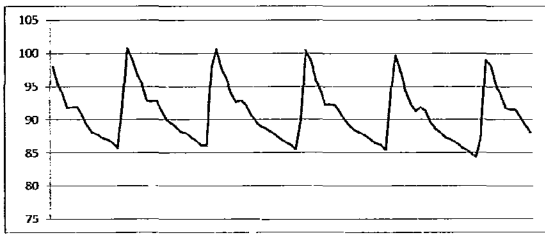

Waveform from Cun, 23 year male

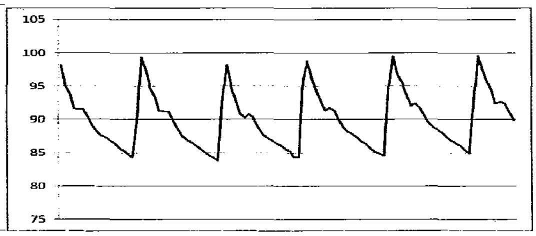

Waveform from Guan, 23 year male

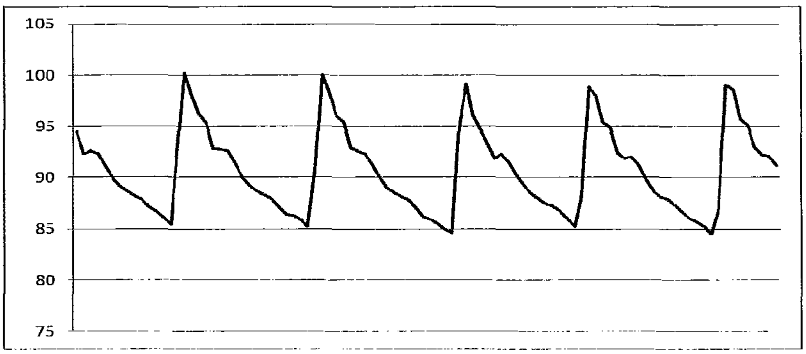

Waveform from Chi, 23 year male

Figure 4-6. TCPD waveform measurements from Cun, Guan, Chi – 23 years old male.

Waveform from Cun, 56 year male

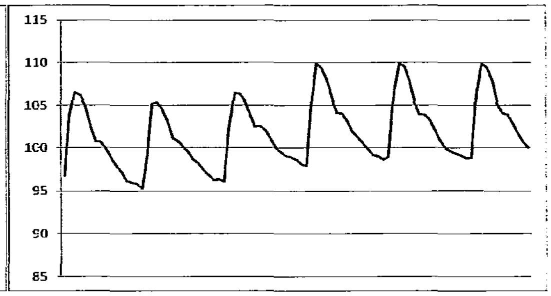

Waveform from Guan, 56 year male

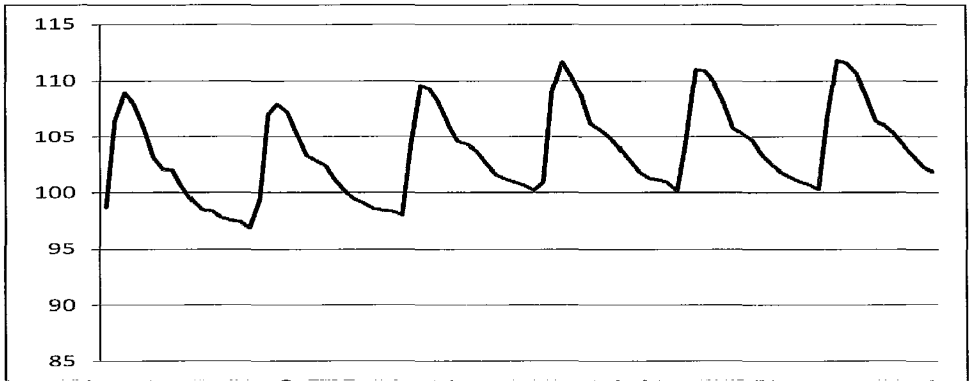

Waveform from Chi, 23 year male

Figure 4-7. TCPD waveform measurements from Cun, Guan, Chi – 56 years old male.

As we can see from the waveforms, some of them have a very stable baseline like the one shown in Figure 4-6. However, in some other waveforms the baseline drift is significant. There are two causes for the baseline wandering. The first is that the diastolic pressure may change during a long period of measurement. The second is due to motion artifact. These causes have to be considered in clinical trials and commercial prototypes.

In each case, the body surface temperature (BST) is also measured. The final value of BST is obtained using the calculation procedure explained in Chapter 3 based on the measurement from the sensor. In this measurement, the body temperature measured during stable state is 32 °C, where stable state means the media in the liquid filled sensor module has the same temperature as the body surface.

4.4 Data processing and result analysis

The discrete tonometry pressure measurements obtained from the digital pressure sensor modules are send to the RS232 port on the PC. The communication is done via 2.4GHz Zigbee transceiver. The pressure points are used to reproduce the tonometry pressure waveform. Several analyses will be made based on the waveform acquired.

4.4.1 Heart Rate

Heart rate represents how frequently the heart contracts. It is simply the inverse of the time duration between heart beats. From the lines below in Figure 4-8, we can easily find out the heart beat duration, which is the peak to peak time. The figure below shows the heart rate is approximately 64 beats per second.

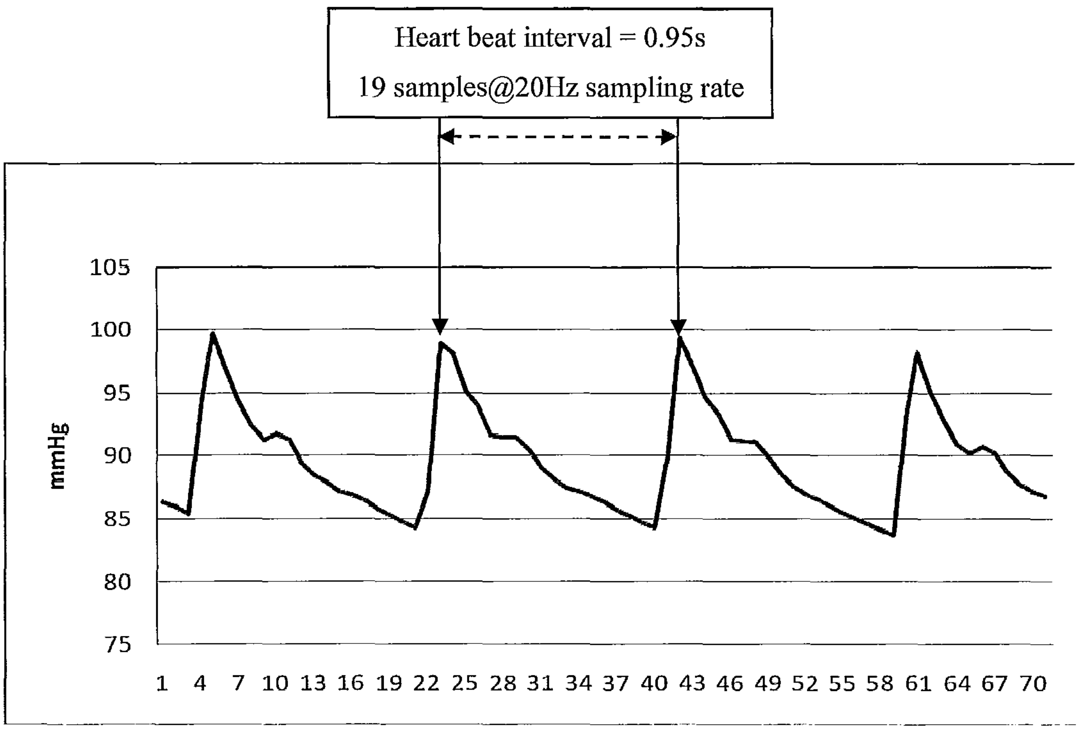

Figure 4-8. Diagram showing the duration between heart beats.

4.4.2 TCPD analysis

In this section, two types of analysis on the pressure waveforms are conducted. The first is the general waveform analysis; its purpose is to compare the shape of the pulse obtained to the pulse described in TCPD in order to perform a basic classification, and to assess the basic characteristics such as frequency and baseline.

The second is individual pulse analysis. A single pulse will be analysed based on certain characteristics, such as rise time, fall time, peak delay, and augmentation index.

4.4.2.1 Waveform comparison

In this section, the measured waveform will be compared with the theoretical peripheral artery pulse waveform, a computer generated waveform based on the quantitative scheme, and waveforms measured by other devices. Figure 4-9 below shows the theoretical waveform of a single pulse [67].

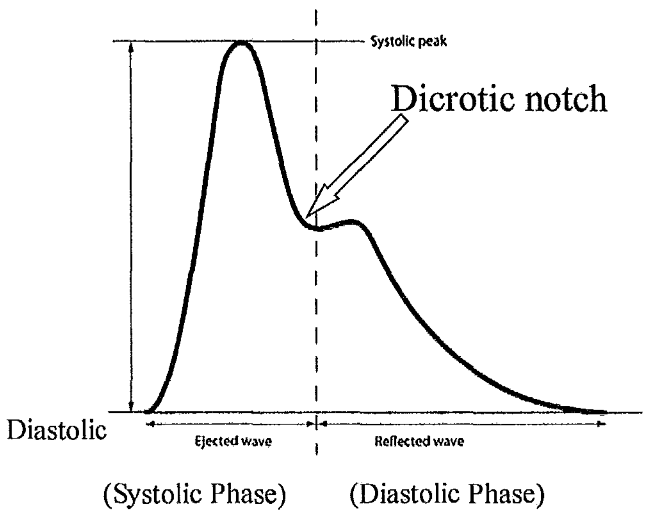

Figure 4-9 Typical artery pulse waveform, single pulse

When the left ventricle of the heart ejects blood into the aorta in systole, the perturbation generates a wave that initially travels through the arteries from the heart towards the arterial tree. The pulse waveform consists of two components, one is forward traveling wave when the left ventricle contracts; and the other one is the reflected wave reflected at the end of the limb [67].

Recall in Chapter 2, the research that described the established quantitative pulse models and proposed mathematical models for the twelve typical TCPD pulse patterns. The model provides several indices in order to distinguish different pulses. The figures below (Figure 4-10) show the twelve pulse waveforms generated in Matlab based on the given indices.

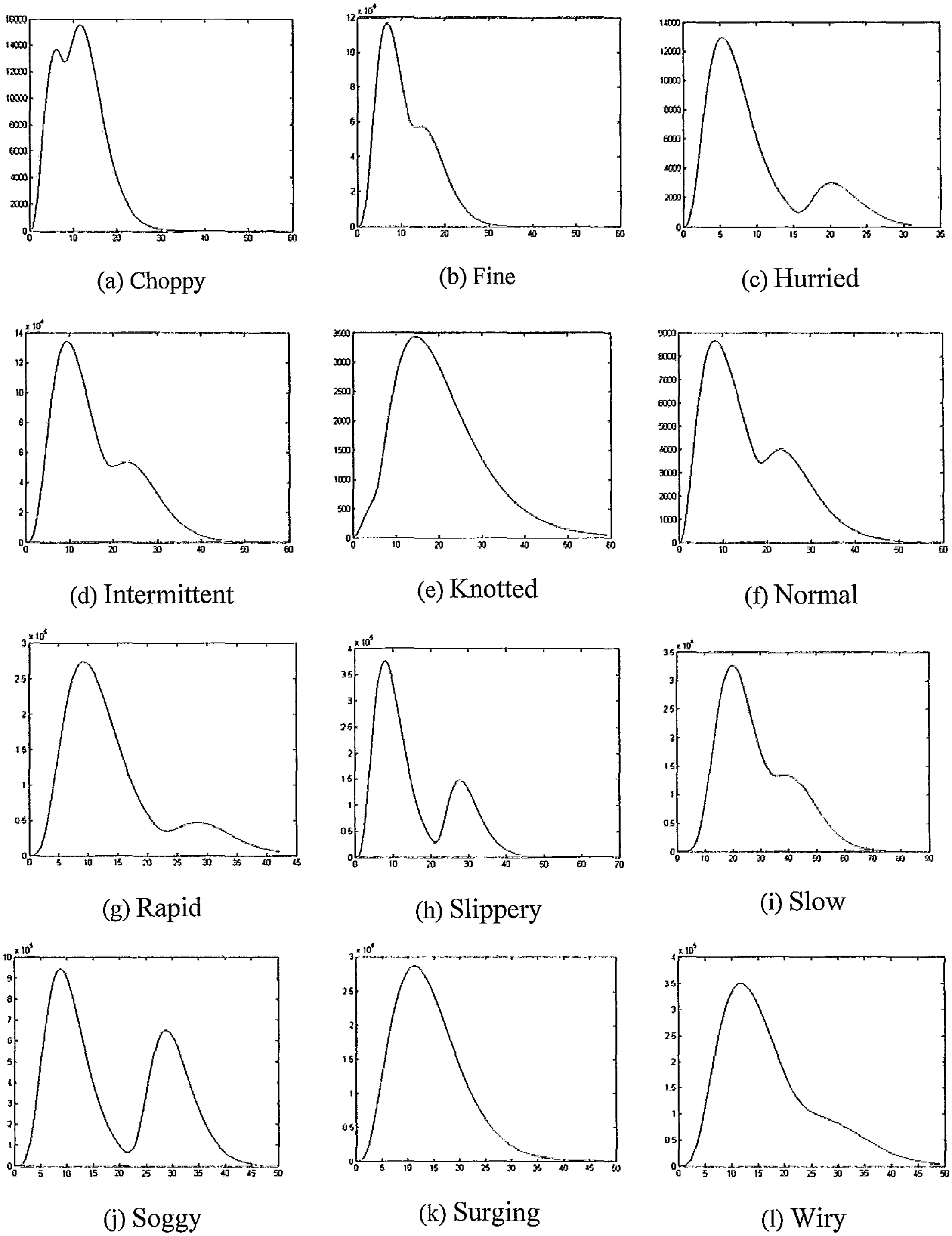

Figure 4-10. Computer generated typical pulse waveforms based on the 12 indices. From [26]

Several pulse waveforms are reproduced using applanation tonometry pressure data acquired from different subjects using our system. The first comparison is between multiple pulse recording and typical "Normal" pattern in TCPD.

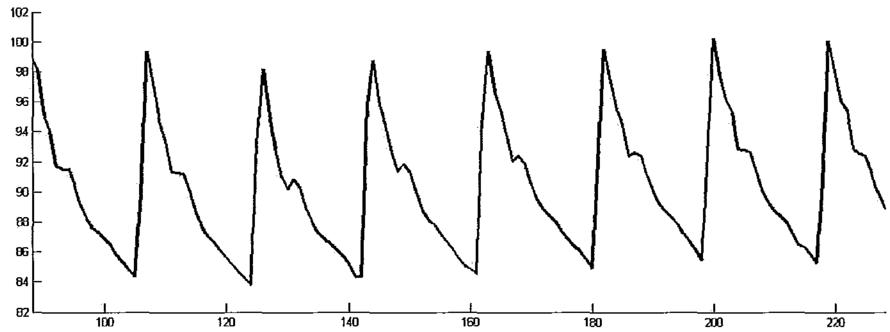

(a) Pulse waveform from 23year male subject.

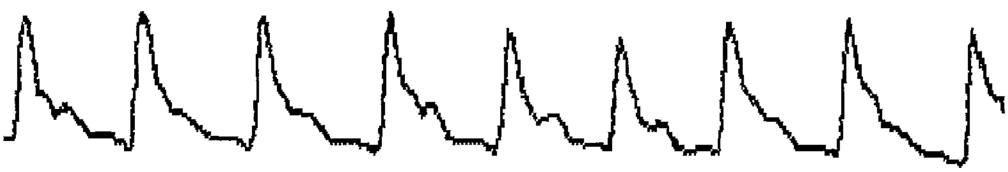

(b) Typical pulse pattern “Normal” [26].

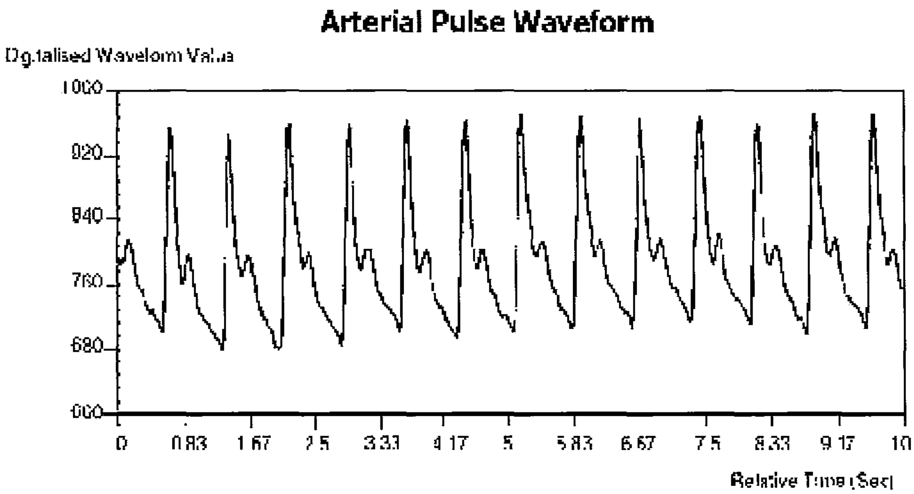

(c) Waveform recorded in other research [68].

Figure 4-11 Comparison between (a) Measured waveform from a 23 year old male and (b) “Normal” waveform. (c) Recorded waveform in other research [68].

Comparison between the recorded general waveform from a 23 year old healthy male subject and the typical “Normal” waveform shows great similarity. Further examination on individual pulse will provide additional information in pulse pattern recognition.

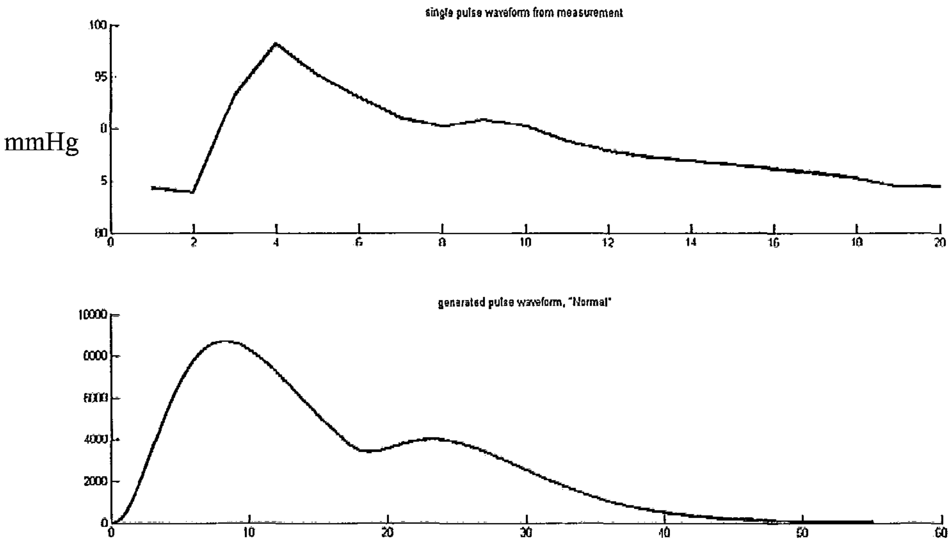

Figure 4-12. Single pulse waveform from measurement of 23 year male (top) and "Normal" pattern generated by computer (bottom).

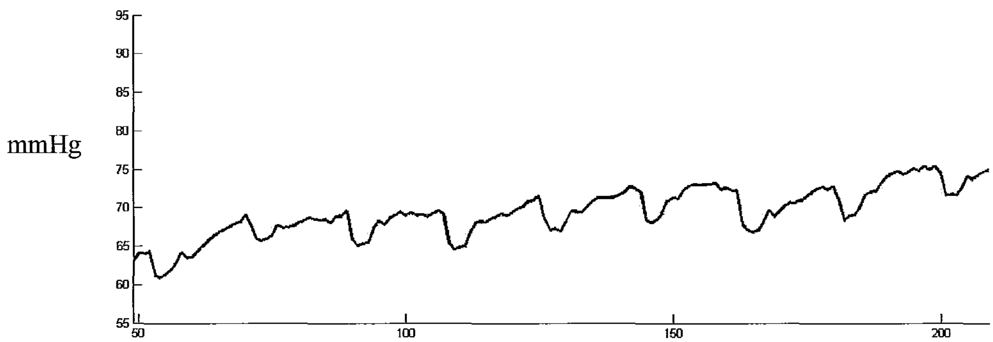

No. of samples

(a) Pulse waveform from a 50 year old male

(b) Pulse pattern "Choppy" [26]

Figure 4-13 Comparison between measured waveform from a 50 year old male and "Choppy" waveform

The measured "Choppy" waveform shares some similarities with the described "Choppy" waveform. However, the single pulse width in the measured waveform is wider.

No. of samples

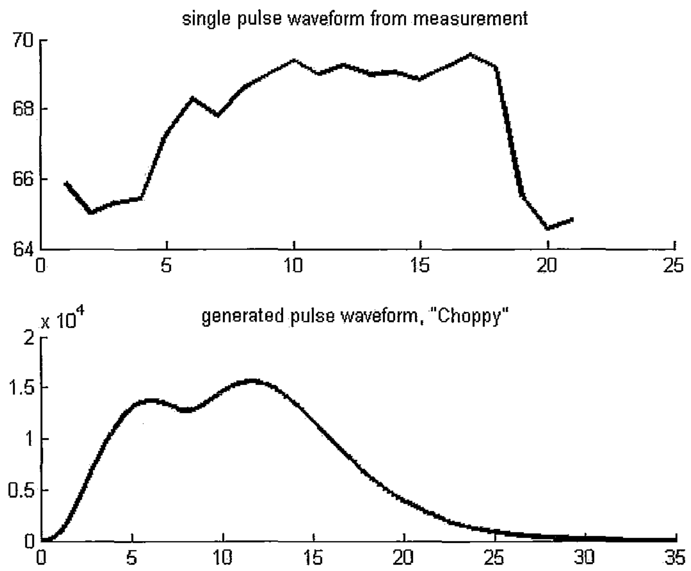

Figure 4-14 Single pulse waveform from measurement of 50 year male (top) and "Choppy" pattern generated by computer (bottom)

4.4.2.2 Waveform analysis

Individual pulse analysis can provide detailed information regarding the pulse characters. In this section the individual pulses will be assessed based on several TCPD standards.

Figure 4-15 shows, on single pulse waveform extracted from the continuous measurement of 23year male, markers indicating point locations on the waveform. In each group of numbers, the top one represents the horizontal axis value which is the n^{th} sample, and the bottom value represents the applanation tonometry pressure, in mmHg.

With these key values show on the waveform the following analysis can be conducted.

a) Rise time diastolic baseline → systolic peak

In TCPD, one characteristic of the pulse is how fast it changes from the bottom to top. This can be described in terms of time delay between first diastolic baseline and the systolic peak. In Figure 4-15 the rise time is $\Delta t_{D1 \to S} = 101.5ms$.

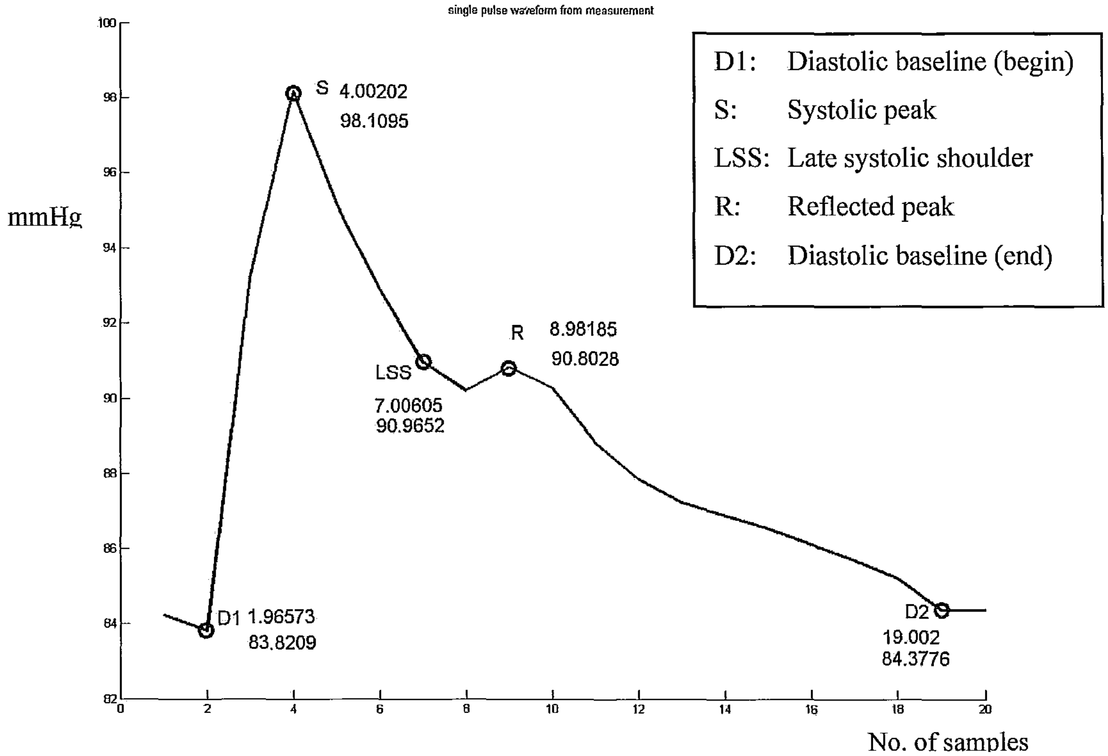

Figure 4-15 Single pulse waveform from measurement of 23 year male. Markers show the key values for pulse analysis.

b) 1st and 2nd peak amplitude difference in percentage

Here, the percentage difference in amplitude of the incident wave and reflected wave is given. In Figure 4-15, the overall pressure difference from diastolic to systolic is $\Delta P_{D \to S} = 14.3mmHg$. The peak difference is $\Delta P_{R \to S} = 6.98mmHg$. Therefore the percentage difference obtained is $\% \Delta P_{S \to R} = 48.81\%$. Usually, the peak difference can be viewed as a factor in cardiovascular disease assessment [69].

c) Augmentation Index

Augmentation index (AI) is a parameter from pulse wave analysis (PWA) and is used as a surrogate measure of arterial stiffness [70]. AI is associated with cardiovascular risk and therefore it is very useful parameter [71]. The augmentation of central arterial pressure and peripheral amplification have been regarded as largely unrelated phenomena, with the former being determined by characteristics of the wave propagation in the aorta and by reflections from the head and lower body, and the latter by reflections from the upper limb. However, the central AI is closely related to the peripheral AI. In this case the peripheral augmentation index calculated based on the waveform is 50%. The definition of AI is given in the figure below (Figure 4-16).

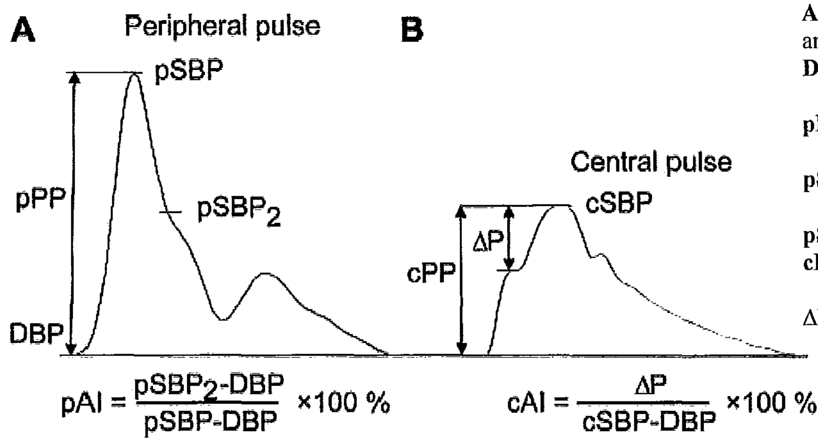

A shows the peripheral AI and **B** shows central AI.

DBP: diastolic blood pressure
pPP: peripheral pulse pressure
pSBP: peripheral systolic blood pressure
pSBP2: late systolic shoulder
cPP: central pulse pressure,
ΔP: augmentation of central systolic pressure above the first systolic shoulder,
cSBP: central systolic peak.

Figure 4-16 Illustration of augmentation index [72].

Parameters extracted from selected measurements, and then comparisons are performed. The table below (Figure 4-17) shows the parameters. There are several observations based on these results:

1. The 1st and 2nd peak time delay is longer for old people than for younger persons.
2. The rise time from diastolic base line to systolic peak is shorter for younger persons since their heart are expected to be stronger.
3. The Augmentation index is larger for older people since their arteries are stiffer.

Male23									
Trial1	t	P		Tds(ms)	Tpp(ms)	Pds	Prs	PP%	AI
D1	1.97	83.82		101.50	7.01	14.30	6.98	48.81	0.50
S peak	4	98.12							
LSS	7.01	90.97							
R peak	8.98	90.8							
D2	19	84							
Trial2	t	P							
D1	10.01	82.3		99.50	6.97	10.35	4.42	42.71	0.50
S peak	12	92.65							
LSS	13.78	87.47							
R peak	16.98	86.72							
D2	21.98	82.3							
Male50									
Trial1	t	P							
D1	11	73.02		149.50	9.03	6.29	2.39	38.00	0.78
S peak	13.99	79.31							
LSS	15.99	77.92							
R peak	20.03	75.41							
D2	27.01	72.93							
Male56									
Trial1	t	P							
D1	9	98.67		150.00	7.99	11.20	5.29	47.23	0.60
S peak	12	109.87							
LSS	14.99	105.42							
R peak	16.99	103.96							
D2	25.02	98.82							

Figure 4-17 Parameter comparison in selected measurements.

4.5 Chapter summary

In this chapter, the experimental procedure and selected measurements were provided and discussed. The measurements were compared with theory and results from other researchers. The results obtained from our system shows consistency with other researchers' results. In addition, the single pulse waveform is analyzed based on characters described in TCPD and cardiovascular diagnosis. The analysis provides ideas towards a future expert system for pattern identification and classification.

Chapter 5 Conclusion and future work

5.1 Conclusion

In this thesis work, research in a wireless sensor system towards individual home healthcare and using the Traditional Chinese Pulse Diagnosis (TCPD) technique is proposed. This designed and constructed system can continuously measure real-time radial artery waveforms. The measurements can then be transmitted wirelessly to a personal computer (PC) for data processing and classification. Once analyzed, the waveform obtained contains significant health-related information. Analyses are performed using the overall wave pattern as well as the single pulse. Measured results show consistency between measured and typical TCPD patterns. In addition, proper single pulse analysis can provide useful insights into cardiovascular health. This research work is innovative because it is a solid attempt at applying TCPD into individual home healthcare.

The system designed consisted of three components: data acquisition, control and wireless transmission units. The data acquisition unit features a novel design which employs three parallel liquid-filled digital piezoresistive pressure sensor modules. They collect radial pulse waveform from Cun, Guan and Chi. The liquid-filled method is used to firstly, simulate doctor's finger tips; secondly, to reduce the discomfort introduced by using solid transducer; and thirdly, but most importantly, to limit the off-axis loading problem incurred using a force transducer.

The control unit consists of four microcontrollers operating at 3V. They are designed to ensure synchronized data acquisition from Cun, Guan and Chi. This is important since in TCPD, certain pulse examinations are conducted simultaneously on the three points. The three sub-level microcontrollers are directly connected with three sensor modules to read pressure measurements. These are controlled by a master-level microcontroller for data acquisition, signals acquisition cycle, temporary storage and to establish communication with wireless transceiver unit.

The wireless transceiver unit includes two 2.4GHz Zigbee transceivers that are operating at 3V. One transceiver is connected to the master-level microcontroller and the other is connected to PC RS232 port through an adapter. The transmission rate is set to 19.2 kBps for minimum USART error rate [59]. The wireless function is verified with the cable transmission results.

The measurements from this system are discrete radial artery tonometry pressure sampled at 50ms interval and the temperature of the liquid. Measurement subjects are adults with ages ranging from 23 to 56 years. The waveforms are reproduced on a PC from discrete measurements. The measurements are consistent with published peripheral radial artery waveforms of other researchers. Several analyses are conducted. These include pulse pattern matching, parameter extraction and comparison. Measured waveforms are compared with TCPD typical patterns and certain consistencies between "Normal" pattern and "Wiry" pattern are found. In addition, several parameters are extracted from the waveforms. They are diastolic baseline pressure, systolic peak pressure, late systolic shoulder and reflected peak pressure. Based on these extracted parameters, the following information are determined: time delay between systolic peak and reflected peak, rise time between diastolic baseline and systolic peak, and augmentation index. The analyzed results show rise time between diastolic baseline to systolic peak is significantly shorter in younger persons with stronger hearts than in older persons with weaker hearts. Also the augmentation index is higher for older stiffer artery than younger less stiff artery.

The system operates from 3V supply and has a current consumption of 12mA when in active require of acquisition; and 3mA when idle. The radial artery pulse and body surface temperature have been successfully recorded and transmitted wirelessly. The prototype system and analyses approaches provide helpful insight into how TCPD may be incorporated into individual home healthcare.

5.2 Future work

The work performed in this thesis demonstrated the concept of an individual home healthcare monitoring system using Traditional Chinese Pulse Diagnosis. The wireless sensor system was designed and constructed using commercial off-the-shelf components. Using the experience gained form this research work, several recommendations for further improvements are now provided.

First, a digital pressure sensor with a faster analog-to-digital converter (ADC) should be used. The sensor used in this work has excellent performance, but a fairly low ADC conversion rate, which is 35ms minimum. This limits the sampling rate of radial pulse and therefore limits the quality of reproduced waveform. One alternative is to use the sensor with the same performance, but with a separate ADC. However, this approach may increase the chances of errors in data processing, and also increase the power consumption. If the approach is considered, the trade-off between every aspect of performance need to a carefully studied.

Second, better membranes should be used. The membrane used in this work is rubber latex. The elastic property of the rubber latex suits our application well. However, it has two major disadvantages. The first one is the pore size. Rubber latex has pore sizes about 5 microns. Depending the liquid being used, the rubber latex membrane may gradually leak over time. The second is that the rubber latex tends to naturally deteriorate when exposed in air. Through experimentation, it was observed that the working lifetime of rubber latex in our system is about two weeks. Therefore, membranes with smaller pore size and longer lifetime should be used.

Third, better expert knowledge should be obtained if an expert classification and diagnostic system is required. This knowledge includes pulse quantification scheme, standard rules for pulse pattern classification, and rules for TCPD three points differential analysis. In this work, the three-point differential analysis did lead to significant conclusions. The knowledge should be obtained from the doctor and clinical researches and "encoded" in software.

Fourth, optimization of the firmware in the system and software analysis on the PC is required so that more stable waveforms over repeating measurements can be obtained. One obstacle to stable waveform is baseline wandering due to motion artefacts. Motion artefacts are caused by the subject's movement or incorrect placement of the device. They will introduce noise to the baseline of the waveform. Therefore, an adaptive baseline wandering removal technique is recommended for this system.

Fifth, the ultimate goal of this research is to integrate this wireless sensor system into a complete home healthcare monitoring systems. One possible scheme of complete system is shown below (Figure 5-1).

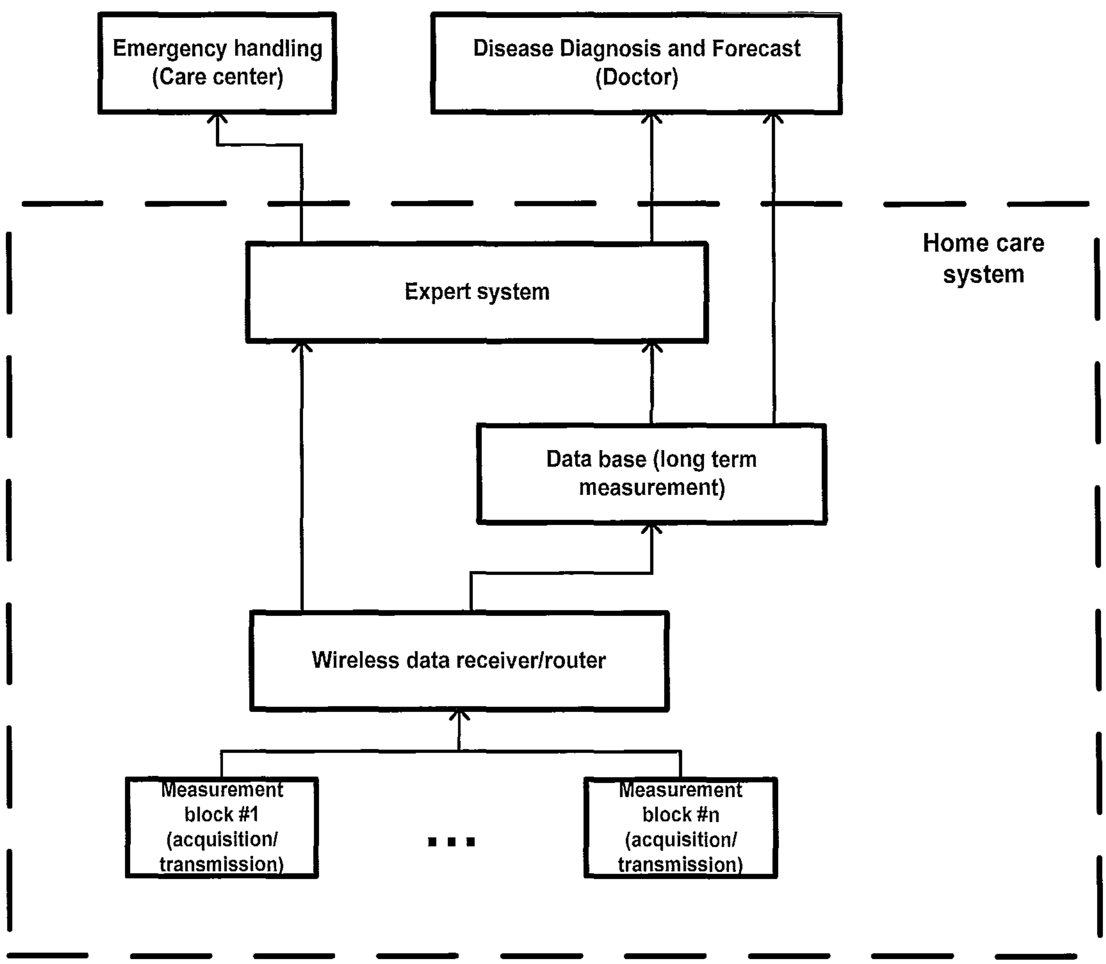

Figure 5-1 Block diagram for home care system

The work done in this thesis includes one measurement block, wireless data transceivers, data logging and basic data analysis. It therefore only contributes to part of the complete home healthcare system.

References

[1] F. Castanie, C. Maihes and M. Ferhaoui, "The U-R-Safe project: A multidisciplinary approach for fully 'nomad' care of patients," *SETIT*, Tunisia, March17-21, 2003.

[2] Martin Turcotte and Grant Schellenberg, "A portrait of seniors in Canada." *Statistic Canada*, Cat. no. 89-519-XIE. Ottawa: Statistics Canada, 1999.

[3] "Population projections for Canada, provinces and territories 2000 to 2026," *Statistics Canada*. Cat. No. 91-520-XPB. Ottawa: Statistics Canada, 2001.

[4] Canadian Institute for Health Information, National Health Expenditure Database (Ottawa, Ont.: CIHI, 2008).

[5] Canadian Institute for Health Information, National Health Expenditure Trends, 1975–2007 (Ottawa, Ont.: CIHI, 2007).

[6] Canadian Institute for Health Information, "Provincial and Territorial Government Health Expenditure by Age Group, Sex and Major Category. Recent and Future Growth Rates." *CIHI*, 2005.

[7] E. Duthie, "Falls," *Medical Clinics of North America*, Vol. 73, pp. 1321–1335, 1989.

[8] A. Sixsmith and N. Johnson. "A smart sensor to detect the falls of the elderly," *IEEE Pervasive Computing*, Volume 3, Issue 2, pp. 42-47, April-June 2004

[9] D.E. Allen, "Building Vibrations from Human Activities." *Concrete International: Design and Construction*, American Concrete Institute, Vol. 12, No. 6. pp. 66-73, 1990.

[10] Majd Alwan , Prabhu Jude Rajendran, Steve Kell, David Mack , Siddharth Dalal, Matt Wolfe and Robin Felder "A Smart and Passive Floor-Vibration Based Fall Detector for Elderly" *Department of Electrical and Computer Engineering, University of Virginia*, 2006.

[11] Earl E. Bakken. "Timeline of Earl E. Bakken." Earl E. Bakken 2006 http://www.earlbakken.com/content/timeline/timeline.html

[12] Peng Cong, Darrin J. Young, and Wen H. Ko, "Novel Long-Term Implantable Blood Pressure Monitoring System." *Proceedings of IEEE Sensors Conference*,. Vol. 3, pp. 1359-1362, 24-27 Oct. 2004.

[13] F. L. Wuyts, V. J Vanhuyse, G. J. Langewouters, W. F. Decraemer, E. R. Raman, and S. Buyle, "Elastic Properties of Human Aortas in Relation to Age and Atherosclerosis: a Structural model," *Phys. Med. Biol.*, Vol. 40, pp. 1577-1597, 1995.

[14] R. G. Gosling and M. M. Budge, "Terminology for Describing the Elastic Behavior of Arteries," *Hypertension*, Vol. 41, No. 6, pp. 1180-1182, June 2003.

[15] Thomas Degen, Heinz Jaeckel, Michael Rufer and Stefan Wyss, "SPEEDY: A Fall Detector in a Wrist Watch," *Electronic Laboratory, Swiss Federal Institute of Technology*, Switzerland, 2003.

[16] Bob Flaws, "The secret of Chinese pulse diagnosis", *Blue Poppy Pr*, 2 edition, 1995

[17] Huiyan Wang, Yiyu Cheng, "A quantitative system for pulse diagnosis in Traditional Chinese Medicine," *Proceedings of the 2005 IEEE Engineering in Medicine and Biology 27th Annual Conference,* Shanghai, China, September 1-4, 2005.

[18] Lisheng Xu, "Modern Researches on Pulse Waveform of TCPD." *IEEE 2002 International Conference on Communications, Circuits and Systems and West Sino Expositions*, June 29- July 1 2002.

[19] H. L. Lee, S. Suzuki, Y. Adachi, M. Umeno and Shan K, "Fuzzy Theory in Traditional Chinese Pulse Diagnosis," *Proceeding of International Joint Conference on Neural Networks*, Nagoya, Japan, vol. 10, pp. 774-778, 1993.

[20] Y. Z. Yoon, M. H. Lee and K. S. Soh., "Pulse Type Classification by Varying Contact Pressure," *IEEE Engineering in Medicine and Biology Magazine*, vol. 19, pp. 106-110, 2000.

[21] B. H. Wang and X. J. Lin, "Detecting system and power-spectral analysis of pulse signals of human body," *Fourth International Conference on Signal Processing*, vol. 2, pp. 1646 - 1649, 1998.

[22] S. E. Fu and S. P. Lai, "A system for pulse measurement and analysis of Chinese medicine," *Proceedings of the Annual International Conference of the IEEE Engineering in Medicine and Biology Society*, vol. 5, pp. 1695-1696, 1989.

[23] The SphygmoCor system, AtCor medical. http:// www.atcormedical.com

[24] C. C. Chiu, S.J. Yeh and Y.C. Yu, "Classification of the pulse signals based on self-organizing neural network for the analysis of the autonomic nervous system," *Chinese Journal of Medical and Biological Engineering*, vol. 16, pp. 461- 476, 1996.

[25] Illustration of the positions of Cun, Guan and Chi. http://www.tcm-kelker.de

[26] Jian-Jun Shu, Yuguabg Sun, "Developing classification indices for Chinese pulse diagnosis", *Complementary Therapies in Medicine*. vol.15, pp. 190—198, Aug. 2006

[27] BQ, Huang, "Discussion on the Identification of Pulse Tracings." *Guiding Journal of TCM*, vol. 12, No.5, May 2006

[28] Lu WA, Wang YYL, and Wang WK, "Pulse Analysis of Patients with severe Liver problems," *IEEE Eng MedBol Mag*, Vol. 18, Issue 1, pp. 73-75, 1999

[29] The human body -- the radial artery www.theodora.com/anatomy/the_radial_artery.html

[30] "Blood pressure." *Wikipedia*

[31] Saima Chaudhry, "Hypertension and its management in diabetics and ethnic minorities." *Journal of student medical science*, Vol1, Issue1, Apr 5th 2009

[32] Cardiac catheterization, *The New York Times Company* http://www.nytimes.com/imagepages/2007/08/01/health/adam/18143Leftheartcatheterization.html

[33] Auscultatory method of measuring the blood pressure, ADInstrument, http://www.adinstruments.com/solutions/experiments/labtutor_experiments/full.php?exp_id=161&section_id=14&name_id=205&template=teaching.

[34] Yury L. Shevchenko, MD; Joshua E. Tsitlik, PhD, "90th Anniversary of the Development by Nikolai S. Korotkoff of the Auscultatory Method of Measuring Blood Pressure" *Circulation*, Vol. 94, pp. 116-118, 1996.

[35] Patrick Davey, Stephen CP Collins, "Blood pressure measurement." Net Doctor

[36] H. Goldman, TH. Schmidt, "Uber Applanations-tonometrie", *Ophthalmologica.* Vol. 134, pp. 221-242, 1957.

[37] R. Kelly, M. Karamanoglu, H. Gibbs, AP. Avolio, MF. O'Rourke, "Noninvasive carotid pressure wave registration as an indicator of ascending aortic pressure." *J Vasc Med Biol.* Vol. 1, pp. 241-247, 1989

[38] R. Kelly, C. Hayward, J. Ganis, J. Daley, A. Avolio, M. O'Rourke, "Noninvasive registration of the arterial pressure pulse waveform using high-fidelity applanation tonometry." *J Vasc Med Biol*, Vol. 1, pp.142-149, 1989.

[39] GM. Drzewiecki, J. Melbin, A. Noordergraaf, "Arterial tonometry review and analysis." *J Biomech*, Vol. 16, pp. 141-152, 1983.

[40] Chen CH, Ting CT, Nussbacher A, Nevo E, Kass DA, Pak P, Wang SP, Chang MS, Yin FCP. "Validation of carotid artery tonometry as a means of estimating augmentation index of ascending aortic pressure." *Hypertension.* Vol. 27, pp.168-175, 1996.

[41] Chen-Huan Chen, Erez Nevo, Barry Fetics, H. Pak. Peter, C.P. Yin Frank W. Lowell Maughan, A. Kass David, "Estimation of Central Aortic Pressure Waveform by Mathematical Transformation of Radial Tonometry Pressure." *Circulation.* Vol. 95, pp. 1827-1936, 1997.

[42] AL. Pauca, SL. Wallenhaupt, ND. Kon, WY. Tucker, "Does radial artery pressure accurately reflect aortic pressure?" *Chest*, Vol. 102 1193-1198, 1992.

[43] Karamanoglu M, O'Rourke MF, Avolio AP, Kelly RP. "An analysis of the relationship between central aortic and peripheral upper limb pressure waves in man." *Eur Heart J.* Vol. 14, pp. 160-167, 1993.

[44] Ljung L. "System Identification: Theory for the User." *NJ: Prentice Hall,* 1st ed., 1987.

[45] Philippe Renevey, Rolf Vetter, Jens Krauss, Patrick Celka and Yves Depeursinge, "Wrist-Located pulse detection using IR signals, activity and nonlinear artifact cancellation," *Proceedings of the 23rd Annual EMBS international Conference*, October 25-28, Istanbul, Turkey, 2001

[46] "blood oxygenation." *Wikipedia*

[47] "Pulse oximetry." *Wikipedia*

[48] Jae Min Kang, Taiwoo Yoo, and Hee Chan Kim, "A Wrist-Worn Integrated Health Monitoring Instrument with a Tele-Reporting Device for Telemedicine and Telecare," *IEEE Transactions on Instrumentation and Measurement*, Vol. 55, No. 5, October 2006

[49] Jug-Man Hwang, Jung-Min Park, and Seong-Dok Park, "Wrist-Located Pulse Detection using IR Reflection due to Pulse Added Volume of Arterial Blood." *3rd International Conference on Computational Electromagnetics and Its Applications Proceedings*, pp. 438-441, 2004

[50] Berkow, Robert. The Merck Manual of Medical Information. New Jersey: Merck, 1997.

[51] Honeywell Model 13 Subminiature load cell

[52] Wikipedia, "Load cell"

[53] Wikipedia, "Strain gauge"

[54] "Wheatstone bridge circuit" *Daytronic.* http:// www.daytronic.com/products/trans/t-loadcells.htm

[55] Wikipedia, "Piezoelectric effect"

[56] Tekscan FlexiForce specification. http://www.tekscan.com/flexiforce/flexiforce.html

[57] Jukka Hast. "Self-mixing interferometry and its applications in noninvasive pulse detection" *Department of Electrical and Information Engineering, University of Oulu.* 2003.

[58] Intersema, "MS5536C SMD Gage Pressure MODULE", Datasheet 2008.

[59] Atmel, "8-bit AVR with 8K Bytes In-System programmable flash, Atmega8L", Datasheet 2007

[60] Atmel ATMega8L http://www.solarbotics.com/assets/images/atmega8l/atmega8l_pl.jpg

[61] Nick Baker, "Bluetooth strengths and weaknesses for industrial applications" *IEEE Computing & Control Engineering,* Vol. 16, Issue 2, pp. 20-25, 2005

[62] Jin-Shyan Lee, Yu-Wei Su, Chung-Chou Shen, "A comparative study of wireless protocols: Bluetooth, UWB, ZigBee and Wi-Fi", *The 33rd Annual Conference of IEEE Industrial Electronics Society (IECON)* Nov. 5-8, 2007, Taipei, Taiwan

[63] D. Porcino and W. Hirt, "Ultra-wideband radio technology: Potential and challenges ahead," *IEEE Commun. Mag.*, vol. 41, no. 7, pp. 66-74, July 2003.

[64] J. S. Lee, "Performance evaluation of IEEE 802.15.4 for low-rate wireless personal area networks," *IEEE Trans. Consumer Electron.*, vol.52, no. 3, pp. 742-749, Aug. 2006

[65] J. S. Lee and Y. C. Huang, "ITRI ZBnode: A ZigBee/IEEE 802.15.4 platform for wireless sensor networks," *in Proc. IEEE Int. Conf. Systems,Man & Cybernetics*, pp. 1462-1467, Taipei, Taiwan, Oct. 2006

[66] Digi, "XBEE 802.15.4 2.4G ZigBee wireless transceiver," Datasheet 2008.

[67] Cardio pulse waveform http://www.proargi9store.com/index.php/category/cardio-pulse-wave

[68] Bryan Williams, "Measurement of Ambulatory Central Aortic Pressure in Clinical Trials using the BPro™ Device" *Department of Cardiovascular Sciences University of Leicester School of Medicine*, United Kingdom August 2008

[69] Motohiro Shimizu and Kazuomi Kario, "Role of augmentation index in hypertension." *Therapeutic Advances in Cardiovascular Disease,* Vol. 2, Issue 1, pp. 25-35, 2008

[70] Patrick Segers; Ahmad Qasem; Tine De Backer; Stephane Carlier; Pascal Verdonck; Albert Avolio. "Peripheral Oscillatory Compliance Is Associated With Aortic Augmentation Index." *Hypertension.* Vol. 37, pp.1434, 2001

[71] J. Nürnberger, A. Keflioglu-Scheiber, AM. Opazo Saez , RR. Wenzel, T. Philipp, RF. Schäfers. "Augmentation index is associated with cardiovascular risk." *Journal of Hypertension.* Vol. 20, Issue 12, pp. 2337-2340, 2002.

[72] Shahzad Munir, Antoine Guilcher, Tamra Kamalesh, Brian Clapp, Simon Redwood, Michael Marber, Philip Chowienczyk. "Peripheral Augmentation Index Defines the Relationship Between Central and Peripheral Pulse Pressure" *Hypertension,* Vol. 51, pp. 112-118, 2008

Appendix

A.1 Firmware for designed sensor module system

LowLv_1.h

```
/*
#ifndef F_CPU
#define F_CPU 2000000UL
#endif
*/
#include <avr/io.h>
#include <util/delay.h>
#include <avr/pgmspace.h>

#define USART_BAUDRATE      19200//error rate .2
#define BAUD_PRESCALE       (((F_CPU/(USART_BAUDRATE * 16UL)))-1)
#define Data_Ready 0x01;
#define TxData_Ready 0x02;
#define Para_Ready 0x04;

//typedef struct{
        volatile uint8_t Tx[5]; // |source|count|D1H|D1L|checksum|
//      }SD;// Shifting_Data

//typedef struct{
        volatile uint8_t C0_H[6];
        volatile uint8_t C0_L[6];
        volatile uint8_t C1_H[6];
        volatile uint8_t C1_L[6];
        volatile uint8_t C2_H[6];
        volatile uint8_t C2_L[6];
        volatile uint8_t D2H[3];
        volatile uint8_t D2L[3];
//}Parameters; //Sensor_Parameters

/*int IsEmpty(Queue );
int IsFull(Queue );
Queue CreateQueue(prog_int16_t );
void DisposeQueue(Queue );
void MakeEmpty(Queue );
void EnQueue(prog_uchar , Queue );
prog_char Front(Queue Q);
void Dequeue (Queue Q);
prog_char FrontAndDequeue(Queue Q);
*/
```

LowLv_1.c

```
//Device: ATmega8L
//Function: read sensor via SPI, send data via USART to Top level
//Name: LowLv_1
//Function: initiate Shifting_Data
```

```
#include <avr/io.h>
//#include<util/delay.h>
#include<avr/pgmspace.h>
#include<stdlib.h>
#include<avr/interrupt.h>
#include<avr/sleep.h>
#include"LowLv_1_ver3.h"
static const prog_int16_t MaxElements = 256;

void MCLK_ON(void);
void MCLK_OFF(void);
void SPI_MasterInit(void);
void SPI_MasterTransmit(uint8_t);
void USART_Init(void);
void USART_SendByte(uint8_t);
uint8_t USART_ReceiveByte(void);

//data saved in rom

static prog_uchar
	read_D1H=0x0f,
	read_D1L=0x40,//read pressure measurement

	read_D2H=0x0f,
	read_D2L=0x20,//read temperature measurement

	read_W1H=0x1d,
	read_W1L=0x50,//read calibration word 1

	read_W2H=0x1d,
	read_W2L=0x60,//read calibration word 2

	read_W3H=0x1d,
	read_W3L=0x90,//read calibration word 3

	read_W4H=0x1d,
	read_W4L=0xa0,//read calibration word 4

	reset_1=0x15,
	reset_2=0x55,
	reset_3=0x40;//reset sequence

//initial calibration data read from sensor
volatile uint8_t W1H,W2H,W3H,W4H, W1L,W2L,W3L,W4L;

//system flags
volatile uint8_t flags;

int main(void){
	int i=0;
	flags &= ~Data_Ready;
	flags &= ~TxData_Ready;
	flags &= ~Para_Ready;
	cli();
```

```
	SPI_MasterInit();
	MCLK_ON();
//	set_sleep_mode(SLEEP_MODE_PWR_DOWN);
	USART_Init();
	SPCR &= ~(1<<CPHA);
	MCUCR = (1<<ISC01) | (1<<ISC00); //rising edge on INT0 generates interrupt
	GICR |= (1<<INT0); //enable INT0
	DDRC = ~(1<<PC0) & ~(1<<PC1); // status light on PINC0 and PINC1, 00:IDLE 01:send
calibration data 11:send measurement
	for(i=0;i<5;i++){
		Tx[i] = 0;
	}
	Tx[0] = 0x11; //source: slave unit #1
	Tx[1] = 0xff;

	SPI_MasterTransmit(reset_1);
	SPI_MasterTransmit(reset_2);
	SPI_MasterTransmit(reset_3);

	SPI_MasterTransmit(read_W1H);
	SPI_MasterTransmit(read_W1L);

	SPCR |= (1<<CPHA);// transmit at falling edge
	SPI_MasterTransmit(0x00);
	W1H=SPDR;
	SPI_MasterTransmit(0x00);
	W1L=SPDR;

	SPCR &= ~(1<<CPHA);
	SPI_MasterTransmit(read_W2H);
	SPI_MasterTransmit(read_W2L);

	SPCR |= (1<<CPHA);// transmit at falling edge
	SPI_MasterTransmit(0x00);
	W2H=SPDR;
	SPI_MasterTransmit(0x00);
	W2L=SPDR;

	SPCR &= ~(1<<CPHA);
	SPI_MasterTransmit(read_W3H);
	SPI_MasterTransmit(read_W3L);

	SPCR |= (1<<CPHA);// transmit at falling edge
	SPI_MasterTransmit(0x00);
	W3H=SPDR;
	SPI_MasterTransmit(0x00);
	W3L=SPDR;

	SPCR &= ~(1<<CPHA);
	SPI_MasterTransmit(read_W4H);
	SPI_MasterTransmit(read_W4L);

	SPCR |= (1<<CPHA);// transmit at falling edge
	SPI_MasterTransmit(0x00);
```

```
            W4H=SPDR;
            SPI_MasterTransmit(0x00);
            W4L=SPDR;
/*
//          MCLK_ON();
            SPCR &= ~(1<<CPHA);
            SPI_MasterTransmit(read_D2H);
            SPI_MasterTransmit(read_D2L);
            SPCR |= (1<<CPHA);// transmit at falling edge

            SPI_MasterTransmit(0x00);
            Init_Para->D2H[0]=SPDR;
            SPI_MasterTransmit(0x00);
            Init_Para->D2L[0]=SPDR;
*/
/////////////////extract C1..C6/////////////

            C0_H[0] = (0x10 & (W4H>>3)) | (0x0f & W3H); //unit 1, C1
            C0_L[0] = W3L;

            C0_H[1] = (0x1f & W4H);//unit 1, C2
            C0_L[1] = W4L;

            C0_H[2] = (0x01 & (W4H>>5));//unit 1, C3
            C0_L[2] = W1H;

            C0_H[3] = (0x01 & (W4H>>6));//unit 1, C4
            C0_L[3] = W2H;

            C0_H[4] = (0x0f & (W3H>>4));//unit 1, C5
            C0_L[4] = W1L;

            C0_H[5] = 0x00;//unit 1, C6
            C0_L[5] = W2L;

            flags |= Para_Ready;

            sei();
//check status light before sending, only 01 may pass
            for(;;){
                        if(( (PINC&(1<<PINC1)) && (!(PINC&(1<<PINC0))) ) ){
                                    if(flags & Para_Ready){
                                                for (i=0;i<6;i++){
                                                            USART_SendByte(C0_H[i]);
                                                }
                                                for (i=0;i<6;i++){
                                                            USART_SendByte(C0_L[i]);
                                                }
                                                flags &= ~Para_Ready;
                                    }
                        }

                        //calculate checksum: sum Tx
                        if(flags & Data_Ready){
```

```
                for(i=0;i<3;i++){
                        Tx[4]=Tx[i]+Tx[4];
                }
                flags &= ~Data_Ready;
                flags |= TxData_Ready;
        }

        if((PINC&(1<<PINC1)) && (PINC&(1<<PINC0))){
                if(flags & TxData_Ready){
                        for(i=0;i<5;i++){
                                USART_SendByte(Tx[i]);
                        }
                        Tx[1]++;

                        if(Tx[1] == 255){
                                Tx[1] = 0;
                        }
                        flags &= ~TxData_Ready;
                }
        }
    }
    return 0;
}

ISR(INT0_vect){
    cli();
//read sensor
    SPCR |= (1<<CPHA);// read at falling edge
    SPI_MasterTransmit(0x00);
    Tx[2]=SPDR;
    SPI_MasterTransmit(0x00);
    Tx[3]=SPDR;

//signal the next reading
    SPCR &= ~(1<<CPHA);
    SPI_MasterTransmit(read_D1H);
    SPI_MasterTransmit(read_D1L);

    flags |= Data_Ready;
    sei();
}


void SPI_MasterInit(void){
    SPCR = (1<<SPE) | (1<<MSTR); // enable SPI, Master mode
//  SPCR &= ~(1<<CPOL); // SCK is low when idle
    SPSR |= (1<<SPI2X);//SCK is 500kHz
    DDRB = (1<<PB2) | (1<<PB3) | (1<<PB5); // set SS (PB2), MOSI (PB3), SCK (PB5) as output
//  DDRB |= (1<<PB6);
//  SFIOR |= (1<<PUD);
    PORTB=0x00;


}
```

```
void SPI_MasterTransmit(uint8_t Data){
            SPDR = Data;
            while (!(SPSR & (1<<SPIF)))
                        ;
}

void USART_Init(void)
{
   //Enable USART
            UCSRB = (1<<RXEN) | (1<<TXEN);
            //Define bit length
            UCSRC = (1<<URSEL) | (1<<UCSZ1) | (1<<UCSZ0);
            // Set baud rate TO 9600
            UBRRL = BAUD_PRESCALE;
            UBRRH = (BAUD_PRESCALE >> 8);
}

void USART_SendByte(uint8_t u8Data)
{
   // Wait if a byte is being transmitted
   while((UCSRA&(1<<UDRE)) == 0)
   {
      ;
   }

   // Transmit data
   UDR = u8Data;
}

/*
uint8_t USART_ReceiveByte( void )
{
            //Wait for data to be received
            while ( !(UCSRA & (1<<RXC)) )
                        ;
            // Get and return received data from buffer
            return UDR;
}
*/


void MCLK_ON(void){

            DDRB |= (1<<DDB1);
            OCR1AL = 0x0e; //Opt_freq= 32.768kHz, Set_freq=35.714kHz, Observed_freq=33kHz
            OCR1AH = 0x00;
            TCCR1A |= (1<<COM1A0); // CTC MODE, TOGGLE OC1A, NO PRESCALE
            TCCR1B = (1<<WGM12) | (1<<CS10);
}

void MCLK_OFF(void){

            TCCR1B &= ~(1<<CS10);
```

```
}
```

LowLv_2.h

```
//Device: ATmega8L
//Function: read sensor via SPI, send data via USART to Top level
//Name: LowLv_2
//Function: initiate Shifting_Data
#include <avr/io.h>
#include<util/delay.h>
#include<avr/pgmspace.h>
#include<stdlib.h>
#include<avr/interrupt.h>
#include<avr/sleep.h>
#include"LowLv_1_ver3.h"
static const prog_int16_t MaxElements = 256;

void MCLK_ON(void);
void MCLK_OFF(void);
void SPI_MasterInit(void);
void SPI_MasterTransmit(uint8_t);
void USART_Init(void);
void USART_SendByte(uint8_t);
void Status_Light_Init(void);
void Status_Receive_Para(void);
void Status_Reveive_Data(void);
uint8_t USART_ReceiveByte(void);

//data saved in rom
static prog_uchar
        read_D1H=0x0f,
        read_D1L=0x40,//read pressure measurement

        read_D2H=0x0f,
        read_D2L=0x20,//read temperature measurement

        read_W1H=0x1d,
        read_W1L=0x50,//read calibration word 1

        read_W2H=0x1d,
        read_W2L=0x60,//read calibration word 2

        read_W3H=0x1d,
        read_W3L=0x90,//read calibration word 3

        read_W4H=0x1d,
        read_W4L=0xa0,//read calibration word 4

        reset_1=0x15,
        reset_2=0x55,
        reset_3=0x40;//reset sequence

//initial calibration data read from sensor
volatile uint8_t W1H,W2H,W3H,W4H, W1L,W2L,W3L,W4L;
```

```
volatile uint8_t ECHO;

//presusre data queue
volatile SD *P;
volatile Parameters *Init_Para;
//P->addr=0x00;

int main(void){
	int i=0;
	cli();
	SPI_MasterInit();
	MCLK_ON();
	USART_Init();
	SPCR &= ~(1<<CPHA);
	MCUCR = (1<<ISC01) | (1<<ISC00); //rising edge on INT0 generates interrupt
	GICR |= (1<<INT0); //enable INT0
	Status_Light_Init();
	P->count[1]=0xff;
	ECHO=0x00;

	SPI_MasterTransmit(reset_1);
	SPI_MasterTransmit(reset_2);
	SPI_MasterTransmit(reset_3);

	SPI_MasterTransmit(read_W1H);
	SPI_MasterTransmit(read_W1L);

	SPCR |= (1<<CPHA);// transmit at falling edge
	SPI_MasterTransmit(0x00);
	W1H=SPDR;
	SPI_MasterTransmit(0x00);
	W1L=SPDR;

	SPCR &= ~(1<<CPHA);
	SPI_MasterTransmit(read_W2H);
	SPI_MasterTransmit(read_W2L);

	SPCR |= (1<<CPHA);// transmit at falling edge
	SPI_MasterTransmit(0x00);
	W2H=SPDR;
	SPI_MasterTransmit(0x00);
	W2L=SPDR;

	SPCR &= ~(1<<CPHA);
	SPI_MasterTransmit(read_W3H);
	SPI_MasterTransmit(read_W3L);

	SPCR |= (1<<CPHA);// transmit at falling edge
	SPI_MasterTransmit(0x00);
	W3H=SPDR;
	SPI_MasterTransmit(0x00);
	W3L=SPDR;

	SPCR &= ~(1<<CPHA);
```

```
        SPI_MasterTransmit(read_W4H);
        SPI_MasterTransmit(read_W4L);

        SPCR |= (1<<CPHA);// transmit at falling edge
        SPI_MasterTransmit(0x00);
        W4H=SPDR;
        SPI_MasterTransmit(0x00);
        W4L=SPDR;

        MCLK_ON();
        SPCR &= ~(1<<CPHA);
        SPI_MasterTransmit(read_D2H);
        SPI_MasterTransmit(read_D2L);
        SPCR |= (1<<CPHA);// transmit at falling edge

        SPI_MasterTransmit(0x00);
        Init_Para->D2H[1]=SPDR;
        SPI_MasterTransmit(0x00);
        Init_Para->D2L[1]=SPDR;

////////////////extract C1..C6////////////
        Init_Para->C1_H[0] = (0x10 & (W4H>>3)) | (0x0f & W3H); //unit 1, C1
        Init_Para->C1_L[0] = W3L;

        Init_Para->C1_H[1] = (0x1f & W4H);//unit 1, C2
        Init_Para->C1_L[1] = W4L;

        Init_Para->C1_H[2] = (0x01 & (W4H>>5));//unit 1, C3
        Init_Para->C1_L[2] = W1H;

        Init_Para->C1_H[3] = (0x01 & (W4H>>6));//unit 1, C4
        Init_Para->C1_L[3] = W2H;

        Init_Para->C1_H[4] = (0x0f & (W3H>>4));//unit 1, C5
        Init_Para->C1_L[4] = W1L;

        Init_Para->C1_H[5] = 0x00;//unit 1, C6
        Init_Para->C1_L[5] = W2L;

//receive calibration data from U1
        PORTC |= (1<<PORTC1); //set status light to 01
//send initial parameters, i.e C1..6 and temperature

        for (i=0;i<6;i++){
                Init_Para->C0_H[i] = USART_ReceiveByte();
        };
        for (i=0;i<6;i++){
                Init_Para->C0_L[i] = USART_ReceiveByte();
        };
        Init_Para->D2H[0] = USART_ReceiveByte();
        Init_Para->D2L[0] = USART_ReceiveByte();

        PORTC &= ~(1<<PORTC1);
//start sending initial parameters
```

```
	while ( !((PINC&(1<<PINC2))==0 && (PINC&(1<<PINC3))==1)){
				;
	}

	for (i=0;i<6;i++){
		USART_SendByte(Init_Para->C0_H[i]);
	};
	for (i=0;i<6;i++){
		USART_SendByte(Init_Para->C0_L[i]);
	};
	USART_SendByte(Init_Para->D2H[0]);
	USART_SendByte(Init_Para->D2L[0]);

	for (i=0;i<6;i++){
		USART_SendByte(Init_Para->C1_H[i]);
	};
	for (i=0;i<6;i++){
		USART_SendByte(Init_Para->C1_L[i]);
	};
	USART_SendByte(Init_Para->D2H[1]);
	USART_SendByte(Init_Para->D2L[1]);
	//note: loop forever if no responce from U3

	MCLK_OFF();
	set_sleep_mode(SLEEP_MODE_PWR_DOWN);
	sei();
	sleep_mode();

	return 0;
}

ISR(INT0_vect){
	cli();
//read sensor
	SPCR |= (1<<CPHA);// read at falling edge
	SPI_MasterTransmit(0x00);
	P->D1H[1]=SPDR;
	SPI_MasterTransmit(0x00);
	P->D1L[1]=SPDR;

//signal the next reading
	SPCR &= ~(1<<CPHA);
	SPI_MasterTransmit(read_D1H);
	SPI_MasterTransmit(read_D1L);

	PORTC = (1<<PORTC0) | (1<<PORTC1); //set status light to 11
//pass data
	P->count[0] = USART_ReceiveByte();
	P->D1H[0] = USART_ReceiveByte();
	P->D1L[0] = USART_ReceiveByte();
//	_delay_ms(10);

	while(!((PINC&(1<<PINC2))==1 && (PINC&(1<<PINC3))==1)){
		;
```

```
        }
        USART_SendByte(P->count[0]);
        USART_SendByte(P->D1H[0]);
        USART_SendByte(P->D1L[0]);
        USART_SendByte(P->count[1]);
        USART_SendByte(P->D1H[1]);
        USART_SendByte(P->D1L[1]);

        if(P->count[1] == 255)
                P->count[1] = 0;

        P->count[1]++;
        sei();

}


void SPI_MasterInit(void){
        SPCR = (1<<SPE) | (1<<MSTR); // enable SPI, Master mode
//      SPCR &= ~(1<<CPOL); // SCK is low when idle
        SPSR |= (1<<SPI2X);//SCK is 500kHz
        DDRB = (1<<PB2) | (1<<PB3) | (1<<PB5); // set SS (PB4), MOSI (PB5), SCK (PB7) as output
//      DDRB |= (1<<PB6);
//      SFIOR |= (1<<PUD);
        PORTB=0x00;


}

void SPI_MasterTransmit(uint8_t Data){
        SPDR = Data;
        while (!(SPSR & (1<<SPIF)))
                ;
}

void USART_Init(void)
{
  //Enable USART
        UCSRB = (1<<RXEN) | (1<<TXEN);
        //Define bit length
        UCSRC = (1<<URSEL) | (1<<UCSZ1) | (1<<UCSZ0);
        // Set baud rate TO 9600
        UBRRL = BAUD_PRESCALE;
        UBRRH = (BAUD_PRESCALE >> 8);
}

void USART_SendByte(uint8_t u8Data)
{
  // Wait if a byte is being transmitted
  while((UCSRA&(1<<UDRE)) == 0)
  {
    ;
  }
```

```
   // Transmit data
   UDR = u8Data;
}


uint8_t USART_ReceiveByte( void )
{
        /* Wait for data to be received */
        while ( !(UCSRA & (1<<RXC)) )
                ;
        /* Get and return received data from buffer */
        return UDR;
}



void MCLK_ON(void){

        DDRB |= (1<<DDB1);
        OCR1AL = 0x0e; //Opt_freq= 32.768kHz, Set_freq=35.714kHz, Observed_freq=33kHz
        OCR1AH = 0x00;
        TCCR1A = (1<<COM1A0) | (1<<CS00); // CTC MODE, TOGGLE OC1A, NO PRESCALE
        TCCR1B = (1<<WGM12) | (CS10);
}

void MCLK_OFF(void){

        TCCR0 &= ~(1<<CS10);
}

void Status_Light_Init(void){
        DDRC = (1<<DDC0) | (1<<DDC1);
        DDRC = ~(1<<DDC2) & ~(1<<DDC3);
        PORTC &= ~(1<<PORTC0);
        PORTC &= ~(1<<PORTC1);
}
```

LowLv_3.c

```
//Device: ATmega8L
//Function: read sensor via SPI, send data via USART to Top level
//Name: LowLv_3
//Function: initiate Shifting_Data
#include <avr/io.h>
#include<util/delay.h>
#include<avr/pgmspace.h>
#include<stdlib.h>
#include<avr/interrupt.h>
#include<avr/sleep.h>
#include"Atmega8_LowLv.h"
static const prog_int16_t MaxElements = 256;

void MCLK_ON(void);
void MCLK_OFF(void);
```

```
void SPI_MasterInit(void);
void SPI_MasterTransmit(uint8_t);
void USART_Init(void);
void USART_SendByte(uint8_t);
uint8_t USART_ReceiveByte(void);

//data saved in rom
static prog_uchar
	read_D1H=0x0f,
	read_D1L=0x40,//read pressure measurement

	read_D2H=0x0f,
	read_D2L=0x20,//read temperature measurement

	read_W1H=0x1d,
	read_W1L=0x50,//read calibration word 1

	read_W2H=0x1d,
	read_W2L=0x60,//read calibration word 2

	read_W3H=0x1d,
	read_W3L=0x90,//read calibration word 3

	read_W4H=0x1d,
	read_W4L=0xa0,//read calibration word 4

	reset_1=0x15,
	reset_2=0x55,
	reset_3=0x40;//reset sequence

//initial calibration data read from sensor
volatile uint8_t W1H,W2H,W3H,W4H, W1L,W2L,W3L,W4L;
volatile uint8_t ECHO;

//presusre data queue
volatile SD *P;
volatile Parameters *Init_Para;

int main(void){
	int i=0;
	cli();
	SPI_MasterInit();
	MCLK_ON();
	USART_Init();
	SPCR &= ~(1<<CPHA);
	MCUCR = (1<<ISC01) | (1<<ISC00); //rising edge on INT0 generates interrupt
	GICR |= (1<<INT0); //enable INT0
	P->count[2]=0xff;
	ECHO=0x00;

	SPI_MasterTransmit(reset_1);
	SPI_MasterTransmit(reset_2);
	SPI_MasterTransmit(reset_3);
```

```
	SPI_MasterTransmit(read_W1H);
	SPI_MasterTransmit(read_W1L);

	SPCR |= (1<<CPHA);// transmit at falling edge
	SPI_MasterTransmit(0x00);
	W1H=SPDR;
	SPI_MasterTransmit(0x00);
	W1L=SPDR;

	SPCR &= ~(1<<CPHA);
	SPI_MasterTransmit(read_W2H);
	SPI_MasterTransmit(read_W2L);

	SPCR |= (1<<CPHA);// transmit at falling edge
	SPI_MasterTransmit(0x00);
	W2H=SPDR;
	SPI_MasterTransmit(0x00);
	W2L=SPDR;

	SPCR &= ~(1<<CPHA);
	SPI_MasterTransmit(read_W3H);
	SPI_MasterTransmit(read_W3L);

	SPCR |= (1<<CPHA);// transmit at falling edge
	SPI_MasterTransmit(0x00);
	W3H=SPDR;
	SPI_MasterTransmit(0x00);
	W3L=SPDR;

	SPCR &= ~(1<<CPHA);
	SPI_MasterTransmit(read_W4H);
	SPI_MasterTransmit(read_W4L);

	SPCR |= (1<<CPHA);// transmit at falling edge
	SPI_MasterTransmit(0x00);
	W4H=SPDR;
	SPI_MasterTransmit(0x00);
	W4L=SPDR;

	MCLK_ON();
	SPCR &= ~(1<<CPHA);
	SPI_MasterTransmit(read_D2H);
	SPI_MasterTransmit(read_D2L);
	SPCR |= (1<<CPHA);// transmit at falling edge

	SPI_MasterTransmit(0x00);
	Init_Para->D2H[1]=SPDR;
	SPI_MasterTransmit(0x00);
	Init_Para->D2L[1]=SPDR;

////////////////extract C1..C6////////////
	Init_Para->C1_H[0] = (0x10 & (W4H>>3)) | (0x0f & W3H); //unit 1, C1
	Init_Para->C1_L[0] = W3L;
```

```
	Init_Para->C1_H[1] = (0x1f & W4H);//unit 1, C2
	Init_Para->C1_L[1] = W4L;

	Init_Para->C1_H[2] = (0x01 & (W4H>>5));//unit 1, C3
	Init_Para->C1_L[2] = W1H;

	Init_Para->C1_H[3] = (0x01 & (W4H>>6));//unit 1, C4
	Init_Para->C1_L[3] = W2H;

	Init_Para->C1_H[4] = (0x0f & (W3H>>4));//unit 1, C5
	Init_Para->C1_L[4] = W1L;

	Init_Para->C1_H[5] = 0x00;//unit 1, C6
	Init_Para->C1_L[5] = W2L;


//send initial parameters, i.e C1..6 and temperature

//send ECHO back to U2, start receiving initial parameters from U2
	do{
		ECHO = USART_ReceiveByte();
		USART_SendByte(ECHO);
	}while(!(ECHO & U1_READY));

	for (i=0;i<6;i++){
		Init_Para->C0_H[i] = USART_ReceiveByte();
	};
	for (i=0;i<6;i++){
		Init_Para->C0_L[i] = USART_ReceiveByte();
	};
	Init_Para->D2H[0] = USART_ReceiveByte();
	Init_Para->D2L[0] = USART_ReceiveByte();

	for (i=0;i<6;i++){
		Init_Para->C1_H[i] = USART_ReceiveByte();
	};
	for (i=0;i<6;i++){
		Init_Para->C1_L[i] = USART_ReceiveByte();
	};
	Init_Para->D2H[1] = USART_ReceiveByte();
	Init_Para->D2L[1] = USART_ReceiveByte();

//wait ECHO from Master, start sending initial parameters
	while(!(ECHO & U2_READY)){
		USART_SendByte(U2_READY);
		ECHO = USART_ReceiveByte();
	};

	for (i=0;i<6;i++){
		USART_SendByte(Init_Para->C0_H[i]);
	};
	for (i=0;i<6;i++){
		USART_SendByte(Init_Para->C0_L[i]);
	};
```

```
        USART_SendByte(Init_Para->D2H[0]);
        USART_SendByte(Init_Para->D2L[0]);

        for (i=0;i<6;i++){
                USART_SendByte(Init_Para->C1_H[i]);
        };
        for (i=0;i<6;i++){
                USART_SendByte(Init_Para->C1_L[i]);
        };
        USART_SendByte(Init_Para->D2H[1]);
        USART_SendByte(Init_Para->D2L[1]);

        for (i=0;i<6;i++){
                USART_SendByte(Init_Para->C2_H[i]);
        };
        for (i=0;i<6;i++){
                USART_SendByte(Init_Para->C2_L[i]);
        };
        USART_SendByte(Init_Para->D2H[2]);
        USART_SendByte(Init_Para->D2L[2]);
        //note: loop forever if no responce from Master

        MCLK_OFF();
        set_sleep_mode(SLEEP_MODE_PWR_DOWN);
        sei();
        sleep_mode();

        return 0;
}

ISR(INT0_vect){
        cli();
//read sensor
        SPCR |= (1<<CPHA);// read at falling edge
        SPI_MasterTransmit(0x00);
        P->D1H[2]=SPDR;
        SPI_MasterTransmit(0x00);
        P->D1L[2]=SPDR;

//signal the next reading
        SPCR &= ~(1<<CPHA);
        SPI_MasterTransmit(read_D1H);
        SPI_MasterTransmit(read_D1L);

//pass data
        P->count[0] = USART_ReceiveByte();
        P->D1H[0] = USART_ReceiveByte();
        P->D1L[0] = USART_ReceiveByte();
        P->count[1] = USART_ReceiveByte();
        P->D1H[1] = USART_ReceiveByte();
        P->D1L[1] = USART_ReceiveByte();

        for(i=0;i<3;i++){
                USART_SendByte(P->count[i]);
```

```
                USART_SendByte(P->D1H[i]);
                USART_SendByte(P->D1L[i]);
        };

        if(P->count[2] == 255)
                P->count[2] = 0;

        P->count[2]++;
        sei();

}


void SPI_MasterInit(void){
        SPCR = (1<<SPE) | (1<<MSTR); // enable SPI, Master mode
//      SPCR &= ~(1<<CPOL); // SCK is low when idle
        SPSR |= (1<<SPI2X);//SCK is 500kHz
        DDRB = (1<<PB4) | (1<<PB5) | (1<<PB7); // set SS (PB4), MOSI (PB5), SCK (PB7) as output
//      DDRB |= (1<<PB6);
//      SFIOR |= (1<<PUD);
        PORTB=0x00;
}

void SPI_MasterTransmit(uint8_t Data){
        SPDR = Data;
        while (!(SPSR & (1<<SPIF)))
                ;
}

void USART_Init(void)
{
  //Enable USART
        UCSRB = (1<<RXEN) | (1<<TXEN);
        //Define bit length
        UCSRC = (1<<URSEL) | (1<<UCSZ1) | (1<<UCSZ0);
        // Set baud rate TO 9600
        UBRRL = BAUD_PRESCALE;
        UBRRH = (BAUD_PRESCALE >> 8);
}

void USART_SendByte(uint8_t u8Data)
{
  // Wait if a byte is being transmitted
  while((UCSRA&(1<<UDRE)) == 0)
  {
    ;
  }

  // Transmit data
  UDR = u8Data;
}


uint8_t USART_ReceiveByte( void )
```

```
{
        /* Wait for data to be received */
        while ( !(UCSRA & (1<<RXC)) )
                ;
        /* Get and return received data from buffer */
        return UDR;
}


void MCLK_ON(void){

        DDRB |= (1<<PB1);
        OCR1AL = 0x0e; //Opt_freq= 32.768kHz, Set_freq=35.714kHz, Observed_freq=33kHz
        OCR1AH = 0x00;
        TCCR1A = (1<<COM1A0) | (1<<CS00); // CTC MODE, TOGGLE OC1A, NO PRESCALE
        TCCR1B = (1<<WGM12) | (CS10);
}

void MCLK_OFF(void){

        TCCR0 &= ~(1<<CS10);
}
```

TopLv.h

```
#include <avr/io.h>
#include<util/delay.h>
#include<avr/pgmspace.h>

#define USART_BAUDRATE      28800 // theoretically multiples of 1.8432MHz could lead to 0 error,
set to 4800 could reduce error, 0.2%(according to datasheet)
#define BAUD_PRESCALE       (((F_CPU/(USART_BAUDRATE * 16UL)))-1)
#define U0_READY 0x81 //10000001
#define U1_READY 0x82 //10000010
#define U2_READY 0x83 //10000011
//#define SENSOR2_READY 0x02 //00000010
//#define SENSOR3_READY 0x03 //00000011

//struct QueueRecord;
//typedef struct QueueRecord *Queue;

typedef struct{
                uint8_t count[3];
                uint8_t D1H[3];
                uint8_t D1L[3];
        }SD;// Shifting_Data

typedef struct{
        uint8_t C0_H[6];
        uint8_t C0_L[6];
        uint8_t C1_H[6];
        uint8_t C1_L[6];
        uint8_t C2_H[6];
```

```
		uint8_t C2_L[6];
		uint8_t D2H[3];
		uint8_t D2L[3];
}Parameters; //Sensor_Parameters

/*int IsEmpty(Queue );
int IsFull(Queue );
Queue CreateQueue(prog_int16_t );
void DisposeQueue(Queue );
void MakeEmpty(Queue );
void EnQueue(prog_uchar , Queue );
prog_char Front(Queue Q);
void Dequeue (Queue Q);
prog_char FrontAndDequeue(Queue Q);
*/
```

TopLv.c

```
//Device: ATmega8535L
//Function: read sensor via SPI, send data via USART to PC
#include <avr/io.h>
#include<util/delay.h>
#include<avr/pgmspace.h>

#define USART_BAUDRATE		4800 // reduce error, 0.2%(according to 8535L datasheet)
#define BAUD_PRESCALE		(((F_CPU/(USART_BAUDRATE * 16UL)))-1)

#ifndef _ Queue_h
struct QueueRecord;
typedef struct QueueRecord *Queue;
int IsEmpty(Queue Q);
int IsFull(Queue Q);
Queue CreateQueue(int MaxElements);
void DisposeQueue(Queue Q);
void MakeEmpty(Queue Q);
void Enqueue (prog_char X, Queue Q);
prog_char Front(Queue Q);
void Dequeue (Queue Q);
prog_char FrontAndDequeue(Queue Q);
#endif

struct QueueRecord{
			int Capacity;
			int Front;
			int Rear;
			int Size;
			char *Array;
		};

void MCLK_ON(void);
void MCLK_OFF(void);
void SPI_MasterInit(void);
void SPI_MasterTransmit(char);
void EEPROM_write(unsigned int, unsigned char);
```

```
unsigned char EEPROM_read(unsigned int);
void USART_Init(void);
void USART_SendByte(char);

int main (void){

	char read_D1H, read_D1L, read_D2H, read_D2L, read_W1H, read_W1L,
			read_W2H, read_W2L, read_W3H, read_W3L, read_W4H, read_W4L,
reset_1,reset_2, reset_3;
	char tempH, tempL;
	uint8_t W1H,W2H,W3H,W4H, W1L,W2L,W3L,W4L, D1H,D1L, D2H,D2L;
	uint8_t addr_W=0, addr_D=0;
	uint8_t C1H,C1L,C2H,C2L,C3H,C3L,C4H,C4L,C5H,C5L,C6H,C6L;
	uint16_t C1=0,C2=0,C3=0,C4=0,C5=0,C6=0;
	read_D1H=0x0f;
	read_D1L=0x40;//read pressure measurement

	read_D2H=0x0f;
	read_D2L=0x20;//read temperature measurement

	read_W1H=0x1d;
	read_W1L=0x50;//read calibration word 1

	read_W2H=0x1d;
	read_W2L=0x60;//read calibration word 2

	read_W3H=0x1d;
	read_W3L=0x90;//read calibration word 3

	read_W4H=0x1d;
	read_W4L=0xa0;//read calibration word 4

	reset_1=0x15;
	reset_2=0x55;
	reset_3=0x40;//reset sequence

	SPI_MasterInit();
	MCLK_ON();
	USART_Init();

////////////Read W1 to W4, each occupies 2 bytes, strore in 0x00 to 0x07//////////////
	SPCR &= ~(1<<CPHA);

	SPI_MasterTransmit(reset_1);
	SPI_MasterTransmit(reset_2);
	SPI_MasterTransmit(reset_3);

	SPI_MasterTransmit(read_W1H);
	SPI_MasterTransmit(read_W1L);

	SPCR |= (1<<CPHA);// transmit at falling edge
	SPI_MasterTransmit(0x00);
	W1H=SPDR;
	SPI_MasterTransmit(0x00);
```

```
            W1L=SPDR;
            EEPROM_write(addr_W, W1H);
            addr_W++;
            EEPROM_write(addr_W, W1L);
            addr_W++;

            SPCR &= ~(1<<CPHA);
            SPI_MasterTransmit(read_W2H);
            SPI_MasterTransmit(read_W2L);

            SPCR |= (1<<CPHA);// transmit at falling edge
            SPI_MasterTransmit(0x00);
            W2H=SPDR;
            SPI_MasterTransmit(0x00);
            W2L=SPDR;
            EEPROM_write(addr_W, W2H);
            addr_W++;
            EEPROM_write(addr_W, W2L);
            addr_W++;

            SPCR &= ~(1<<CPHA);
            SPI_MasterTransmit(read_W3H);
            SPI_MasterTransmit(read_W3L);

            SPCR |= (1<<CPHA);// transmit at falling edge
            SPI_MasterTransmit(0x00);
            W3H=SPDR;
            SPI_MasterTransmit(0x00);
            W3L=SPDR;
            EEPROM_write(addr_W, W3H);
            addr_W++;
            EEPROM_write(addr_W, W3L);
            addr_W++;

            SPCR &= ~(1<<CPHA);
            SPI_MasterTransmit(read_W4H);
            SPI_MasterTransmit(read_W4L);

            SPCR |= (1<<CPHA);// transmit at falling edge
            SPI_MasterTransmit(0x00);
            W4H=SPDR;
            SPI_MasterTransmit(0x00);
            W4L=SPDR;
            EEPROM_write(addr_W, W4H);
            addr_W++;
            EEPROM_write(addr_W, W4L);
            addr_W++;

/////////////////extract C1..C6, each 2 bytes, store in 0x08 to 0x13////////////
/*          C1=((0x01 & W1H)<<8) & (0xff & W1L);
            C2=((0x0f & W2H)<<8) & (0xff & W2L);
            C3=((0xe0 & W2H)<<8) & (0x1f & W1L);
            C4=((0x01 & W3H)<<8) & (0xff & W3L);
            C5=((0xfd & W4H)<<8) & (0xfd & W3H);
```

```
//
	C6=((0x01 & W4H)<<8) & (0xff & W4L);
*/
//	C1 = ((C1 + (W1H & 0x03))<<8) + W1L;
	C1H = (0x10 & (W4H>>3)) | (0x0f & W3H);
	C1L = W3L;

//	C2 = ((C2 + (W2H & 0x0f))<<8) + W2L;
	C2H = (0x1f & W4H);
	C2L = W4L;

//	C3 = ((C3 + (0x01 & (W2H>>7)))<<8) + (0xc0 & (W2H<<1)) | (0x3f & (W1H>>2));
	C3H = (0x01 & (W4H>>5));
	C3L = W1H;

//	C4 = ((C4 + (0x01 & W3H))<<8) + W3L;
	C4H = (0x01 & (W4H>>6));
	C4L = W2H;

//	C5 = (C5 + ((0x0f & (W4H>>4))))<<8 + ((0xc0 & (W4H<<4)) | (0x3f & (W3H>>2)));
	C5H = (0x0f & (W3H>>4));
	C5L = W1L;

//	C6 = (C6 + (0x03 & W4H)) + W4L;
	C6H = 0x00;
	C6L = W2L;

//read W1 from sensor, 10 times
	while (1){
//send request
//		_delay_ms(1000);
//		USART_SendByte(C6H);
//		USART_SendByte(C6L);
//		USART_SendByte(W4H);
//		USART_SendByte(W4L);

		SPCR &= ~(1<<CPHA);
//		SPI_MasterTransmit(read_D1H);
//		SPI_MasterTransmit(read_D1L);

//		SPI_MasterTransmit(read_W1H);
//		SPI_MasterTransmit(read_W1L);


//read data
		SPCR |= (1<<CPHA);// transmit at falling edge
		_delay_ms(50);

		SPI_MasterTransmit(0x00);
//		EEPROM_write(0x00, 0xf1);
		D1H=SPDR;
		SPI_MasterTransmit(0x00);
//		EEPROM_write(0x01, SPDR);
		D1L=SPDR;
```

```
/*			SPCR &= ~(1<<CPHA);
			SPI_MasterTransmit(read_D2H);
			SPI_MasterTransmit(read_D2L);

			SPCR |= (1<<CPHA);// transmit at falling edge
			_delay_ms(50);
			SPI_MasterTransmit(0x00);
			D2H=SPDR;
			SPI_MasterTransmit(0x00);
			D2L=SPDR;
*/
/*			USART_SendByte(C1H);
			USART_SendByte(C1L);

			USART_SendByte(C2H);
			USART_SendByte(C2L);

			USART_SendByte(C3H);
			USART_SendByte(C3L);

			USART_SendByte(C4H);
			USART_SendByte(C4L);

			USART_SendByte(C5H);
			USART_SendByte(C5L);

			USART_SendByte(C6H);
			USART_SendByte(C6L);
*/
			USART_SendByte(D1H);
			USART_SendByte(D1L);
//			_delay_us(100);

//			USART_SendByte(D2H);
//			USART_SendByte(D2L);

//			i++;
		}

		return 0;
}


void SPI_MasterInit(void){
		SPCR = (1<<SPE) | (1<<MSTR); // enable SPI, Master mode
//		SPCR &= ~(1<<CPOL); // SCK is low when idle
		SPSR |= (1<<SPI2X);//SCK is 500kHz
		DDRB = (1<<PB4) | (1<<PB5) | (1<<PB7); // set SS (PB4), MOSI (PB5), SCK (PB7) as output
//		DDRB |= (1<<PB6);
//		SFIOR |= (1<<PUD);
		PORTB=0x00;


}
```

```
void SPI_MasterTransmit(char Data){
        SPDR = Data;
        while (!(SPSR & (1<<SPIF)))
                ;
}

void EEPROM_write(unsigned int uiAddress, unsigned char ucData){
        while (EECR & (1<<EEWE))
                ;
        EEAR = uiAddress;
        EEDR = ucData;
        EECR |= (1<<EEMWE);
        EECR |=(1<<EEWE);
}

unsigned char EEPROM_read(unsigned int uiAddress){
        while(EECR & (1<<EEWE))
                ;
        EEAR = uiAddress;
        EECR |= (1<<EERE);
        return EEDR;
}


void USART_Init(void)
{
  //Enable USART
        UCSRB = (1<<RXEN) | (1<<TXEN);
        //Define bit length
        UCSRC = (1<<URSEL) | (1<<UCSZ1) | (1<<UCSZ0);
        // Set baud rate TO 9600
        UBRRL = BAUD_PRESCALE;
        UBRRH = (BAUD_PRESCALE >> 8);
}

void USART_SendByte(char u8Data)
{
  // Wait if a byte is being transmitted
  while((UCSRA&(1<<UDRE)) == 0)
  {
    ;
  }

  // Transmit data
  UDR = u8Data;
}



/*
uint8_t USART0_vReceiveByte()
{
  // Wait until a byte has been received
```

```
    while((UCSR0A&(1<<RXC0)) == 0)
    {
        ;
    }

    // Return received data
    return UDR0;
}
*/


void MCLK_ON(void){

        DDRB |= (1<<PB3);
        OCR0 = 0x0e; //Opt_freq= 32.768kHz, Set_freq=35.714kHz, Observed_freq=33kHz
        TCCR0 = (1<<WGM01) | (1<<COM00) | (1<<CS00); // CTC MODE, TOGGLE OC0, NO
PRESCALE

}

void MCLK_OFF(void){

        TCCR0 &= ~(1<<CS00); // CTC MODE, TOGGLE OC0, NO PRESCALE

}

int IsEmpty(Queue Q){
        return Q->Size==0;
}

void MakeEmpty(Queue Q){
        Q->Size = 0;
        Q->Front = 1;
        Q->Rear = 0;
}

statuc int Succ(int Value, Queue Q){
        if (++Value==Q->Capacity)
                Value=0;
        return Value;
}

void Enqueue (char X, Queue Q){
        if(IsFull(Q))
                return;
        else{
                Q->Size++;
                Q->Rear = Succ(Q->Rear, Q);
                Q->Array[Q->Rear]=X;
        }
}
```

A.2 Bill of material

Components	Quality	Unit price	Total
ATmega8L-8PU Microcontroller	4	3.6	14.4
Capacitor 100nF	4	0.02	0.08
Intersema MS5536c digital pressure sensor	3	27	81
Membrane, sensor module assembly	3	1	3
Xbee 2.4GHz transceiver	2	21.6	43.2

Total 141.68 USD